Spreading of plastics near tidal inlet systems: an understanding of buoyant particle behaviour

Thesis research

Francine van Hee & Floris Pauw

Spreading of plastics near tidal inlet systems: an understanding of buoyant particle behaviour
Thesis research

Francine M. van Hee (000013103) & Floris H. Pauw (000013543)

Module LKZ428: bachelor thesis

Utrecht University: Institute for Marine and Atmospheric Research Utrecht (UU-IMAU)

Van Hall Larenstein: University of Applied Sciences (VHL)

Supervisors:
Huib de Swart & Abdel Nnafie – UU-IMAU
Peter Smit & Alwin van Beem – VHL

Leeuwarden

June 10th, 2020

Front page photo: Kilina, 2019

Abstract

Marine debris is a growing global problem. Due to the wide ocean dynamics worldwide, predicting the transport of floating marine debris, such as plastic, is difficult. Although large-scale distribution patterns and accumulation zones are recognised and reproduced by numerical models, small-scale prediction of plastic particle spreading in coastal zones is complex and has been done little with high-resolution models. The large differences in coastal bathymetry and hydrodynamics cause the prediction of transport pathways of marine debris to be complex. This research aimed at understanding the behaviour of buoyant particles and the extent to which their transport characteristics are influenced by different hydrodynamic processes that are critical to tidal inlet systems, by modelling the transport of buoyant particles under specific hydrodynamic conditions. An idealized model was used to simulate hydrodynamics and transport characteristics (particle dispersion, mean particle transport, spreading time and beaching) of buoyant particles under the influence of tides, swell in combination with tides, and wind conditions in combination with tides and swell.

Results mainly showed differences in the spreading time (time for particles to reach the tidal inlet) and direction, and beaching quantity. For the tides-only scenario, different release times (different tidal phases) resulted in different spreading times (max five days difference for first particle to enter the tidal inlet system). Allowing for both tides and swell in the simulations resulted in an offshore residual (depth-averaged) current along the coastline. This caused particles to move offshore, which in turn resulted in significantly less beaching (max 19.7%) compared to the tides-only scenario (max 63%). Adding a third process, constant wind, showed that wind direction and speed strongly influenced the particle spreading time and direction. The time it took for first particles to reach the tidal inlet decreased significantly when forcing a gentle breeze and even more so with a strong wind. Particles typically moved in the direction of the wind and in case of a strong wind, the effect of the falling and rising tide was suppressed almost completely. Only onshore wind perpendicular to the coast resulted in spreading time and direction of particles similar to the scenarios without wind. In the simulations with wind conditions, wind resulted in a significant decrease of beaching (max 7.3%) compared to the scenarios without wind, except for a strong wind from the west. In the last scenario, variable wind conditions (taken from wind data for the period and location of the MSC Zoe incident) were included in the model. Here, wind influenced particle transport most strongly, mainly in the form of spreading time (max 2.6 days for first particle to enter the tidal inlet system) and beaching quantity (max 3.3%, not including strong wind from the west). As with a constant strong wind, the effect of the tides was suppressed by forcing variable wind conditions.

The results of this research give the extent to which three critical processes (tides, swell, wind) in tidal inlet systems influence the transport of particles. These can be used to improve the complex models that are used for accurate predictions of particle pathways and therefore aid policy decision making about emergency response strategies as well as for future management of tidal inlet systems. As the results reveal the contribution of the processes to particle transport, emphasis can be put on the processes that are important in tidal inlet systems in order to limit computing time in complex models and therefore speed up emergency response.

Table of contents

1. Introduction

"*The movement and circulation of the oceans is tied very closely to the circulation of the atmosphere: both are ultimately driven by the distribution of solar energy, and their motions are linked by friction at the sea surface*" (Kump, Kasting, & Crane, 2014). Caused by the unequal distribution of solar energy on Earth, a surface temperature gradient is created, resulting in surface winds. Earth's pattern of surface wind is the driver of surface-ocean circulation and the major ocean currents. As wind moves over the ocean, friction at the surface (i.e. wind stress) causes wind to drag the ocean surface in the same direction, resulting in surface-ocean wind-drift currents. In the Northern Hemisphere, water is deflected to the right as it is affected by the Coriolis force. Due to the presence of continents, the large-scale surface currents follow a circular pattern (i.e. gyre), that is clockwise in the Northern Hemisphere (see figure 1.1) (Kump, Kasting, & Crane, 2014). Other drivers of ocean circulation are water density and the tides. The tide is considered a massive progressive wave and its speed is determined by the depth of the ocean. As the wave moves towards coastal areas, where the ocean becomes shallower, the tidal range increases (The Open University, 1999).
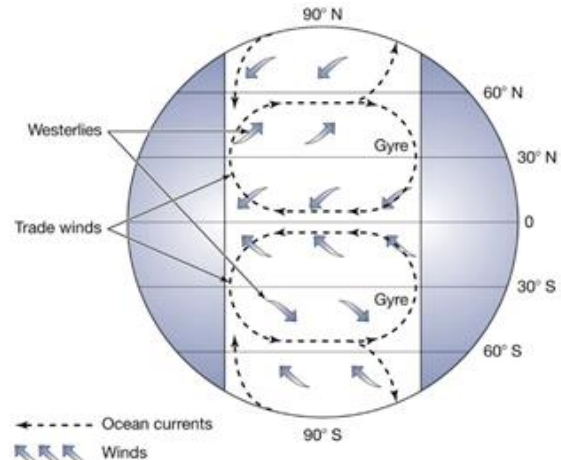

Figure 1.1: Ocean surface circulation (Kump, Kasting, & Crane, 2014). Surface currents of the upper layer (50-100m) are driven by wind but deflected by Coriolis force.

Tidal currents are considerably stronger in shallow seas and along coasts than in the open ocean, typically strong enough to rework sand and gravels. Next to this, oceanic currents, local wind-driven currents and wind-generated waves also play a large role in e.g. sediment transport in shelf seas. The pattern of currents in coastal seas is not only affected by small-scale variations in hydrodynamic conditions, but also by the structure of the coastline, the bathymetry and the presence of fronts, thus more complex than in open seas. This thesis focused on tidal inlet systems, which are part of larger intertidal flat systems and are found worldwide. For example, along the US east coast and Gulf Coast, the east coast of Vietnam and the south coast of Portugal. Another well-known example is in the Wadden Sea: the largest uninterrupted system of intertidal flats in the world (spread over the Netherlands, Germany and Denmark) and one of the last large-scale, intertidal ecosystems that is largely undisturbed. It has been recognized as an area of global importance and is named a World Heritage site (UNESCO, 2020). Tidal inlet systems contain tidal flats in the back-barrier basin, which are alternately submerged by water and exposed to air. Tidal inlets are narrow openings in the shoreline through which the water flows (see figure 1.2). They act as a connection between the ocean and inland bays, marshes, lagoons or tidal creeks (FitzGerald & Buynevich, 1978; Oost, de Groot, Duren, & van der Valk, 2014).

What makes water transport in tidal inlet systems complex is a combination of morphological features (figure 1.2) and hydrodynamic processes. Intertidal flats and tidal inlets are aptly named, as their most important hydrodynamic process is the tides. The tide "*determines the existence of the intertidal flat*"

Figure 1.2: Schematic overview of a tidal inlet system (Oost, de Groot, Duren, & van der Valk, 2014).

(Hir, et al., 2000), as it influences the physical appearance of the tidal flats system given that it mostly consists of erodible sand and mud. The difference in flood and ebb determines the strength of the current and therefore influences the size of inlets. Next to the tides, other important hydrodynamic drivers of water motion in tidal inlet systems are waves, wind and density differences. Waves contribute to the continuously changing morphology of the tidal inlet system by eroding sand and mud (Hir, et al., 2000), as their orbital motion stirs up sediments. Waves can also generate net movements, such as longshore currents in the zones where waves break (The Open University, 1999). Usually, waves originating from the sea are unable to penetrate the narrow tidal inlet as the energy dissipates in e.g. the ebb-tidal delta (Wang, Louters, & de Vriend, 1995). Although tidal currents and storm waves are the main drivers of water motion that affect the seabed, local wind-driven currents can also contribute to sediment transport. Next to this, tidal flats are often connected to estuaries, the areas in which rivers discharge into the sea. In this shallow area, the fresh water from the river mixes with the salt water in the delta area, resulting in a lower density. This in turn leads to horizontal density gradients, which can also be caused by the heating of surface water that decreases water density. Combined with the slope in bed-level from open sea to coast, the density-driven currents that are created lead to a net current of the surface water offshore and an onshore current at the bottom, a process known as gravitational circulation (Burchard & Badewien, 2015).

Marine debris
The processes described above are essential for the influx of nutrients to tidal basins, but they also offer a way for marine debris to enter the tidal basin system. Marine debris, consisting mostly of plastic, has been recognized worldwide as a global problem having severe ecological, economic and human health impacts (Mansui, Molcard, & Ourmieres, 2015; van Utenhove, 2019). Examples of the impact of marine plastic include ingestion or entanglement by marine organisms, human consumption through seafood and decreasing the attractiveness of the sea towards people (van Utenhove, 2019). Marine debris is typically classified into two categories: land- or ocean based. Land-based debris originates from land surfaces and is transported through waterways such as rivers, whereas ocean-based debris originates directly from activities at sea, such as fisheries, marine traffic and container spills (Sheavly & Register, 2007).

In January 2019 a containership by the name of MSC Zoe lost 341 of its containers during stormy weather in the Wadden Sea (Janssen, 2019). Part of the resulting debris washed up on shores, while a large portion remained in the sea (Stichting de Noordzee, 2020). Accidents such as the MSC Zoe could happen again and coincidentally one recently did. North of the Dutch Wadden island Ameland, containership OOCL Rauma lost 7 of its containers due to heavy weather on February 11th, 2020 (Netherlands Coastguard, 2020). The extent of plastic pollutions seemed limited for the containers

Figure 1.3: Plastic granules washed up on shores (<5 mm) (Plastic Soup Foundation, 2019).

lost by OOCL Rauma. After the MSC Zoe incident, beaches of the Wadden islands were covered in debris, namely plastic granules (see figure 1.3) (Baptist, et al., 2019). The buoyant characteristic of plastic causes it to widely disperse under the influence of oceanic currents and other hydrodynamic processes, making it difficult to collect. It is therefore a problem for the marine environment (van Utenhove, 2019). Different hydrodynamic conditions (e.g. wind speed/direction) might results in different transport pathways of buoyant plastic particles. Upon entering tidal inlets, particles may end up beaching on tidal flats. With the falling tide, the water level drops and tidal flats fall dry. As a result, particles may become stuck in the sediment, which would harm for example benthic organisms. Moreover, plastic particles in the water column may enter the food chain as they are eaten by organisms (Zandt, 2019).

Existing research

Research has been done on the transport of plastic particles in the vast oceans. For example, the oceanic garbage patches have gained much attention in the media and general public and are well-researched (Lebreton, Greer, & Borrero, 2012; Van Sebille, England, & Froyland, 2019; Howell, Bograd, Morishige, Seki, & Polovina, 2012). The fate of an item, when spilled in the sea, is predictable to some extent given the well-known large-scale distribution patterns. Scientific models are often designed to portray particle dispersion over large ocean systems, containing lower spatial resolutions. However, these models do not resolve the smaller-scale coastal zones, in which there is a higher complexity of hydrodynamic processes. Consequently, there is a lack of fundamental understanding about particle spreading on these smaller scales (e.g. a magnitude of 100 m) (Critchell, et al., 2015; Hardesty, et al., 2017; van Utenhove, 2019).

A research on numerical modelling of floating debris in the world's oceans, simulating 30 years of worldwide input and circulation, suggests that the largest accumulation zones for floating debris are the ocean gyres of the Northern Hemisphere. However, coastal seas with a net inflow without outlets, such as the Mediterranean, also show high accumulation numbers (Lebreton, Greer, & Borrero, 2012). A more coastal-oriented smaller scale study by van Utenhove (2019) modelled the transport of buoyant macro-plastics in the Wadden Sea. This research applied numerical modelling to analyse the effect of windage (the direct effect of wind on particles), diffusion coefficients and beaching and different release locations. Van Utenhove concluded there was a significant discrepancy between transport in nearshore and open waters and that wind strongly influences local currents. Furthermore, release location was an important parameter due to complex shorelines and local topography differences. Recommendations were to further investigate the effect of the hydrodynamic processes (van Utenhove, 2019).

Existing literature on particle transport in tidal inlet systems is often focussed on particles with large densities, such as sediments, while leaving more buoyant particles with smaller densities that behave more like water out of the question (van Utenhove, 2019). Critical processes determining buoyant particle dispersal in tidal inlet systems have been relatively underexplored. Despite its negative effects, the MSC Zoe incident above the Wadden Sea offered opportunities in improving numerical modelling of particle dispersal in these systems. Janssen (2019) compared observations from waddenplastic.nl, a citizen science project by Groningen University, with his results of modelling the dispersal of small particles in the North Sea. The citizen science field study mapped small plastic granules that washed ashore after the MSC Zoe container loss and found the highest concentration of granules on Schiermonnikoog, east of the location of the incident (see figure 1.4). Although the research by Jansen (2019) was focused on particle dispersal in the North Sea and even included results of dispersal into the Wadden Sea, it did not resolve the small-scale spatial variations in water motion, as occurs in
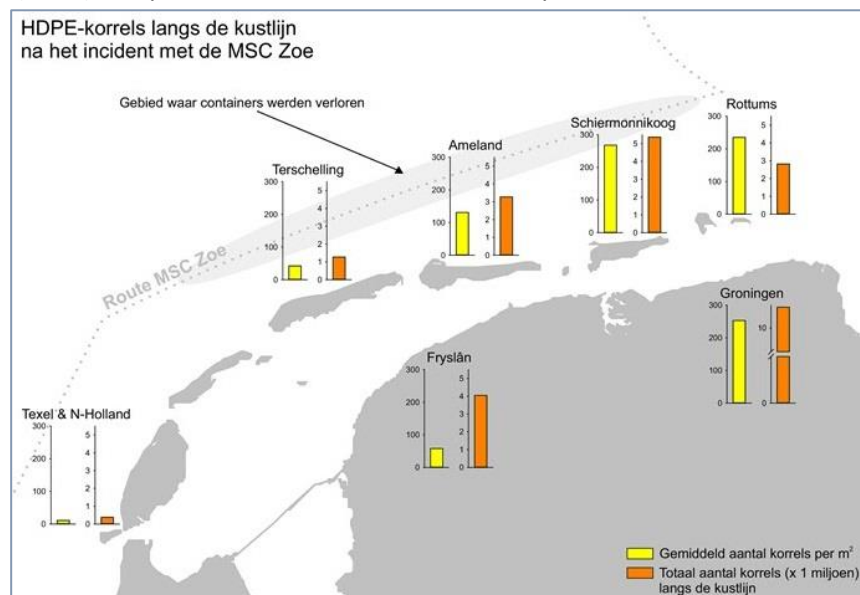

Figure 1.4: The HDPE granule count (x 1 million) along the shores of the eastern Wadden area (Groningen University, 2019). Arrow marks location incident. Yellow = mean per m2; orange = total count.

tidal inlet systems. To accurately predict particle dispersal in tidal inlet systems, a fundamental understanding of the processes at play is necessary, which can help improve numerical modelling for these systems.

At the Institute for Marine and Atmospheric research Utrecht (IMAU), an institute of Utrecht University, transport of matter in coastal and inland seas is an important topic of research. Part of this work is motivated by questions from policymakers such as Rijkswaterstaat, requiring knowledge to help in the decision-making process. This research was established with supervisors of IMAU, whom were inspired by the MSC Zoe incident to investigate the spreading of plastic particles in tidal inlet systems, and to gain fundamental knowledge on how particles bypass tidal inlets. For obtaining a better fundamental understanding of the hydrodynamic processes and the extent they influence transport of buoyant particles, so-called idealized models are employed. These models make specific simplifying assumptions regarding geometry and physical processes. Computation times of such models are much shorter than those of complex models, hence they are suitable tools to assess sensitivity of results to different values and scenarios. This results in a better understanding of the importance of different physical processes, which can be used to improve complex models (Murray, 2003).

Problem statement
Tidal inlets offer a way into intertidal flat systems for plastic particles. The hydrodynamics influencing particle transport are complex and not yet understood. Plastic particle spreading cannot be predicted without an understanding of the processes that are critical to the water flow in tidal inlet systems.

Aim
The aim of this research is to understand the behaviour of buoyant particles and the extent to which their transport characteristics are influenced by different hydrodynamic processes that are critical to tidal inlet systems, by simulating the transport of buoyant particles under specific hydrodynamic conditions with an idealized model.

Research questions
Main question
To what extent are transport characteristics of buoyant particles, released from a perturbing source outside of the tidal inlet system, influenced by the hydrodynamic processes in a tidal inlet system?

Sub questions
1. To what extent are transport characteristics of buoyant particles influenced by tides only and how do these characteristics depend on release times (tidal phases)?
2. To what extent are transport characteristics of buoyant particles influenced by the contribution of swell to tides and how do these characteristics depend on release times?
3. To what extent are transport characteristics of buoyant particles influenced by the contribution of wind-driven currents to tides and swell?
4. To what extent are transport characteristics of buoyant particles influenced by realistic time-variable wind conditions (based on the MSC Zoe incident), in combination with tides and swell and how do these characteristics depend on release times?

The report first proceeds with the methodology (chapter 2), which elaborates on background theory (chapter 2.1) of hydrodynamics applicable to this research, before going over the tools (chapter 2.2) used to simulate and visualise the scenarios later listed in the operationalisation (chapter 2.3). Here, the model

domain and the design of experiments were described in detail. The analysis (chapter 2.4) then explains how the output of the simulations were analysed to obtain answers to the research questions.

In the results (chapter 3), a default case (chapter 3.1) is introduced, covering one of the simulations in detail. Built on this base, the findings of the scenarios and their corresponding simulations are subsequently presented in chapter 3.2 – 3.5.

The discussion (chapter 4) makes sense of the results found in the previous chapter and presented some of the limitations in this research. Here, the results of this research are also compared with other literature.

In the conclusions (chapter 5), answers are formulated to the defined research questions. And finally, recommendations (chapter 6) are given for further research.

2. Methodology

To address the research questions, first, relevant knowledge about the hydrodynamics in tidal inlets and particle transport is given in section 2.1, to understand the processes at play. This is essential to interpret the results. In the next section, different modelling tools are discussed that were used during this research to model currents, swell, particle transport and beaching. This is followed by a section that discusses the operationalisation for this research, which includes the model set-up and design of experiments. The chapter ends with a section explaining the analysis of the results.

2.1 Hydrodynamics in tidal inlets and particle transport

Processes

Tides

The tides are the result of processes that have periodically constant cycles (the Moon its orbit around the Earth and Earth's orbit upon its own axis and the Sun), therefore making tides rather predictable (The Open University, 1999). A tidal period is typically 12 hours and 25 minutes (semi-diurnal), but in some coastal seas diurnal tides (periods of around 24 hours) are observed. Thus, in locations with a diurnal tidal cycle, high and low tide can be observed once a day, whereas this is twice a day in locations with a semi-diurnal tidal cycle. The observed tides are a mix of many tidal constituents (Haigh, 2017). The dominant constituents are commonly known as M2 and S2 sine waves. The M2 wave refers to the lunar semi-diurnal tide, induced by the gravitational pull of the moon, whereas the S2 wave refers to the solar semi-diurnal tide (a period of 12 hours), caused by the gravity of the Sun. Combining these constituents, as in reality, results in spring and neap tides (see figure 2.1). It should be kept in mind there are many other constituents influencing the observed tides.
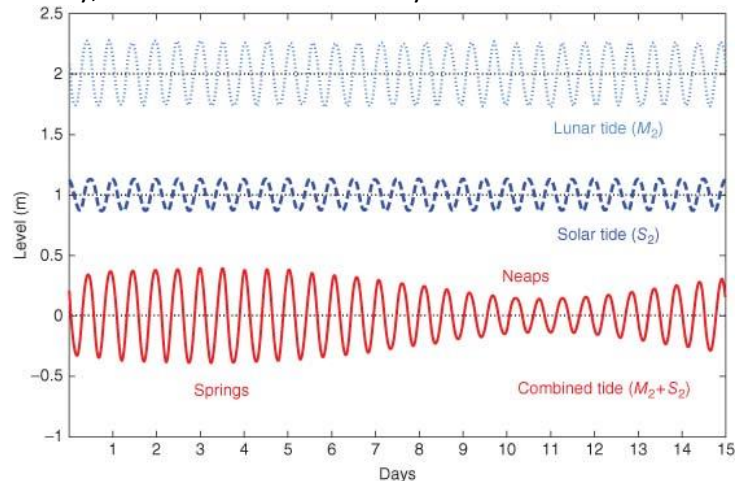

Figure 2.1: Lunar, solar and combined tides over a period of 15 days (Haigh, 2017).

Following the movement of the tides, they can be seen as massive progressive waves moving over the surface of the Earth. Tidal waves have a long wavelength compared to the depth of the oceans, causing them to behave as shallow water waves. However, rather than directly circumnavigating the Earth, the tidal current is constrained by the presence of land masses. The effect of the Coriolis force, an apparent force due to the rotation of the Earth about its axis, results in amphidromic systems in water basins. "*The crest of the tidal wave at high water circulates around an amphidromic point during each tidal period*" (The Open University, 1999). The tidal range (i.e. difference between high water and low water) is zero at the amphidromic point and increases as one moves further away from it. The Coriolis force deflects water in an anti-clockwise direction in the Northern Hemisphere, so that tidal waves propagate with the coast on the right (Haigh, 2017).

In coastal zones, the tidal current is influenced by other factors as well, such as the structure of the coastline, bathymetry and local weather conditions (The Open University, 1999; Buonaiuto & Bokuniewicz, 2008).

Swell

Surface waves are mostly initiated by processes that are not constant, namely local wind. Swell is not influenced by local wind conditions. These so-called swell waves were formed in distant storms and as they propagate further from that storm, their wave height decreases, and their wavelengths increase. Local winds have no significant influence on the amplitudes of swell in tidal inlet systems as the area for wave propagation is too small (The Open University, 1999).

Wind-induced currents

At the sea-surface, water and wind are in contact, resulting in frictional stress (i.e. wind stress). This results in energy of the air to be transferred to the surface layer of the water. The movement of that layer drags along the water layer below, and so on, thus a transfer of energy down the water column occurs. However, as energy moves downward, it dissipates and the current therefore slows down with depth. Next to this, the Coriolis effect deflects water to the right (in the Northern Hemisphere) further with increasing depth. The result is a net movement of water to the right relative to the wind direction, called Ekman transport (Kump, Kasting, & Crane, 2014). Depending on the direction of the wind and of the surface current, Ekman transport pushes water onshore or away from the shore. Onshore wind tends to cause water to pile up near the coast, leading to a downward slope of the surface water due to gravity in an offshore direction. This so-called pressure-driven current is deflected to the right by the Coriolis force, which causes a flow of water along the shore (The Open University, 1999).

Tidal residual velocity

In the presence of islands along a coastline, such as the Wadden Islands, the tidal current is constrained resulting in higher velocities. The current is forced to narrow as it flows through a tidal inlet and must therefore speed up according to the requirement for continuity (The Open University, 1999). In the case of a tidal inlet, when the tide comes in, water gradually flows into the inlet from all directions. When the tide turns, the outflow of water is pushed through the narrow tidal inlet with a high velocity, resulting in a so called 'ebb-tide jet', a concept first proposed by Stommel & Farmer (1952) (see figure 2.2).

In terms of the residual velocities, which is defined as "*the averaged velocities at a fixed location over multiple tidal periods*" (Wang, Hirose, Moon, & Yuan, 2013), the net current here is ebb-dominated in the middle of the tidal inlet, towards the sea, but flood-dominated at the sides of the inlet (see figure 2.2).
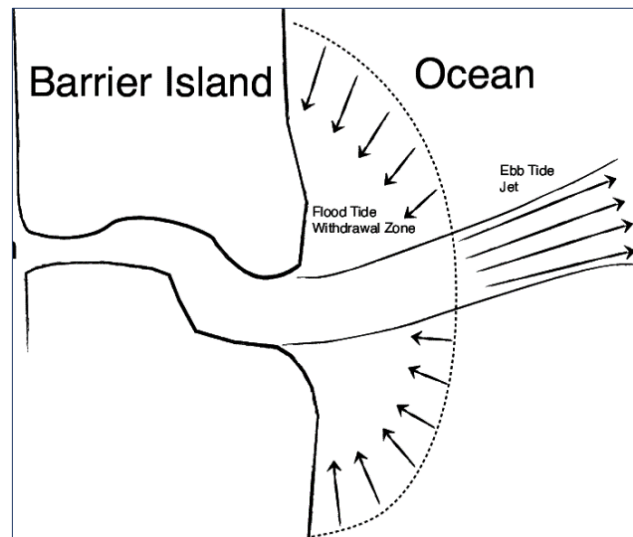

Figure 2.2: Schematic overview of the ebb-tide jet occurring as the tide is falling (Rynne, 2016).

There are also other sources of tidal residual currents. The bottom friction that the tidal current experiences depends on local depth. Away from the inlet, it results in a residual current that is parallel to the coast and in the direction of the tidal wave.

Wave induced residual velocity

Residual velocities are also contributed to by waves. Waves cause a net transfer of momentum in their direction of propagation, meaning energy is moving through the material (water). Approaching the coast, the accumulation of momentum results in set-up of water level towards the coast and a net current parallel to the coastline. The longshore current arises as waves usually approach shorelines at an inclined angle.

Waves transfer energy through the water and displace individual water particles in an almost circular motion. As this motion is not completely circular, there is a small net forward displacement of water in the direction of wave propagation, a concept termed 'Stokes drift' (see figure 2.3) (Dyke, 1980; Henry, 2019). However, as waves approach the shore, an offshore current (i.e. undertow) results to compensate for the onshore Stokes drift (Lentz, Fewings, Howd, Fredericks, & Hathaway, 2008). The undertow is in the water column below the surface waves. For this reason, in terms of buoyant particle transport, a net movement in the same direction as the wave can be observed, whereas in terms of sediment transport, particles move away from the coast (Guannel & Özkan-Haller, 2014). These movements cannot be observed separately in a depth-averaged residual velocity.
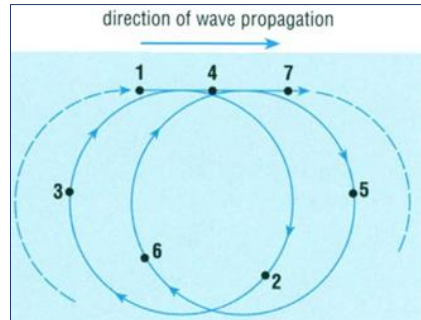

Figure 2.3: Particle motion in a wave, visualising Stokes drift (The Open University, 1999).

Bypassing of material

Bypassing of material, a process defined in research of sediment transport, occurs in ebb-dominated tidal systems. Particles enter a tidal inlet system from the surf-zone with the flood phase and move back out through the channels with the ebb phase due to the strong ebb-directed currents, leaving the system seaward of the ebb-tidal delta. Subsequently, as the flood phase returns, particles are swept past the ebb-tidal delta by wave- and tide-driven longshore currents, essentially bypassing the tidal inlet system and its channels (see figure 2.4) (Herrling & Winter, 2018).
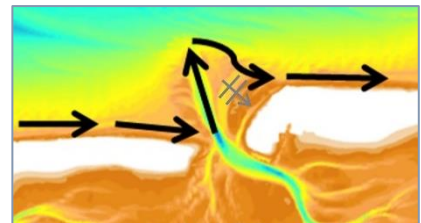

Figure 2.4: A simplified overview of how material bypasses a tidal inlet system (Herrling & Winter, 2018).
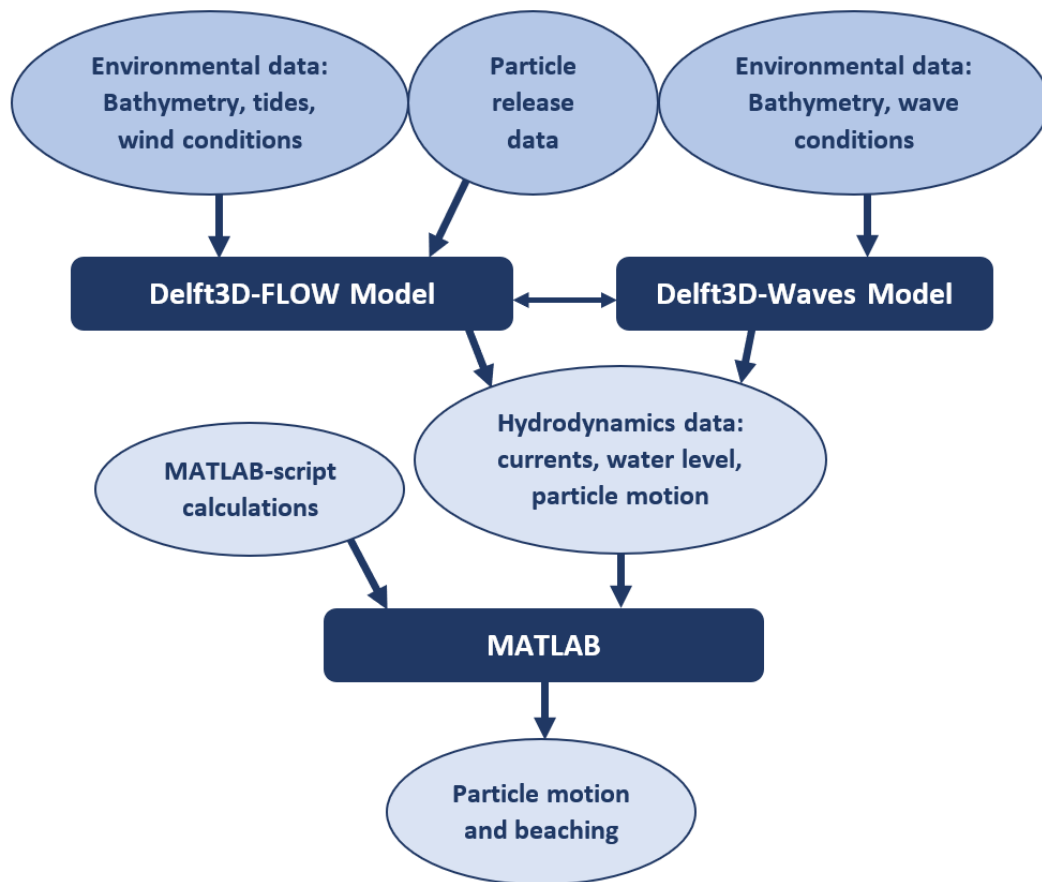
2.2 Tools

Figure 2.5: Overview of the modelling framework. Data output from the Delft3D model was used as input for MATLAB routines that calculate beaching.

Delft3D-FLOW

In order to understand the spreading of buoyant particles and to determine the number of particles that potentially end up in a tidal inlet and basin, it is important to gain fundamental insight into the hydrodynamic processes in tidal inlet systems that influence the spreading of buoyant particles. A Delft3D-FLOW model was used to simulate the motion of these particles under different hydrodynamic conditions. Delft3D software is designed to simulate two-dimensional and three-dimensional currents, sediment transport and morphology, waves, water quality and ecology, as well as interactions between these processes.

The hydrodynamic module, Delft3D-FLOW, "*calculates non-steady (tide and wind-driven) flow and transport phenomena that result from tidal and meteorological forcing on a boundary fitted grid*" (Deltares, 2019). An idealized (simplified) Delft3D-FLOW model is used that represents a tidal inlet and ebb-tidal delta, based on the model as presented by Ridderinkhof et al. (2014). They state: "*the numerical model is used in its 2D mode. Thus, the hydrodynamics are described by depth-averaged shallow water equations*". This is kept the same for this research. To simulate the tides, the model forces a harmonic variation in water level at the alongshore boundary (*conditions: Frequency = 30 degrees/hour; Amplitude begin = 0.68571 m; Phase begin = 0 degrees; Amplitude end = 0.836697 m; Phase end = 42 degrees*), and harmonic Neumann conditions at the cross-shore boundaries (*western boundary conditions: Frequency =*

30 degrees/hour; Amplitude begin = 9.7924*10⁻⁶ m; Phase begin = 65 degrees; Amplitude end =
9.7924*10⁻⁶ m; Phase end = 65 degrees. Eastern boundary conditions: Frequency = 30 degrees/hour;
Amplitude begin = 9.7924*10⁻⁶ m; Phase begin = 102 degrees; Amplitude end = 9.7924*10⁻⁶ m; Phase end
= 102 degrees).

Different from tides, wind conditions are defined in the model as a uniform field that is time dependent. This means spatially, the computational domain contains the same wind conditions, but wind speed and direction can vary in time. In this research, both types of wind inclusion (time-varying and constant) were used.

Delft3D-WAVES
To simulate swell in the model, SWAN (i.e. Delft3D-WAVES) is used. Swell is generated outside the computational domain and enters at the north-oriented open boundary. Boundary conditions used to force waves (here swell) at the open boundary are:
- significant wave height = 1 metre;
- peak period Tp = 5.75 seconds;
- direction (nautical) = 335 degrees;
- directional spreading = 4 degrees.

To calculate currents including waves in the computational domain, the Delft3D-FLOW module communicates with SWAN (see figure 2.5), which in turn calculates how these waves change as they approach the coast, and how currents are being affected and generated by waves (Lesser, Roelvink, van Kester, & Stelling, 2004).

MATLAB
In Delft3D, particles are defined as passive tracers (no mass) and therefore behave as fluid parcels. However, the process of beaching is important to include, as tidal flats (areas that fall dry) are very prevalent in tidal inlet systems. These are areas that are above water level during low tidal phases. The software MATLAB (a programming platform to analyse data, develop algorithms and create models and applications) was used to overcome this model limitation. MATLAB de-activated the motion of particles when they reached dry land (i.e. beaching), which were defined as areas at which the water level is momentarily below 0 m. In this way, the simulated particles differed from fluid parcels. Once particles were frozen (de-activated), they remained frozen for the rest of the simulation period.

2.3 Operationalisation

In order to meet the wishes of IMAU, the operationalisation of this research was determined in weekly meetings with supervisors of the institute. These weekly meetings continued throughout the project, thus also including their interests and supervision in analysis.
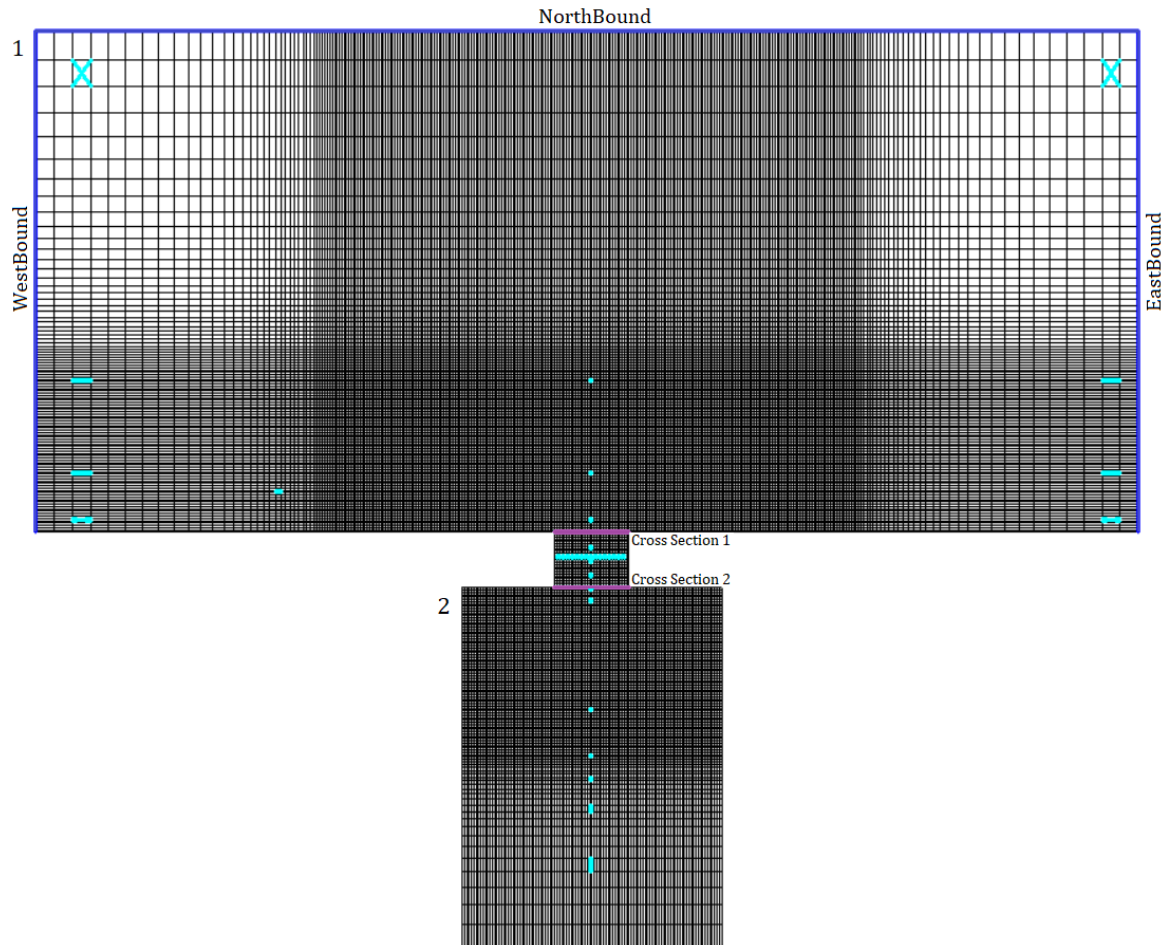
Model domain

Figure 2.6: Computational grid of the Deflt3D-FLOW model, with two subdomains: 1=open sea, 2=back barrier basin. The cross-sections (purple lines) provide information about e.g. the amount of water flowing through the sections, which indicates the exchange of water between open sea and the water basin. So-called observation points (light blue) were added and placed at different positions in the domain, with some more concentrated at the tidal inlet. These are points at which the model outputs values of variables such as water level, velocity, and wave height.

The computational domain of the Delft3D-FLOW model consisted of a rectangular grid with two subdomains (open sea and back-barrier basin) that are connected by the tidal inlet (see figure 2.6). The grid contained 296 grid points in the M-direction (x-coordinates), and 229 grid points in the N-direction (y-coordinates). The spatial resolution was increased in the tidal inlet area to indicate more detail. This was necessary as the velocities were assumed to vary at spatially smaller scales than in the open sea, caused by the larger variety in bottom depth in and nearer to the tidal inlet area. In the Delft3D-WAVES model, a longer (in N-direction) but similar grid was used, although with a lower spatial resolution. This grid was extended at the west and east sides of the domain compared to the Delft3D-FLOW model, in order to remove the so-called shadow area. The extension was necessary because swell was forced from the northern boundary that propagate from north-west to south-east. This means that to the west of the

wave ray that enters the domain at the north-western corner, no swell occurred. Delft3D-FLOW solved the hydrodynamics at a time step of two minutes and stored map results at a time interval of 30 minutes. Coupling with SWAN occurred every 60 minutes.

A realistic bathymetry was implemented. Here, bathymetric data representative for the Vlie tidal inlet were used and retrieved from Ridderinkhof et al. (2014) (see figure 2.7). Due to attention the MSC Zoe event has gained, the location for particle-release was chosen to represent a shipwreck/cargo spill similar to that of the MSC Zoe. A total of 300 particles was released in the model. The model was able to release one particle per grid cell; therefore, the number of particles was limited to 300 (20x15 cells). However, this number was sufficient to analyse particle transport and the effect of hydrodynamic processes on particle spreading.
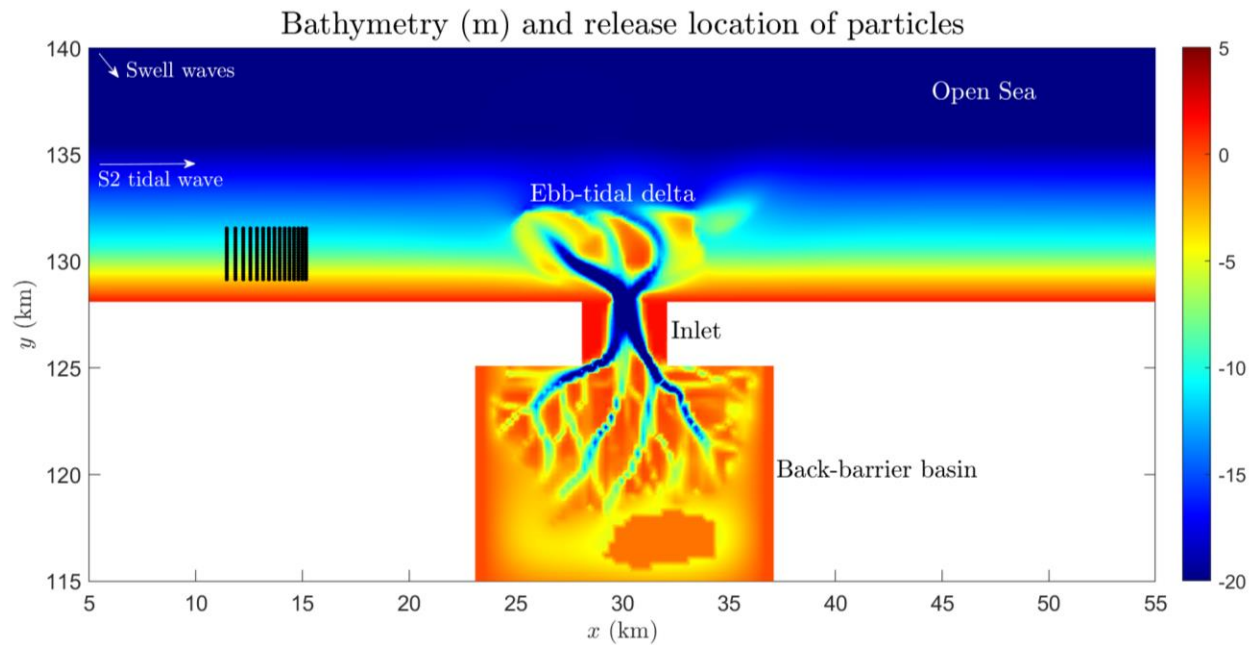

Figure 2.7: Bathymetry of the modelled tidal inlet system. Colours indicate the bathymetry. Open sea = 60x30 km, back-barrier basin = 14x19 km, tidal inlet = 4x3 km. West-eastward propagating S2 tidal wave with a period of 12 hours. Black dots indicate release locations of particles.

Design of experiments

The model needs time to adjust to the given forcing. For this reason, particles were not released at t=0 (hours) in the simulation. A test-run showed that 22 hours was enough time for the model to adjust (see figure 2.8). Therefore, particles were only released at or after t=22 (hours).

The simulations were run for 40 days in case 1 to allow for multiple tidal cycles and sufficient particle spreading to occur, and 20 days for case 2 and 3, as net particle transport turned out to be faster.
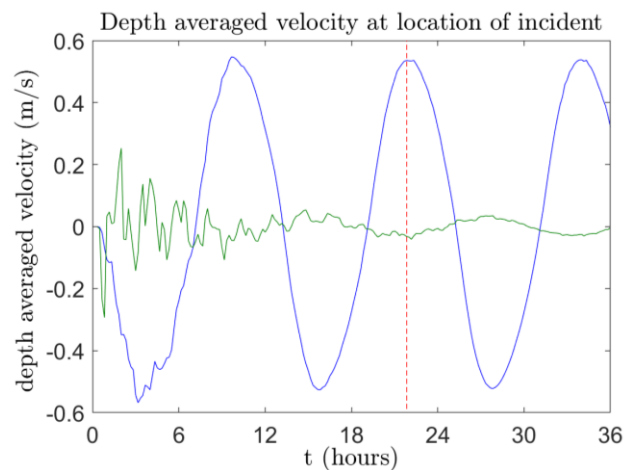

Figure 2.8: Depth-averaged velocity at location incident (test run with tides only). Reference time of model is 00:00 at 01/01/2019 (first time point). Dotted line = 22 hours and corresponds with the flood phase (explained in next section).

Scenarios

In consultation with IMAU supervisors the following scenarios were established.

Case 1) Influence of the tides

In the first scenario, the influence of the tides on particle transport was explored (without the influence of swell and wind). A semi-diurnal tidal frequency of 12 hours was used in the model. This is a major simplification, as the tide consists of many harmonics (explained in section 2.1). However, calculation with all tidal harmonics becomes very complex, hence one constituent was taken as the representative tide. This research focussed on short-term spreading of particles in a relatively small domain with respect to the size of tidal waves and does not include the effect of the spring and neap cycle, so the S2 tidal harmonic with a period of 12 hours was used as the representative constituent. In the simulations, particles were released at four different tidal phases (see figure 2.9). Thus, this scenario included four simulations.
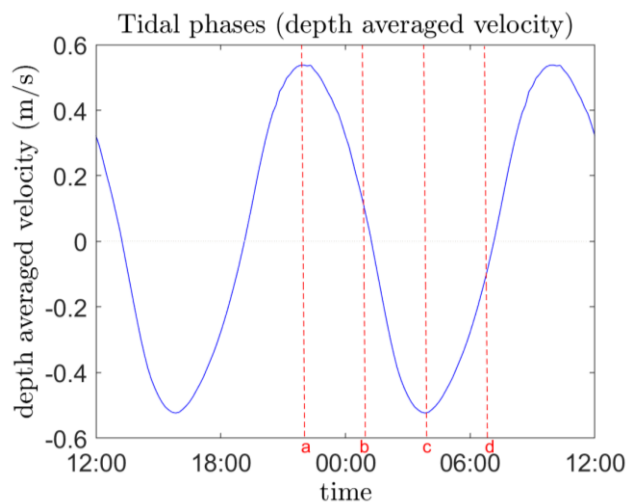

Figure 2.9: Tidal phases indicated on depth averaged velocity (a=flood, b=slack after flood, c=ebb, d=slack after ebb).

Case 2) Influence of swell

In this scenario, waves that are locally generated by wind were not considered. The swell was forced in the model with a direction of 335 degrees (coming from north-west), as swell propagates inwards from the Atlantic/Norwegian Sea (Lavidas & Polinder, 2019). This scenario provides a generalized understanding of the effect of swell, isolated from wind-induced waves to determine their individual effect on particle transport. The release time of particles was also included in this scenario, so four simulations were run in this scenario. A fifth simulation was conducted, which represents a scenario with only swell (no tides). As no particles were released in this simulation, but only the hydrodynamics were computed, this scenario was not presented in the results, but only in the discussion when comparing the residual velocity for different scenarios.

Case 3) Influence of wind

Wind creates a net current in the water surface, thus influencing particle transport (chapter 2.1). Modelling varying wind speeds and directions provides insight into particle transport depending on different wind conditions. In this idealized model, the effect of a coastward wind direction was simulated, as the assumption was made that wind directions away from the coast would result in particles to also move offshore. For this reason, the following wind directions were explored: west (270°), north-west (315°), north (0° or 360°), north-east (45°), east (90°). These directions remained constant during the entire simulation. Similarly, the wind speed during each of these simulations remained constant as well. Two different wind speeds were simulated: a gentle breeze of 4 m/s (3 Beaufort), and a strong wind of 10 m/s (5 Beaufort). These scenarios comprised a total of ten simulations. No variations in particle release times were made in this case as the focus here was on the effect of windspeed and wind direction.

Case 4) MSC Zoe scenario

In the final set of four simulations, more realistic wind conditions over time were analysed to show results that feed back to a more representative situation for particle spreading. As the MSC Zoe event was taken

as an example in this research, the wind conditions from early January 2019 were used in these simulations (see figure 2.10). See appendix II for a table with the values of the wind conditions, retrieved
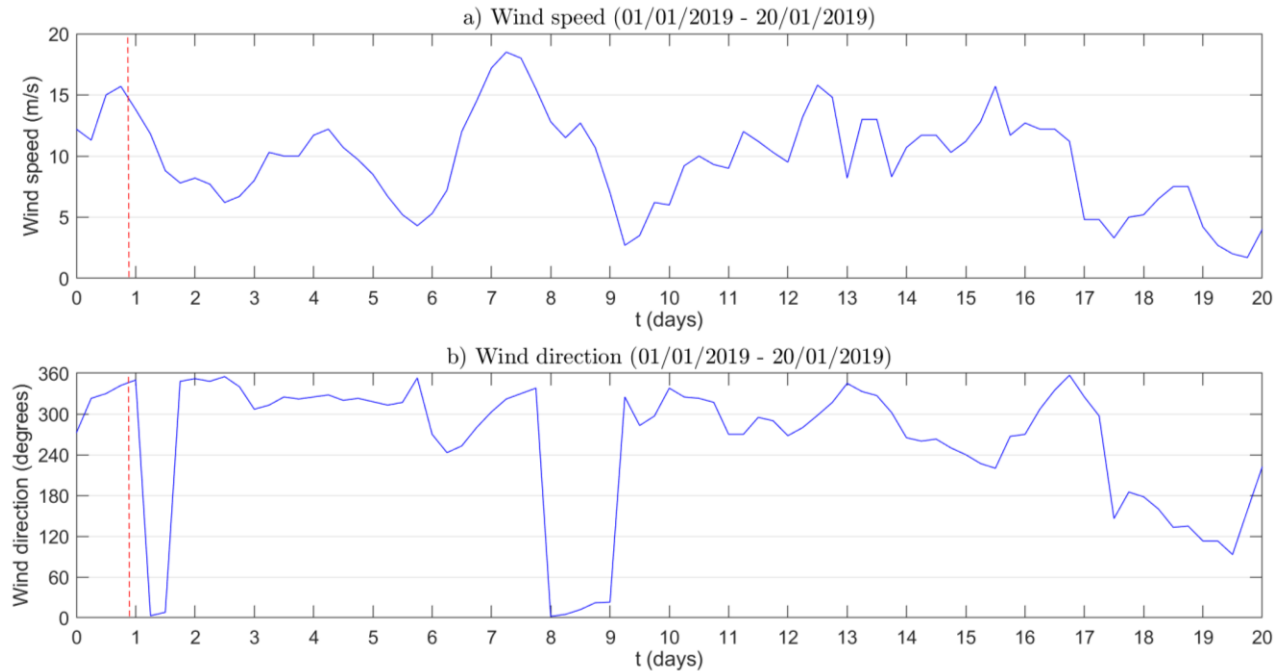

Figure 2.10: Wind speeds (a) and directions (b) over time from 01/01/2019 to 21/01/2019. Red dotted line = time of MSC Zoe container loss. 360 degrees = north (i.e. 0 degrees), 180 degrees = south.

from KNMI (2020). The wind directions and speeds forced in the model changed linearly every six hours. According to an interim investigation report on the loss of containers from the MSC Zoe, the accident occurred at approximately 23:00h on January 1st, when the ebb phase occurred in that location (Dutch Safety Board & Bundesstelle für Seeunfalluntersuchung, 2019; Rijkswaterstaat, 2020). However, this time represents the moment the ship realised they lost cargo. Therefore, there is a possibility that cargo was lost a few hours before, which would correspond with the flood-slack phase. Next to this, the ship lost cargo again later that same night, but at a moment corresponding with the ebb-slack phase. Considering these different times, all three mentioned tidal phases were analysed in this research. To provide the opportunity to compare with the other scenarios, releasing particles during the flood phase in this scenario were also analysed.

Model output

The table (table 2.1) below gives an overview of all run settings. The output of particle spreading (location of each particle) was stored at each computational time step (two minutes), data output at observation points and cross-sections (water level, depth-averaged velocity, discharge) were stored every 10 minutes and data output at all grid points (hydrodynamic and fixed morphologic data) were stored at time intervals of 30 minutes.

Table 2.1: Simulation (run) settings and output.

Run	Included processes			Conditions		Particle release times				Output
	Tides	Swell	Wind	Wind speed	Wind direction	Flood	Flood-slack	Ebb	Ebb-slack	Run time (days)
1	■			-	-	■				40
2	■			-	-		■			40
3	■			-	-			■		40
4	■			-	-				■	40
5	■	■		-	-	■				20
6	■	■		-	-		■			20
7	■	■		-	-			■		20
8	■	■		-	-				■	20
x	■	■		-	-	■			■	20
9	■	■	■	4 m/s	270°	■				20
10	■	■	■	4 m/s	315°	■				20
11	■	■	■	4 m/s	0°	■				20
12	■	■	■	4 m/s	45°	■				20
13	■	■	■	4 m/s	90°	■				20
14	■	■	■	10 m/s	270°	■				20
15	■	■	■	10 m/s	315°	■				20
16	■	■	■	10 m/s	0°	■				20
17	■	■	■	10 m/s	45°	■				20
18	■	■	■	10 m/s	90°	■				20
19	■	■	■	varying	varying	■				20
20	■	■	■	varying	varying		■			20
21	■	■	■	varying	varying			■		20
22	■	■	■	varying	varying				■	20

2.4 Analysis

To analyse the extent that tides, swell and wind influence transport characteristics, these characteristics are given in this section, followed by an explanation and how they were visualized and how they contribute to answering the research questions. This section ends with a description on plotting the residual velocity, which was used to interpret and give possible explanations as to why specific results were received. The following transport characteristics were defined:

- individual particle dispersal;
- mean particle transport;
- particle spreading time;
- beaching quantity.

Individual particle dispersal

Individual particle dispersal refers to the spreading of all modelled particles: the locations of each particle after certain amounts of time have passed in the simulation. This was visualized by plotting a figure showing the **particle locations** in the study area at four to six different times into the simulation (depending on the results). This gives a general overview of how particles disperse within the study area. All snapshots were taken at the same time of day (07:00, corresponding with slack after ebb) to ensure correct comparisons between simulations.

Mean particle transport

This transport characteristic refers to the mean of particles. It provides an indication to the spreading of the bulk of particles and easier comparisons between simulations. To analyse the mean particle transport, three different figures were made. Firstly, the **standard deviation** was plotted as a line-graph, which indicates the range of spreading (in metres) between individual particles relative to the mean. Secondly, a figure was made that shows the **pathway** of the particle mean in the study area. This provides an immediate overview of how the bulk of particles moves in the tidal inlet system. The third figure, a line-graph, separates this mean pathway into the **x- and y-coordinates** of the location of the mean over time.

Particle spreading time

The particle spreading time refers to four variables that were analysed: the time it takes for the first **individual particle** to enter the tidal inlet, below the y-coordinate of 128 km, the time it takes for the **mean of particles** to reach the tidal inlet area (first time to reach past the x-coordinate 28.1 km), the time it takes for the mean of particles to subsequently pass the tidal inlet area (first time to reach past the x-coordinate 31.2 km) (see figure 2.11) and the residence time of the mean of all particles inside the tidal inlet area. The spreading time of the mean was plotted into the previously mentioned graphs of the standard deviation and x- and y-coordinates. Two vertical dotted lines were computed crossing the x-coordinate line at the moments of entering and passing the inlet area. To retrieve the values of the time it takes for first individual particles to enter the tidal inlet (y<128km), a graph that shows the number of particles inside the tidal inlet over time was used. This graph is further explained below, as it is also used to indicate the beaching of particles.
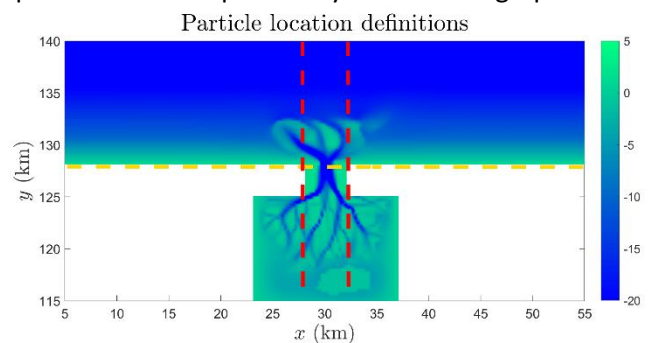

Figure 2.11: X-coordinates of tidal inlet: x=28.1, x=32.1 (red), and y-coordinates of boundary of tidal inlet: y=128.0 (yellow).

<u>Beaching quantity</u>

In analysing the number of particles that end up beached, a difference was made between particles beaching **in the tidal inlet or basin** (y<128km) and particles beaching **along the coastline or on the ebb-tidal delta** (y>128km). For the latter, a line-graph was plotted that shows the number of particles that beach at the coast/ebb-tidal delta over time. This was computed by counting the particles that were 'frozen' above the y-coordinate 128 km (see figure 2.11). A similar graph was plotted to show the number of particles beaching in the tidal inlet over time (as mentioned in the previous section). However, these numbers were computed by counting the particles reaching below the y-coordinate 128 km, therefore also plotting the in- and outflow of particles in the tidal inlet over time.

For all the figures explained above, differences between results indicated the influence of each process on transport characteristics. For the first scenario (tides-only), the extent that release time influences transport characteristics of particles was analysed by comparing the figures between the four tidal phases. Large differences would indicate a high sensitivity to the tidal phase during release time. In analysing results for the second case (tides + swell), the figures were compared with the results of case 1. Considering different tidal phases at release time were also included in this scenario, the result would indicate whether the sensitivity of tidal phases increases or decreases by adding swell. In the third scenario (tides + swell + wind), no difference was made in release time. Figures were compared between the simulations, as well as with results of the previous cases. For these scenarios, the emphasis was on the mean particle transport and spreading time, as that provides an immediate and clear overview of the differences of influence of different wind directions and speeds on particle movement. The last scenario (MSC Zoe), did again include different release times. Figures were compared between these simulations, but the focus was on comparing these results with case three, to see if adding varying (realistic) wind conditions rather than constant wind conditions results in large differences in particle transport. The results of this scenario could indicate whether particle spreading might be supported or limited by the tidal phase if it has the same or opposite direction to wind direction.

Residual velocity

The residual velocity is essential to make sense of the findings in this research and is used as part of the discussion. As mentioned in section 2.1, the residual velocity is the averaged velocity at fixed locations over multiple tidal periods. In the study area of this research, the velocities at for example the moment of a rising tide and the moment of a falling tide were in opposite directions. Although this information showed the flow of water at specific moments, the residual velocity would (partly) explain the net particle movement. Furthermore, the velocity in tidal inlet systems spatially varies greatly, caused by the variety in water depth. This could result in spatial variations of flood- and ebb-dominance (explained in section 2.1). Again, the residual velocity would show the net velocity in the entire domain and was therefore used to analyse net particle movement.

To plot the residual velocities in the computational domain, a period was defined over which the depth-averaged velocities are calculated. This period was for every case the period between 1.5 and 11 simulated days, unless otherwise indicated. At each grid point, a directional arrow was computed to indicate the direction of the residual current and of which the size indicates the force of the current. Per plot, the size of each quiver is determined based on the largest quiver in that scenario. Therefore, it seems that in two different plots (two separate figures), the quivers represent the same force of the velocity, which is not the case. When the residual velocities of two different scenarios were compared, they were plotted in the same figure.

3. Results

This chapter presents the results of all simulations, per case. Firstly, run 1 of case 1, taken as the default case, is extensively described, covering particle spreading and beaching quantity. Secondly, a section on the sensitivity of tidal phases is written, in which results of releasing particles during different tidal phases were presented and compared to the default case. This section ends with a summary on the results of case 1 (tides-only). Thirdly, the results for the simulations of case 2 (influence of swell) are presented in section 3.3, again starting with particle spreading, followed by an analysis on beaching of particles, and finally a summary of case 2. Fourthly, results for case 3 are presented, in which the different wind conditions are compared, again followed by a summary of the case. Finally, the results of the simulations with the MSC Zoe event wind conditions are presented.

3.1 Default case

In this first simulation, in which particles were released at flood (run 1), an immediate movement towards the east was observed. While subsequently oscillating west and eastward, the net movement remained eastward. Particles displaced slower nearest to the coastline. This can be seen in the particle locations after five days: particles nearest to the coast have displaced less than particles that were initially further from the coast (see figure 3.1). After 10 days, about half of the particles was still west of the inlet, while the other half was being dragged into the inlet and pushed back out repeatedly through the channels. Upon 20 days after release, most particles were either beached in the tidal inlet or basin, or moving further east, away from the tidal inlet. Subsequently, particles remained oscillating back and forth, but eventually disappeared from the computational domain within 40 days. It should be noted that figure 3.1 is not a representation of when particles beached, as particles in the same location after 40 days as e.g. after 20 days override the previously plotted particles.
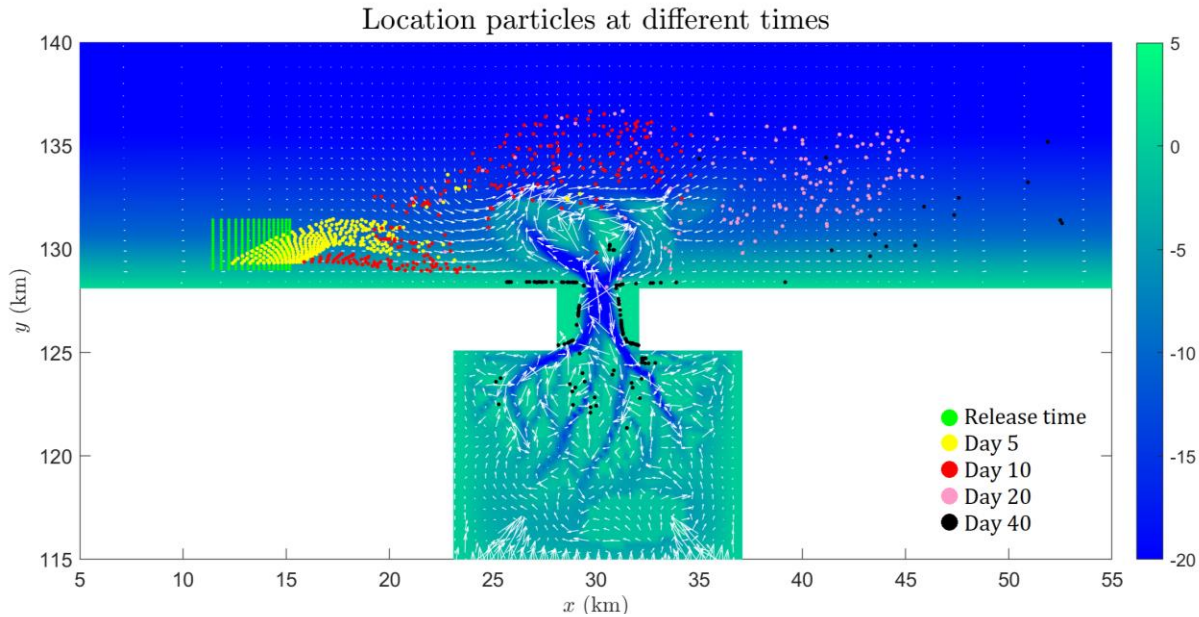

Figure 3.1: Particle locations at different times into the simulation (particles released during flood phase). White arrows represent residual velocities. Colour bar indicates bathymetry.

Whereas the individual particles started entering the tidal inlet after approximately five days, the mean of particles only reached the western boundary x-coordinate of the tidal inlet after eight days (see table 3.1). After entering the inlet area, the mean passed it again three days later, meaning the bulk of particles was in this area for three days.

Table 3.1: Time it takes for first particles to enter the tidal inlet (below y=128), and time it takes for mean of particles to reach and pass x-coordinates of the tidal inlet area, including residence time.

Simulation	Release time	First particles enter inlet	Mean enters inlet area	Mean passes inlet area	Residence time of mean
	tidal phase	days	days	days	days
Run 1	Flood	5.12	8.11	11.12	3.01

Figure 3.2: Standard deviation of mean particle movement and coordinates of mean location of particles over time. Dotted line left = mean of particles reaches western boundary x-coordinate of the tidal inlet. Dotted line right = mean of particles passes east boundary x-coordinate. Thus, the area in between dotted lines gives the time most particles are in or above the tidal inlet.

As particles approached the tidal inlet area, they started to segregate. This is observed in the upward trend of the standard deviation relative to the mean of particles after five days (figure 3.2a). The observed fluctuations in the upward trend of the standard deviation is caused by the tides (rising and falling), so it seems tides influence the segregation of particles to some extent. As particles were pushed in and out of the tidal inlet, analysed here via the mean, north-south oscillations in particle movement were observed next to the net eastward movement. However, after passing the tidal inlet and ebb-tidal delta, the mean particle movement stabilized back to the initially observed movement (east-west oscillations) and hardly any north-south movement was observed anymore (see figure 3.2b).

After reaching the tidal inlet at day 5, particles continuously moved in and back out of the tidal inlet for about 20 days. After this, the number of particles in the tidal inlet stabilized, as no new particles entered the tidal inlet (see figure 3.3a). What stands out, is that all particles that at a certain point reached below y=128km (entering the tidal inlet), seem to end up beached in the tidal inlet or basin. A total of 39% of particles beached in this area (see table 3.2). Next to this, 24% end up beached along the coastline, visualized in figure 3.1 (black dots along the horizontal coastline). Most particles beached on the coastline west of the tidal inlet. After about 25 to 30 days, no new particles beached in this area (see figure 3.3b). This remaining 37% of particles bypassed the tidal inlet area and eventually left the computational domain.

Table 3.2: Particles beaching in the tidal inlet or basin (y<128) and coastline/ebb-tidal delta (y>128).

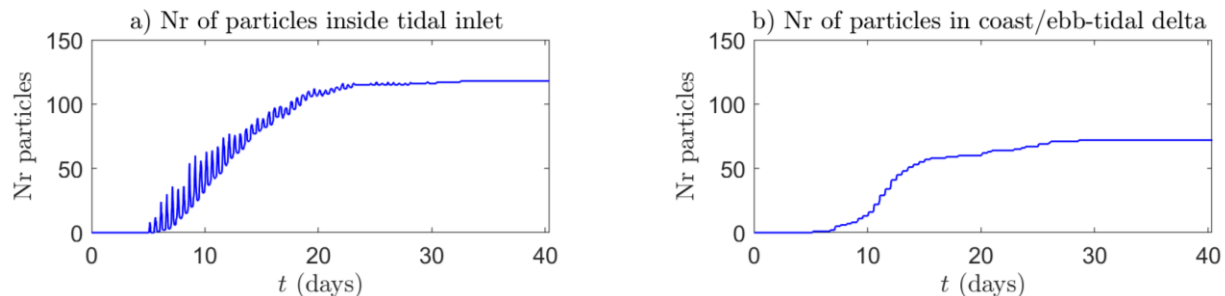| Simulation	Release time	Tidal inlet		Coast/ebb-tidal delta	
	tidal phase	number	%	number	%
Run 1	Flood	118	39	72	24

Figure 3.3: Number of particles in the tidal inlet (y<128) and finally beaching (a), and number of particles beaching at the coast/ebb-tidal delta (b) over time.

3.2 Sensitivity to tidal phase at release time

The sensitivity to the tidal phase at release time influencing the spreading of particles is analysed in this section, starting with particle spreading before continuing with beaching. The four selected release times at different tidal phases were analysed for differences. This section closes with a summary providing a conclusion on the influence of release time on potential particle pathways.
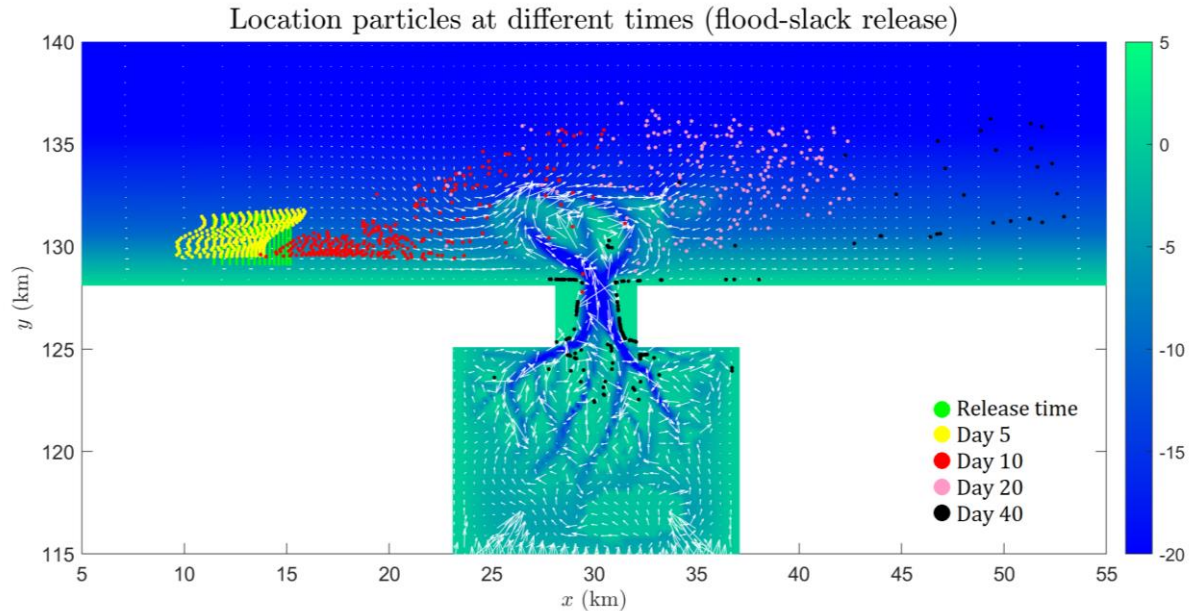
Particle spreading

Figure 3.4: Snapshots of the location of all particles at 5, 10, 20 and 40 days into the simulation, for Run 2 (flood-slack release). Colour bar indicates bathymetry.
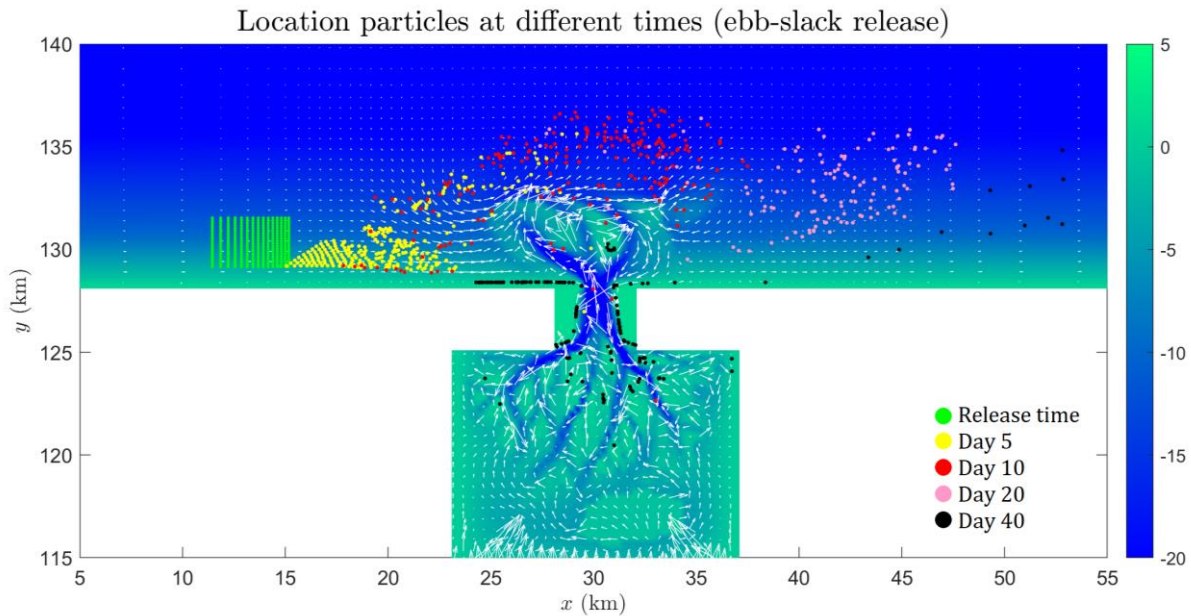

Figure 3.5: Snapshots of the location of all particles at 5, 10, 20 and 40 days into the simulation, for Run 4 (ebb-slack release). Colour bar indicates bathymetry.

Just as for particles released at flood (default case), particles released at other tidal phases generally moved in the direction of the running tide (towards east) and slowly spread. Over time, particles moved towards the tidal inlet, where many of them were pulled into the inlet with the flood phase, after which they were either beached or pushed back out with the ebb phase and continued to move eastward. What stands out is the difference between particles released at flood-slack and particles released at ebb-slack (see figures 3.4 and 3.5). These particles were released in slack-phases (i.e. turn of the tide), meaning they moved with the flood or ebb current for the maximum amount of time, until the tide turned again (6 hours). Particles released at flood-slack, initially moved away from the tidal inlet, causing a delay of arrival at the tidal inlet. After 10 days, most particles were still west of the tidal inlet (figure 3.4). Particles released in the ebb-slack phase, however, were already heavily under the influence of the dynamics in the tidal inlet after 10 days (figure 3.5). The same occurred for particles released in the ebb phase (see supporting figure in appendix I) and flood phase (section 3.1).
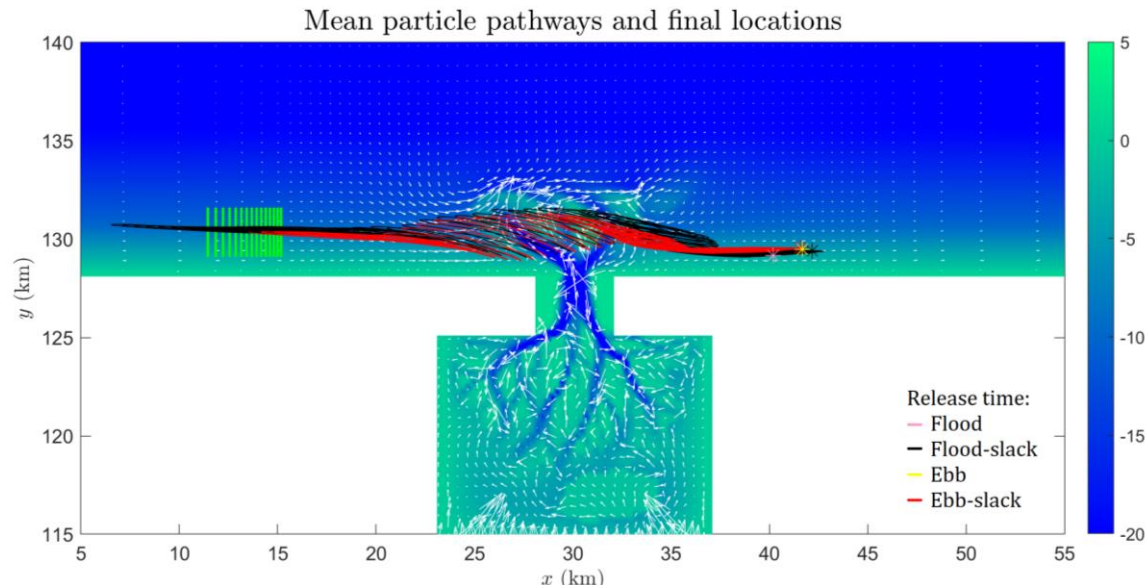

Figure 3.6: Mean pathway of particles for simulation with slack-releases and mean locations at the end of the simulation flood and ebb release times. Green dots represent the release location of all particles. Colour bar indicates bathymetry.

When comparing the mean pathways of particles released in different tidal phases, particles released at flood-slack and ebb-slack have the largest difference among the simulations (see figure 3.6). This was caused by the initial delay of releasing particles at flood-slack compared to the ebb-slack release time. Some supporting graphs for the mean particle pathways are given in appendix I. Although a significant difference was observed initially, after 40 days (end of simulation), the difference in mean final locations was small enough to be considered as negligible. This gives the impression that the tidal phase at release time does not influence particle spreading on the longer term.

Considering the initial differences in the simulations, the time it took for particles to reach the inlet seemed to highly depend on release time (see table 3.3). On average, particles released at flood-slack reached the tidal inlet five days later compared to particles released at ebb-slack. However, the difference in spreading time for particles released at flood and particles released at ebb was insignificant. Although both simulations differed notably from simulations with slack release times, the simulations with flood and ebb releases were very similar. On the contrary, the residence time was similar for all simulations. The means of particles released at flood-slack and ebb passed the inlet area half a day faster than the means of particles released at flood and ebb-slack. Next to this, for all simulations, particles segregated more after passing the inlet (see figure 3.7).

Table 3.3: Time it takes for first particles to enter the tidal inlet (below y=128), and time it takes for mean of particles to reach and pass x-coordinates of the tidal inlet area, including residence time.

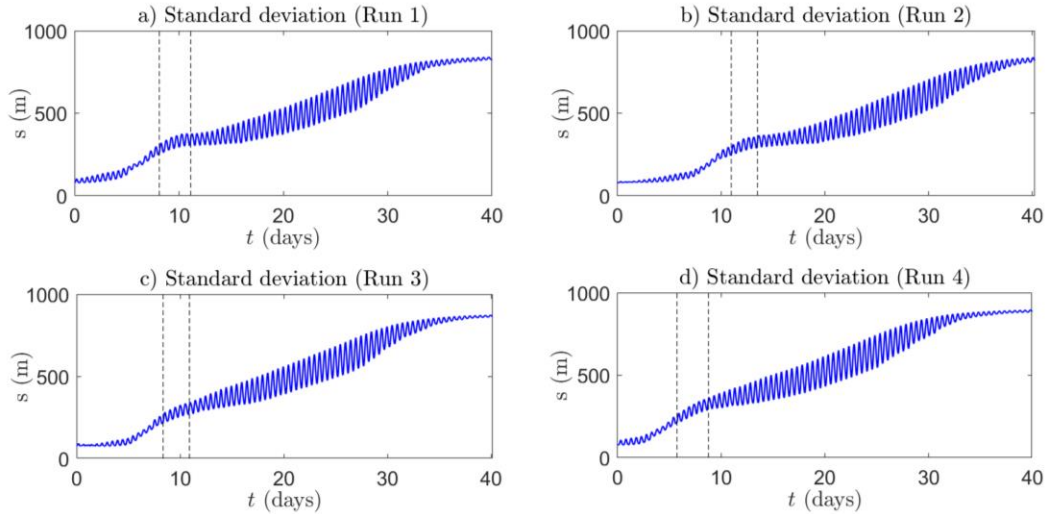| Simulation	Release time	First particles enter inlet	Mean reaches inlet area	Mean passes inlet area	Residence time of mean
	tidal phase	*days*	*days*	*days*	*days*
Run 1	Flood	5.12	8.11	11.12	3.01
Run 2	Flood-slack	7.92	10.97	13.50	2.53
Run 3	Ebb	5.38	8.34	10.88	2.54
Run 4	Ebb-slack	2.76	5.74	8.76	3.02

Figure 3.7: Standard deviation of mean particle movement over time for release times a) flood, b) flood-slack, c) ebb, d) ebb-slack. Dotted lines represent the times the mean of particles reaches the western boundary x-coordinate of the tidal inlet (left) and passes the east boundary x-coordinate (right). Thus, the distance between dotted lines is the time most particles are in or above the tidal inlet.

Beaching

For all simulations, particles oscillated in and out of the tidal inlet with the current of the tidal phases. Over time, an increasing number of particles remained beached in the inlet, but after about 20 to 25 days, this number stabilized (see figure 3.8a). Just as for the time it took for the mean of particles to reach the tidal inlet area, simulations with flood and ebb release also showed a similar percentage of particles that beached in the tidal inlet or basin (see table 3.4). For particles released in the flood-slack phase, the number of particles that beached in the tidal inlet or basin was highest (43%), whereas this was significantly less for particles released in the ebb-slack phase (31%). Remarkably, this seemed to be opposite for particles that beached along the coastline and ebb-tidal delta, in which the simulation with ebb-slack release showed the highest beaching quantity (27%) and the simulation with flood-slack release the lowest (13%) (see figure 3.8). Although for the two runs most beaching occurred in opposite places, it does add up to similar totals (see table 3.4).

Table 3.4: Particles beaching in the tidal inlet or basin (y<128) and coastline/ebb-tidal delta (y>128), and total percentage

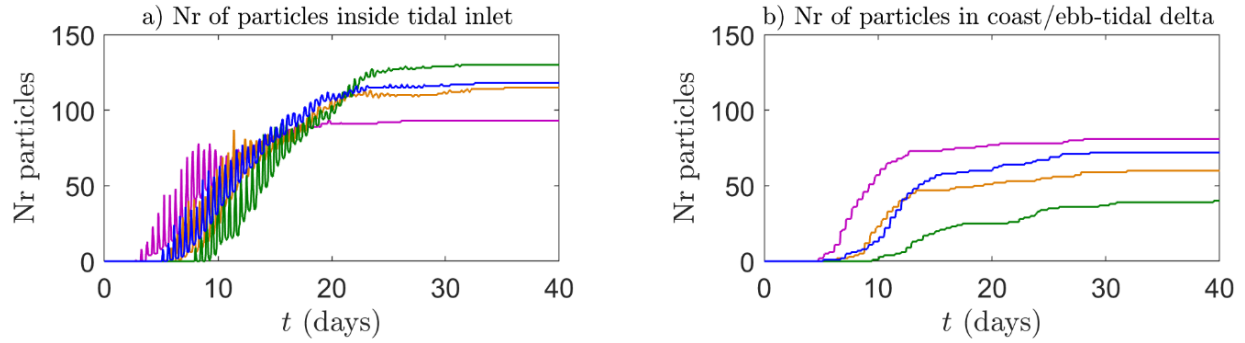| Simulation	Release time	Tidal inlet		Coast/ebb-tidal delta		Total	
	tidal phase	*number*	*%*	*number*	*%*	*number*	*%*
Run 1	Flood	118	39	72	24	190	63
Run 2	Flood-slack	130	43	40	13	170	56
Run 3	Ebb	115	38	60	20	175	58
Run 4	Ebb-slack	93	31	81	27	175	58

Figure 3.8: Difference in number of particles in inlet over time (a) and beaching on the coast and ebb-tidal delta over time (b) between simulations with release times: flood (blue), flood-slack (green), ebb (orange) and ebb-slack (purple).

Summary

The largest differences are seen between particles released in the flood-slack and ebb-slack phase, as particles are being transported with the flood or ebb current in one direction for the maximum period (6 hours). As such, the first particles released at flood-slack, entered the tidal inlet five days later than particles released at ebb-slack. This delay is also seen in the time it took for the mean to enter the tidal inlet area. However, residence times in the area are similar for all simulations.

The percentage of particles that beached in the tidal inlet or basin was highest for the simulation with flood-slack release and lowest for the simulation with ebb-slack release, whereas the opposite was found for the percentages of particles that beached at the coastline and ebb-tidal delta. The total numbers of particles that beached were very similar for all simulations, even though the simulation with flood release exceeded the other simulations to a small extent in total percentage of beached particles.

3.3 Influence of swell on transport of plastics

This section presents results of simulations, in which the water motion was driven by both tides and swell. It starts with particle spreading before continuing with beaching of particles. The four selected release times at different tidal phases were analysed for differences. This section closes with a summary providing a conclusion on the influence of swell on transport characteristics.
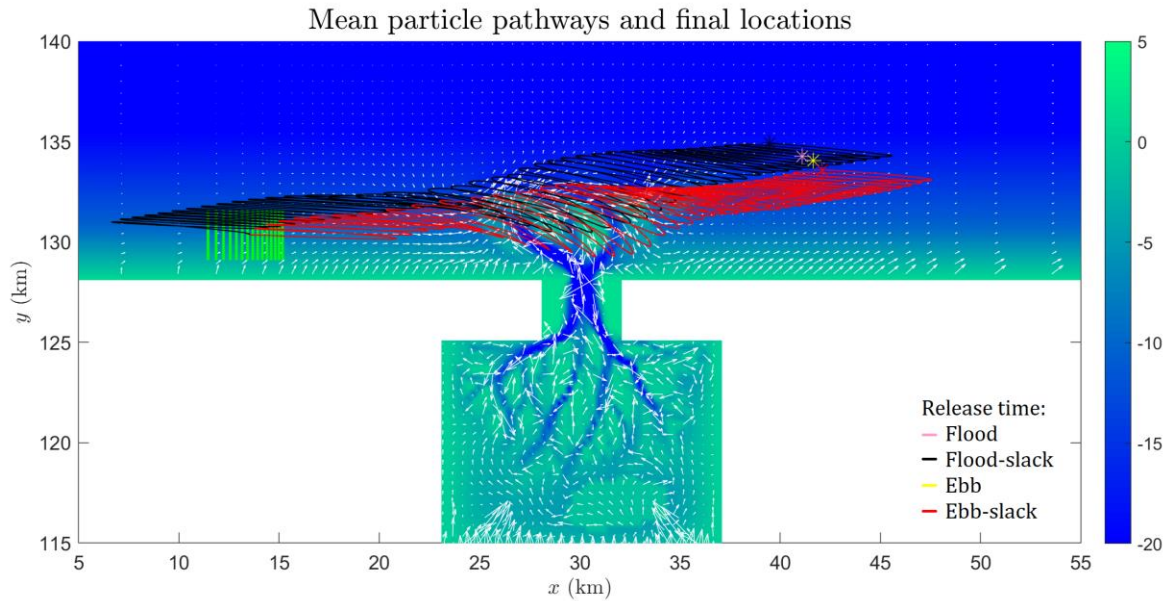
Particle spreading

Figure 3.9: Mean particle pathways of flood-slack (black) and ebb-slack release (red), and mean locations of flood (m) and ebb release (yellow). Colour bar indicates bathymetry.
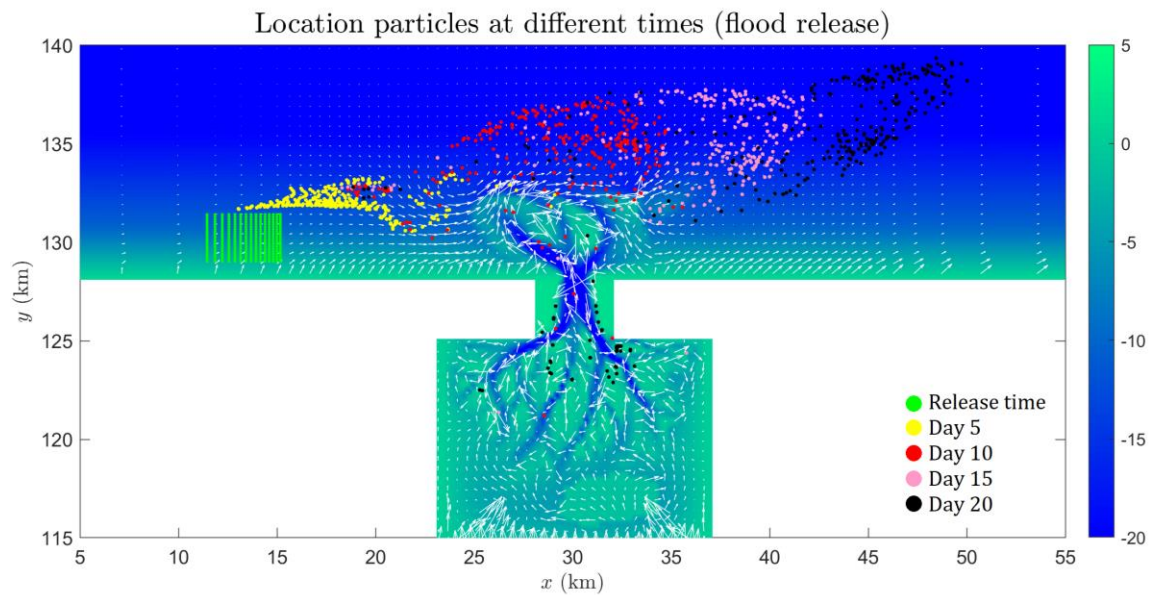

Figure 3.10: Locations of particles at different times into the simulation, particles released during flood phase. Colour bar indicates bathymetry.

While particle movement in the tides-only scenario was initially mainly east-west, including the process of swell increased north-south movement significantly (see figure 3.9). Along the coastline, particles were initially pushed away from the coast by what seems to be an offshore residual current. As a result, the particles entered the tidal inlet area further north compared to particles in the scenario tides-only and therefore entered the tidal inlet mainly through the channels. Some particles passed the ebb-tidal delta after moving through the channel once, but most particles entered the tidal inlet multiple times. Another difference with the tides-only scenario is that by adding swell, particles continued moving towards the north, even after passing the tidal inlet area (see figure 3.10).

The times the first particles entered the tidal inlet for tides + swell were very similar to those of the tides-only scenario, yet here the mean entered the inlet area sooner. The time it took for the means of particles in all four simulations to reach the inlet area did mainly show the same order compared to tides-only. The mean of particles released in the flood-slack phase reached the inlet area last, while the mean of particles released in the ebb-slack phase reached the inlet area first out of all simulations. Between the flood release and ebb release simulations, this only differs marginally (see table 3.5). Residence times were nearly identical for each simulation, except for a half day difference with the ebb release. Compared to the tides-only scenario, the residence time was about a day shorter for the simulations including swell (table 3.5). Thus, it seems swell influences the spreading time of particles to some extent. The standard deviation followed the same trend as that found in the tides-only scenario. After particles reached the tidal inlet, the standard deviation increased (see figure 3.11).

Table 3.5: Time it takes for first particles to enter the tidal inlet (below y=128), and time it takes for mean of particles to reach and pass x-coordinates of the tidal inlet area, including residence time.

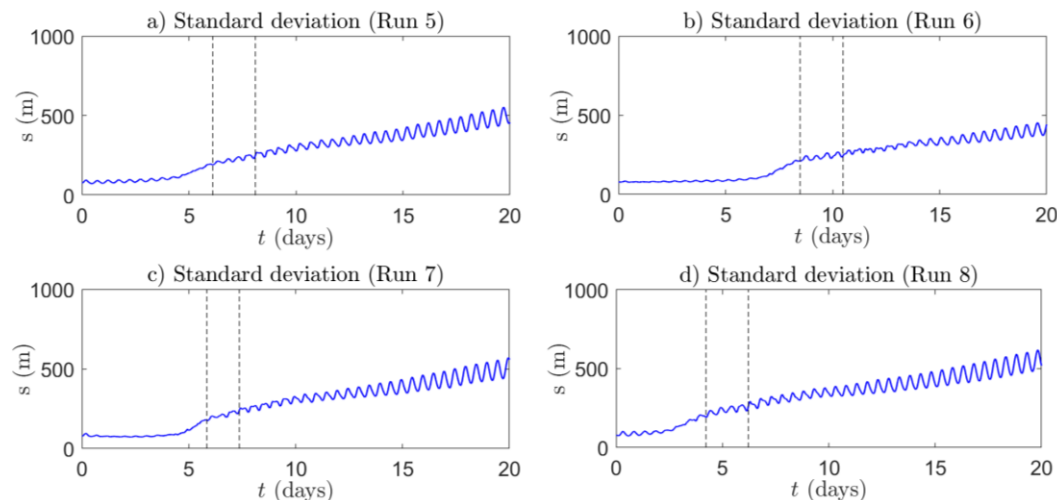| Simulation	Release time	First particles entering inlet	Mean reaches inlet area	Mean passes inlet area	Residence time of mean
	tidal phase	*days*	*days*	*days*	*days*
Run 5	Flood	5.06	6.12	8.11	1.99
Run 6	Flood-slack	7.44	8.48	10.49	2.01
Run 7	Ebb	4.87	5.84	7.36	1.52
Run 8	Ebb-slack	2.70	4.23	6.22	1.99

Figure 3.11: Standard deviation of mean particle movement over time for release times a) flood, b) flood-slack, c) ebb, d) ebb-slack. Dotted lines represent the times the mean of particles reaches the western boundary x-coordinate of the tidal inlet (left) and passes the east boundary x-coordinate (right). Thus, the distance between dotted lines is the time most particles are in or above the tidal inlet.

Beaching

As mention before, particles continuously moved more towards the north due to swell compared to the scenario tides-only. They entered the ebb-tidal delta more north and particles entered the tidal inlet mainly via the channels or even bypassed the tidal inlet. This resulted in less particles entering the tidal inlet (see figure 3.12) compared to the tides-only scenario. Next to this, as particles now moved within these deeper channels, less particles ended up beached, especially along the coastlines. For all four simulations, the number of particles that beached in the tidal inlet or basin and at the coastline/ebb-tidal delta was significantly less than for the tides-only scenario. Between the simulations in this scenario (tides + swell) there were only minor variations, with the most beaching for particles released at ebb-slack (19.67%), and the least for particles released at flood-slack (12.33%) (table 3.6).

Table 3.6: Particles beaching in the tidal inlet or basin (y<128) and coastline/ebb-tidal delta (y>128), and total percentage.

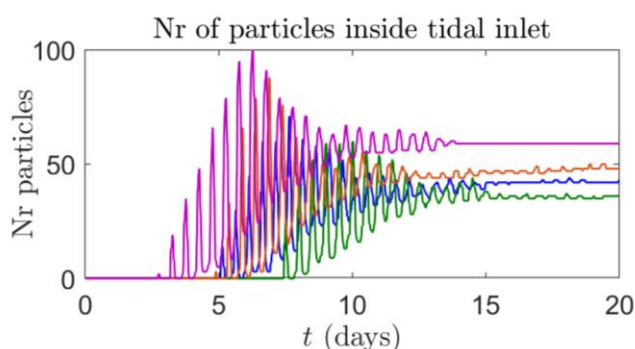| Simulation	Release time	Tidal inlet		Coast/ebb-tidal delta		Total	
	tidal phase	*number*	*%*	*number*	*%*	*number*	*%*
Run 5	Flood	43	14.33	2	0.67	45	15
Run 6	Flood-slack	36	12	1	0.33	37	12.33
Run 7	Ebb	48	16	4	1.33	52	17.33
Run 8	Ebb-slack	59	19.67	0	0	59	19.67

Figure 3.12: Difference between simulations in number of particles in inlet over time, per release time: flood (blue), flood-slack (green), ebb (orange), ebb-slack (purple).

Summary

Swell mainly affects particle pathways by adding an offshore movement. Particles entered the tidal inlet area within less time than in the tides-only scenario and residence times of the means were slightly shorter. Due to the northward movement, particles entered the tidal inlet mainly via the ebb-tidal delta and its channels and considerably less beaching occurred. Hardly any particles beached on the coastline and the ebb-tidal delta (0 to 1.33%) and 12 to 20% of particles beached in the tidal inlet.

3.4 Influence of wind on transport of plastics

In this section, the influence of wind direction and wind speed on transport characteristics is presented. First, particle spreading is described in which comparisons are made between wind directions and wind speeds. Secondly, beaching of particles is described, again comparing wind directions and speeds. In these scenarios, no difference is made in tidal phases. All results presented here are from releasing particles during the flood phase.
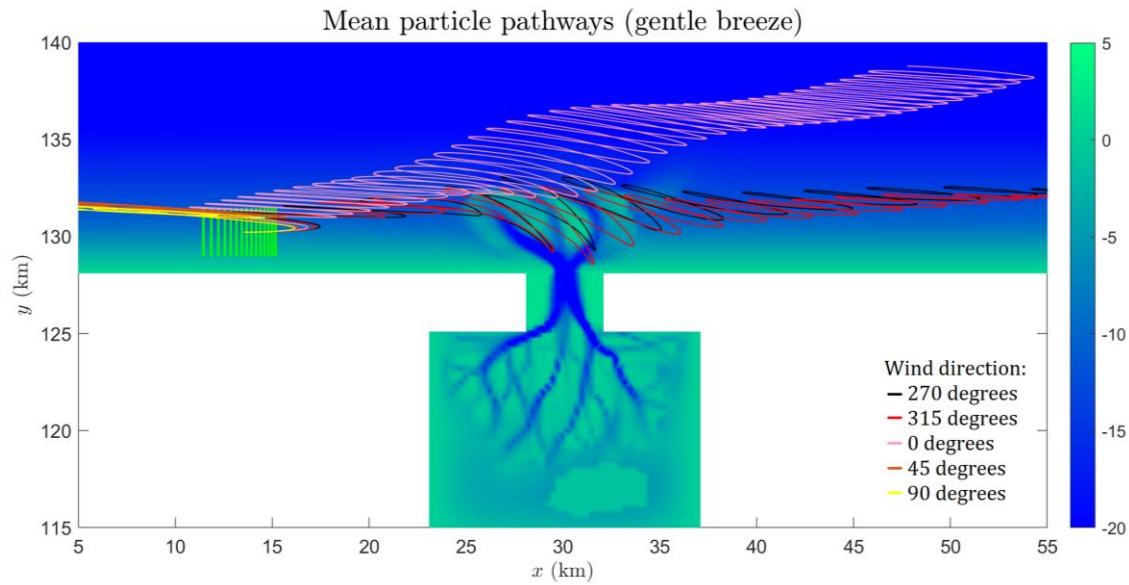
Particle spreading

Figure 3.13: Mean particle pathways of simulations with five different wind directions with gentle breeze (4 m/s). Green dots represent release location. Colour bar indicates bathymetry.
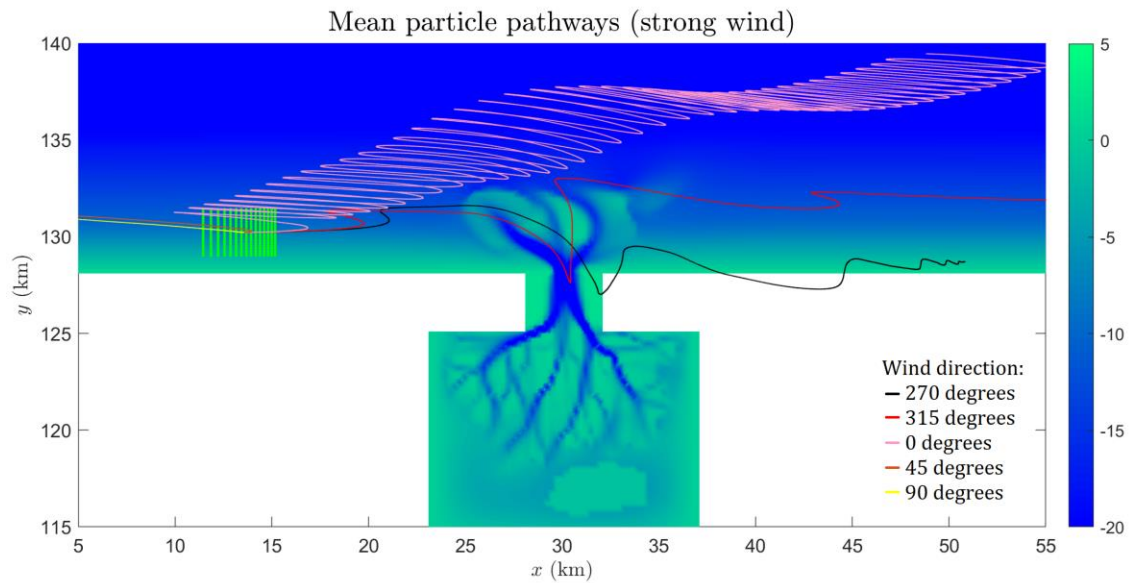

Figure 3.14: Mean particle pathways of simulations with five different wind directions with strong wind (10 m/s). Green dots represent release location. Colour bar indicates bathymetry.

Compared to the scenarios without wind (sections 3.1 – 3.3), adding wind conditions showed a much faster displacement of particles. First of all, for both the gentle breeze scenarios and the strong wind scenarios, wind directions of 45 and 90 degrees (wind from north-east and east respectively) resulted in a net movement towards the west, pushing particles westward, rather than the so far observed eastward movement (see figures 3.13 and 3.14). This indicates wind had a large influence on the direction of particle spreading. Wind directions of 270 and 315 degrees (wind from west and north-west respectively) resulted in a fast net movement of particles towards east. Whereas the effect of the tides was still observed with a gentle breeze, this oscillating back and forth seemed to almost disappear entirely with a strong wind, as the speed of particle transport was considerably faster.

One result that stands out is the particle motion for the scenario with a wind direction coming from the north (0°). In this scenario, for both gentle breeze and strong wind, the particles displaced much slower compared to the other wind directions and the spreading time was more comparable to the scenarios without wind conditions (see table 3.7). Considering wind from the north (0°) is perpendicular to the coast, it seemed particles were not pushed along either sides of the coastline. Therefore, the tides seemed to have a larger influence on particle transport in this scenario. The difference was also seen in the standard deviation of the positions of all particles (see figure 3.15). For the simulation with a gentle breeze, the mean under the influence of wind direction from north behaved similar to that of the scenario 'tides + swell' (section 3.3). After reaching the tidal inlet, particles dispersed to some extent, but remained within the computational domain much longer compared to particles under the influence of wind from the west, in which the line stabilized after about seven days. For the scenario with a strong wind, particles were pushed out of the domain even faster by wind from the west (within approximately two days).

Table 3.7: Time it takes for first particles to enter the tidal inlet (below y=128), and time it takes for mean of particles to reach and pass x-coordinates of the tidal inlet area, including residence time.

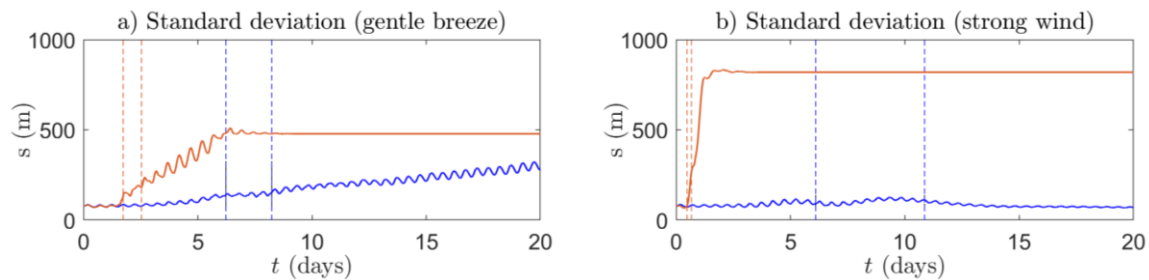| Simulation	Wind direction	Wind speed	First particles enter inlet	Mean reaches inlet area	Mean passes inlet area	Residence time of mean
	degrees	m/s	days	days	days	days
Run 9	270	4	1.60	1.58	2.53	0.95
Run 14	270	10	0.51	0.48	0.64	0.16
Run 10	315	4	2.06	2.07	3.06	0.99
Run 15	315	10	0.56	0.54	0.94	0.40
Run 11	0	4	**5.08**	**5.62**	**7.62**	2.00
Run 16	0	10	-	**5.63**	**7.65**	2.02
Run 12	45	4	-	-	-	-
Run 17	45	10	-	-	-	-
Run 13	90	4	-	-	-	-
Run 18	90	10	-	-	-	-

Figure 3.15: Difference between standard deviations of gentle breeze (a) and strong wind (b), for scenarios with wind from north (blue) and wind from west (orange). The standard deviation for the scenarios with wind from 315 degrees is given in appendix I.

Beaching

For the scenarios with a wind direction towards the west, naturally no particles ended up in the tidal inlet or on the ebb-tidal delta. Here, all particles left the computational domain within four to five days for gentle breeze and one day for strong wind. For the other scenarios, in which particles did move towards the tidal inlet, the number of particles entering the tidal inlet and beaching showed differences (see figure 3.16). A gentle breeze from the north-west (315°) pushed a larger number of particles into the tidal inlet, when compared to a gentle breeze from the west (270°). Next to this, the number of particles that also beached in the inlet or basin was for wind from the north-west doubled, compared to that in the case of wind from west (12.67% and 6.33% respectively) (see table 3.8). Remarkably, these results were quite different when a strong wind was forced in the model. Here, the number of particles that was pushed in (and out of) the inlet over time did not differ much between the two wind directions. But, the number of particles that also beached in the inlet or basin was significantly higher for wind from the west (28%), rather than wind from north-west (1.67%) (see table 3.8).

Again, the results for the scenarios with wind from the north (0°) were noteworthy. It was previously mentioned that these scenarios were most similar to the scenario of 'tides + swell' (no wind). However, the number of particles beaching was very different. Whereas 14.33% of particles beached in the inlet or basin for 'tides + swell', this percentage was significantly lower (2.33% and 0%) when wind from the north was forced in the model (see table 3.8). So, it seemed that wind from the north had a larger influence on beaching than on particle spreading.

Table 3.8: Particles beaching in the tidal inlet or basin (y<128) and coastline/ebb-tidal delta (y>128), and total percentage.

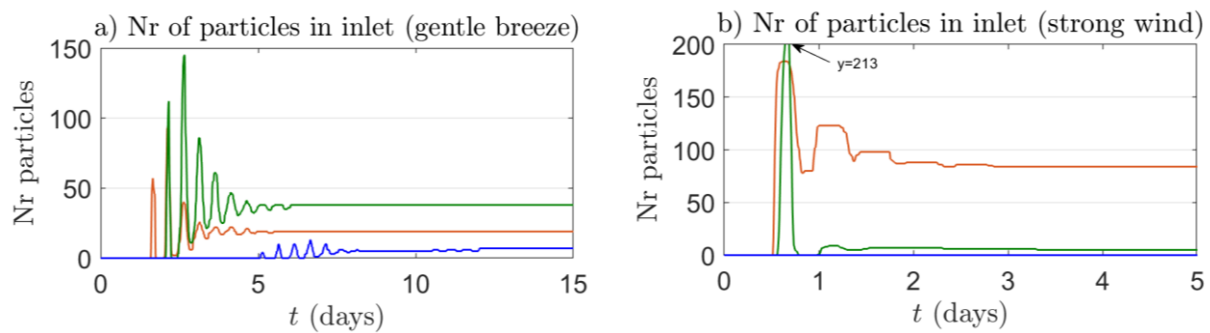| Simulation	Wind direction	Wind speed	Tidal inlet		Coast/ebb-tidal delta		Total
	degrees	*m/s*	*number*	*%*	*number*	*%*	*%*
Run 9	270	4	19	6.33	3	1	7.33
Run 14	270	10	84	28	4	1.3	29.30
Run 10	315	4	38	12.67	7	2.33	15
Run 15	315	10	5	1.67	5	1.67	3.33
Run 11	0	4	7	2.33	0	0	2.33
Run 16	0	10	0	0	0	0	0
Run 12	45	4	0	0	0	0	0
Run 17	45	10	0	0	0	0	0
Run 13	90	4	0	0	0	0	0
Run 18	90	10	0	0	0	0	0

Figure 3.16: Difference in number of particles in inlet, of gentle breeze (a) and strong wind (b), between scenarios with wind from north (blue), wind from north-west (green) and wind from west (orange).

Summary

The influence of wind on particle transport was mainly observed in the direction and speed of particle transport. With a stronger wind speed, particles also moved faster and less influence of the tidal phases was observed. Next to this, in general particles moved in the same direction as the wind direction. However, a wind direction from the north, perpendicular to the coast, showed remarkable results. The movement was more comparable to the scenarios without wind and rather than moving towards the coast, particles showed a counterintuitive movement offshore. This contributed to significantly less particles beaching compared to the other scenarios. The difference between a gentle breeze and a strong wind was remarkably small in the scenario with wind from north, including for beaching, whereas this showed large differences for wind from the west and north-west.

3.5 Influence of time-varying wind conditions (MSC Zoe based) on transport of plastics

This section presents the results for the scenario with more realistic wind conditions. Starting with a description of the particle spreading, including comparisons with previous scenarios, followed by a description of beaching, also comparing to previous scenarios. As mentioned in section 2.3, four release times, with differing tidal phases, are analysed in this scenario.
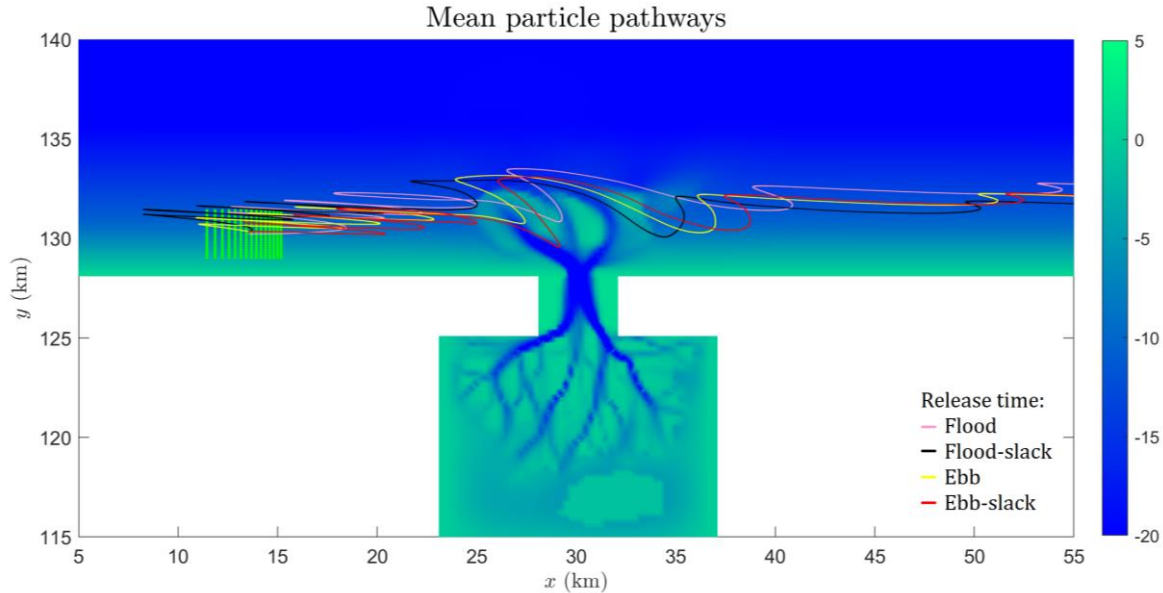
Particle spreading

Figure 3.17: Mean particle pathways for the four runs in this MSC Zoe wind conditions scenario. Green dots represent release location. Colour bar indicates bathymetry.
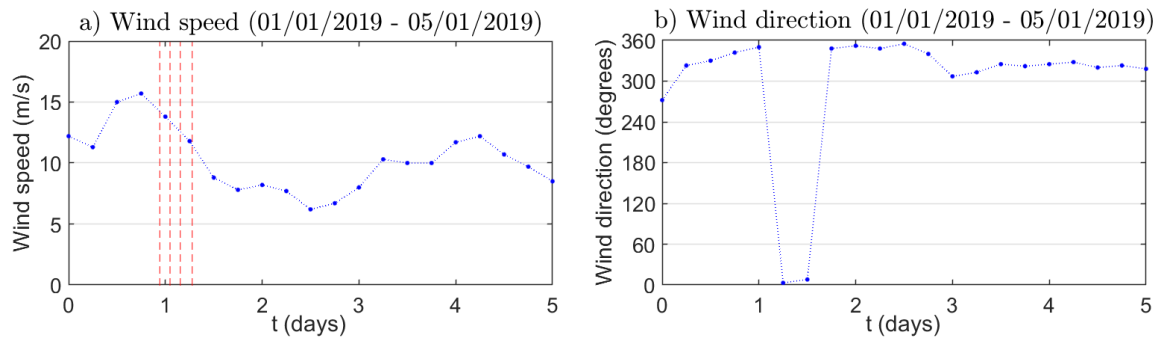

Figure 3.18: Wind speed (a) and direction (b) from January 1st to January 5th. The blue dots mark data points connected linearly. The red dotted lines indicate the release times per simulation in chronological order. It should be noted that the wind direction changes linearly from e.g. 350 to 10 degrees in the model by taking 360 as the intermediate step. The line-graph here (b) does not reckon for this and therefore shows a slight distorted picture.

Even though a varying wind speed and direction was forced in these simulations, the net movement of particles was towards the east, just as with most previous scenarios (see figure 3.17). The means of particles seemed to show an oscillating movement with the tides before having reached the tidal inlet area after approximately two days (see table 3.9). The mean position showed a slight tendency to be transported into the tidal inlet via the channels, yet it bypassed the inlet in a matter of hours. After five days into the simulation, the mean had left the computational domain. This behaviour is similar to that in the scenarios with a strong wind from north-west (315°). This makes sense, considering that the wind came from northern directions with a speed of approximately 10 m/s (strong wind) over the first five days

in this scenario. Different from this scenario, however, was the time it took for the mean to reach the inlet area. For the scenario with a strong wind from 315 degrees, the mean reached the inlet area in half a day, whereas here the mean reached the inlet area after approximately two days, even though the wind speed was on average similar. The difference was that the wind direction in this MSC Zoe scenario was more from the north and even leaned towards north-north-east at the time particles were released (see figure 3.18). As was shown in section 3.4, wind from the north (0°) did not push particles east or west. Thus, this would explain why the mean particle pathways followed the oscillating movement of the tides before reaching the tidal inlet. On January 3rd, wind direction turned to approximately 320 degrees. On the same day, the mean position of all particles had reached the tidal inlet. With the change in wind direction, particle movement suddenly accelerated, as was observed in the very short time it took for particles to pass the inlet area after reaching it (see table 3.9).

Table 3.9: Time it takes for first particles to enter the tidal inlet (below y=128), and time it takes for mean of particles to reach and pass x-coordinates of the tidal inlet area, including residence time

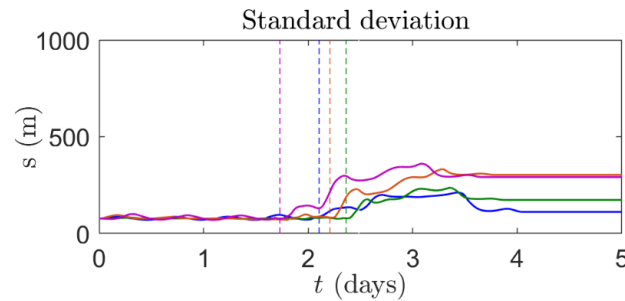| Simulation	Release time	First particles enter inlet	Mean reaches inlet area	Mean passes inlet area	Residence time of mean
	tidal phase	days	days	days	days
Run 19	Flood	2.58	2.10	2.49	0.39
Run 20	Flood-slack	2.47	2.36	2.43	0.07
Run 21	Ebb	2.31	2.21	2.27	0.06
Run 22	Ebb-slack	1.75	1.73	2.11	0.38

Figure 3.19: Standard deviations for simulations in MSC Zoe scenario per release time: flood (blue), flood-slack (green), ebb (orange), ebb-slack (purple). Dotted lines indicate entering of tidal inlet area. Reference time of x-axis is the release time of particles (t=0).

The standard deviation showed that particles segregated less compared to previous scenarios (see figure 3.19). Reaching the tidal inlet area did increase the standard deviation to some extent, but this was minimal compared to the scenarios without wind. It was also seen that, just as with a constant strong wind, particle dispersal was much less influenced by tidal phase, as they were oscillating to a lesser extent. The mean position of particles released in the ebb-slack phase reached the inlet area after 1.73 days (relative to its release time), whereas the mean of particles released during the flood-slack phase reached the inlet area last of all simulations (see table 3.9). This difference between ebb-slack and flood-slack was also seen in the scenarios without wind. Taking a closer look at the time it took for particles (and the mean) to enter the tidal inlet area, the same initial difference was observed, as explained in section 3.2. Particles released during slack after flood, first moved with the ebb current towards the west for the maximum amount of time until the tide turned again (6 hours). Particles released during the ebb-slack phase however, moved towards the east (towards the tidal inlet) with the flood current for the maximum amount of time until the tide turned again. This explains the initial difference, clearly seen at January 2nd at 00:00 (see figure 3.20 and figure 3.21).
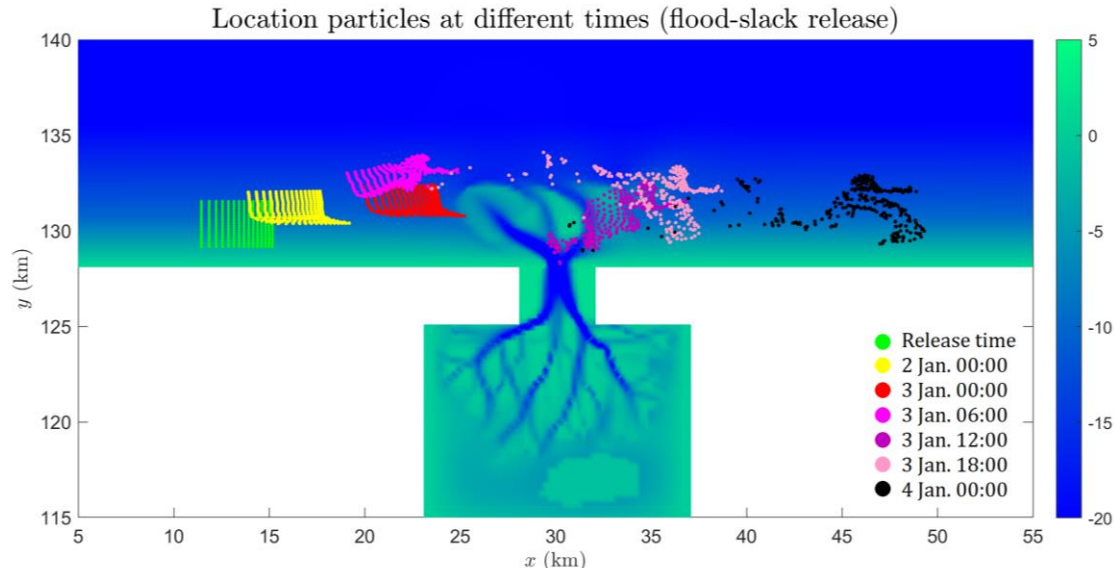
Figure 3.20: Locations of particles at different times into the simulation, for flood-slack release. Colour bar indicates bathymetry.
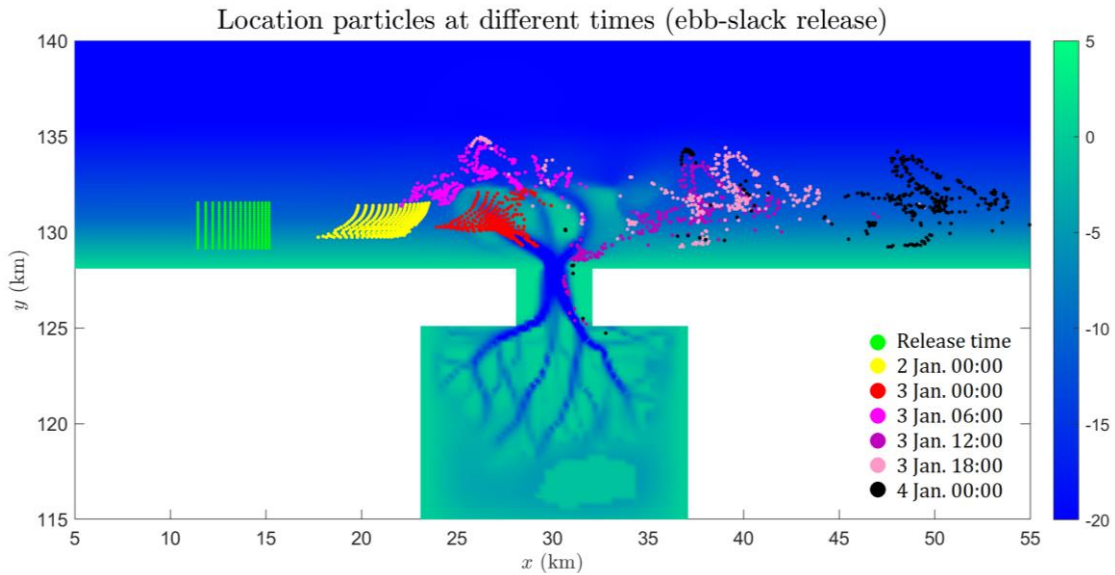

Figure 3.21: Locations of particles at different times into the simulation, for ebb-slack release. Colour bar indicates bathymetry.

Beaching

Considering the observed transport of particles was a similar pattern to the concept of bypassing, as particles were swept passed the inlet after slightly entering one of the channels, very few particles beached (see table 3.10).

Table 3.10: particles beaching in the tidal inlet or basin (y<128), and coastline/ebb-tidal delta (y>128), and total percentage.

Simulation	Release time	Tidal inlet		Coast/ebb-tidal delta		Total
	tidal phase	*number*	*%*	*number*	*%*	*%*
Run 19	Flood	0	0	1	0.33	0.33
Run 20	Flood-slack	0	0	3	1	1
Run 21	Ebb	4	1.33	6	2	3.33
Run 22	Ebb-slack	3	1	6	2	3

Summary

Just as with constant wind conditions, particle transport seemed to depend on the wind direction especially for the direction to which they displaced. The wind speed seemed to highly influence the time it took particles to reach certain points in the domain. Although the difference between the defined gentle breeze and strong wind did not seem to be large, the difference with scenarios excluding wind was significant. In this scenario, net movement of particles was towards the east, which was caused by the wind direction being mainly in the same direction. Although wind started out from an almost northern direction when particles were released, the moment particles reached the tidal inlet, wind direction changed to a direction from north-west, and started speeding up. This resulted in a transport pattern similar to the concept of bypassing and particles suddenly passing the inlet area within one day. This caused a very low number of particles to end up being beached. Between the four different release times, hardly any difference was seen. This probably has to do with wind starting out from the north, not resulting in any initial sudden movements.

4. Discussion

The discussion starts with a summary of the results, with notable findings highlighted in table 4.1. This is followed by a discussion on explaining the results, mainly by discussing what caused the differences in residual velocities and therefore in particle transport. During this, results of this research are simultaneously compared with findings of similar research. The next section is a reflection on model limitations and the chapter ends with a discussion on the relevance to practice.

Table 4.1: Summarized table of results.

Scenario	Release time/ conditions		Spreading time				Beaching quantity		
			First particle enters inlet	Mean enters inlet area	Mean passes inlet area	Residence time	Tidal inlet	Coast/ ebb-tidal delta	Total
	tidal phase		*days*	*days*	*days*	*days*	*%*	*%*	*%*
Tides	Flood		5.12	8.11	11.12	3.01	39	24	**63**
	Flood-slack		7.92	10.97	13.50	2.53	**43**	**13**	**56**
	Ebb		5.38	8.34	10.88	2.54	38	20	58
	Ebb-slack		2.76	5.74	8.76	3.02	**31**	**27**	**58**
Swell	Flood		5.06	6.12	8.11	1.99	14.33	**0.67**	15
	Flood-slack		7.44	**8.48**	10.49	2.01	**12**	**0.33**	12.33
	Ebb		4.87	5.84	7.36	1.52	16	**1.33**	17.33
	Ebb-slack		2.70	**4.23**	6.22	1.99	**19.67**	**0**	19.67
	direction	*speed*							
Wind	270	4 m/s	1.60	1.58	2.53	0.95	6.33	1	7.33
	270	10 m/s	0.51	0.48	0.64	0.16	**28**	1.3	29.3
	315	4 m/s	2.06	2.07	3.06	0.99	12.67	2.33	15
	315	10 m/s	0.56	0.54	0.94	0.40	1.67	1.67	3.33
	0	4 m/s	**5.08**	**5.62**	**7.62**	2.00	2.33	0	2.33
	0	10 m/s	-	**5.63**	**7.65**	2.02	**0**	**0**	**0**
	45	4 m/s	-	-	-	-	**0**	**0**	**0**
	45	10 m/s	-	-	-	-	**0**	**0**	**0**
	90	4 m/s	-	-	-	-	**0**	**0**	**0**
	90	10 m/s	-	-	-	-	**0**	**0**	**0**
	tidal phase								
MSC Zoe	Flood		2.58	2.10	2.49	0.39	0	0.33	0.33
	Flood-slack		2.47	2.36	2.43	0.07	0	1	1
	Ebb		2.31	2.21	2.27	0.06	1.33	2	3.33
	Ebb-slack		1.75	1.73	2.11	0.38	1	2	3

In the tides-only scenario, most beaching occurred for the scenario with a flood release. The beaching quantity per location depended on release time, with a relatively high and low quantity in the tidal inlet for the simulations with flood-slack and ebb-slack releases respectively. For beaching on the coast and ebb-tidal delta the opposite was the case, yet this evened out the totals to very similar percentages of 56 and 58%.

In the tides + swell scenario, the mean of particles released at flood-slack reached the tidal inlet last of the four simulations, and beaching quantity in the tidal inlet was lowest. Conversely, for the simulation with an ebb-slack release the mean of particles reached the tidal inlet after the least amount of time, and beaching quantity in the tidal inlet was highest. Thus, it appeared beaching quantity was related to the time particles reached the tidal inlet. Yet for all release times, little to no beaching occurred on the coast and ebb-tidal delta.

In the scenario with wind conditions, beaching quantity was the highest in the simulation with a strong wind from the west. Particle spreading was fast for most wind directions, with wind from the north being the exception. For this simulation, the spreading times were similar to those found in the tides + swell scenario. No beaching occurred for the simulations with a strong northerly wind and gentle and strong wind from north-east and east.

4.1 Interpretation of results

Influence of the tides on transport of plastics

Particles under the influence of the tides were displaced back and forth with the rising and falling tide. However, there was a net movement in the direction of the running tide (eastward) which was also seen in the residual velocities (figure 4.1). In areas of uniform depth, the velocities pointed consistently towards the east. Nearest to the coast, particle motion was slowest, corresponding with the small residual velocities, which was most likely the result of bottom-friction close to the coastline.

A clear pattern was visible of ebb- and flood-dominance in the tidal inlet and ebb-tidal delta (explained in section 2.1). During the flood phase, water flowed gradually from all directions into the inlet, whereas during the ebb phase, water was pushed through the narrow tidal inlet back into the sea past the ebb-tidal delta. The corresponding residual velocities showed more flood-dominated currents (towards the inlet) at the sides of the inlet and delta, and a stronger ebb-dominated current in the middle. The phenomenon was also seen by observing the particles. They entered the tidal inlet west with the flood phase and they were pushed back out mainly in the middle with the ebb phase. This strong current in the middle might be the reason not all particles beached in the tidal inlet or basin or on the coastlines. As was presented in section 3.1 and 3.2, many particles beached along the coastlines inside the tidal inlet. These locations correspond with residual currents (flood-dominated) from either side of the mouth of the inlet, towards the opposite side into the inlet, thus pushing particles against the coast during the flood phase. The behaviour observed in the spreading of particles was, as expected, the same as the flow pattern of the hydrodynamics. The same was found by Van Utenhove (2019), who also found that particles indeed moved with the hydrodynamics.
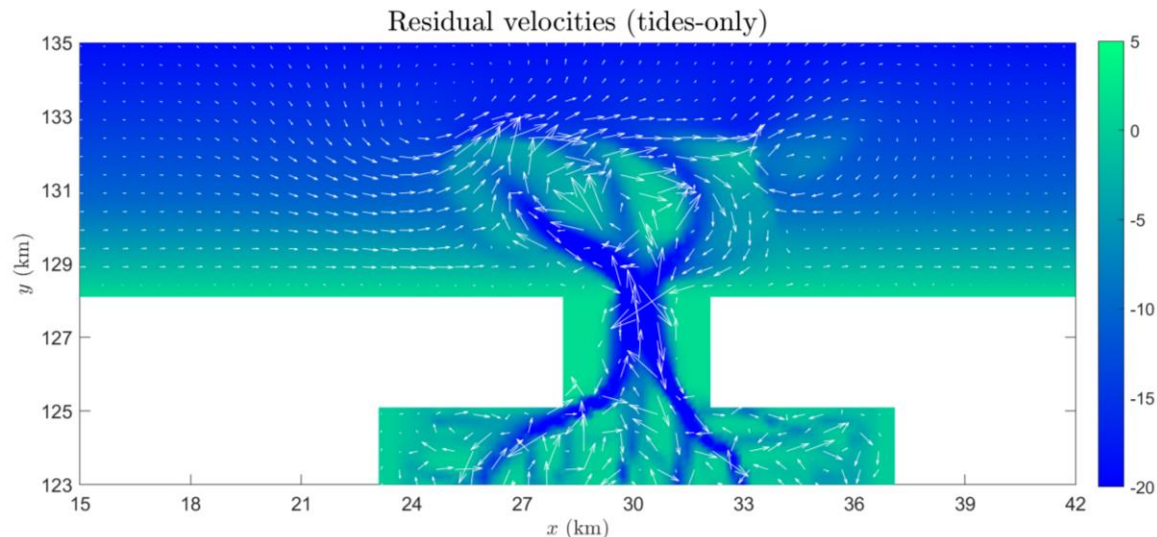

Figure 4.1: Residual velocities in the tidal inlet system (scenario 'Tides-Only'). The release location of particles is now at the west boundary of the displayed domain. Colour bar indicates bathymetry.

The final mean locations of particles per simulation (different release times) were very close to each other, giving the impression that the influence of release time on particle transport was negligible. However, there were very subtle differences in net particle motion between the simulations, which did cause significant differences in beaching. These results correspond with findings by Van Utenhove (2019), who found that the time of release was not a critical parameter but did result in significant difference in particles beaching. Yet another research, also based on a two-dimensional model, found that particles released from ships at sea at different times followed different paths (Critchell, et al., 2015).
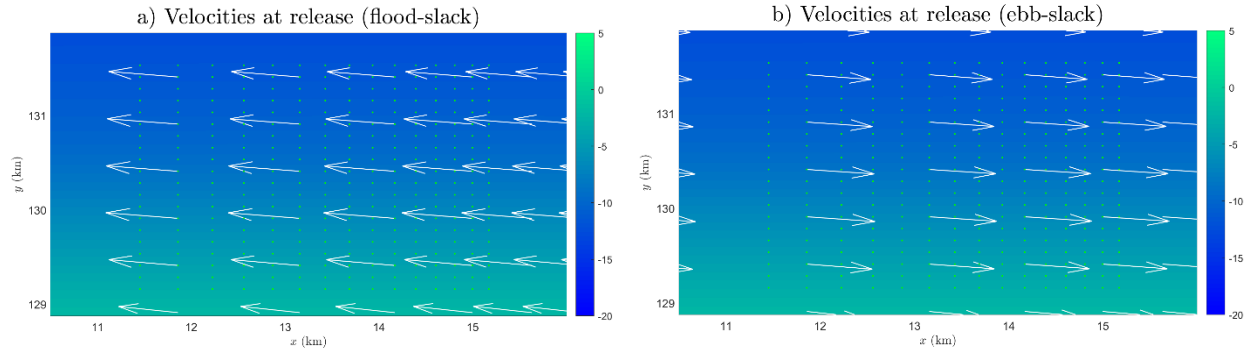
Figure 4.2: Velocities at the location of release averaged from the first 3 hours upon release. a) flood-slack release, b) ebb-slack release. Colour bar indicates bathymetry.

The initial direction of the current at the time of release determined at what y-coordinates (further north or south) the particles entered the tidal inlet system. The first three hours sets the simulations of different release times apart. Particles released in the flood-slack and ebb phases first moved westward and slightly towards the north, corresponding with the velocities at release time (figure 4.2a). They kept moving in this direction for six and three hours respectively, until the tide turned again. This was different from particles released during the flood and ebb-slack phases, which initially moved eastward for three and six hours respectively (see figure 4.2b). Considering particles released in the flood-slack phase initially moved away from the tidal inlet, they reached it later than particles released in the other tidal phases. Particles were under the influence of the oscillating tides longer and moved slightly further north (with every ebb phase) than particles in the other simulations. This explains why particles with a flood-slack release reach the tidal inlet slightly further north than particles released in the other tidal phases. As the opposite occurred for particles released in the ebb-slack phase, their slightly more southern location upon entering the inlet area caused more particles to beach on the coastlines.

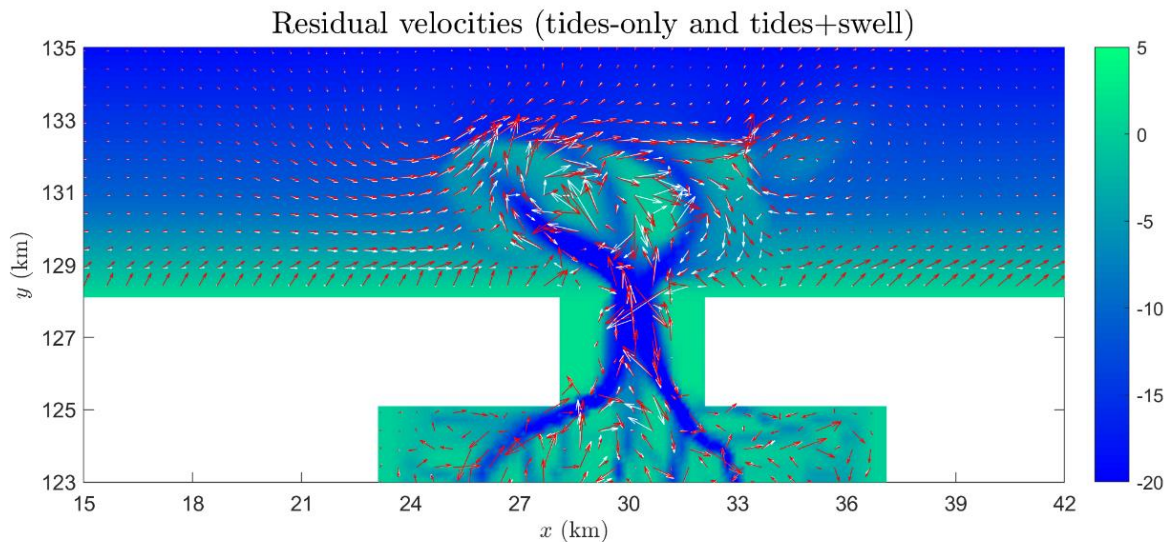**Influence of adding swell on transport of plastics**

Figure 4.3: Difference in residual velocities between the scenarios tides-only (white) and tides + swell (red). Colour bar indicates bathymetry.

While the tides-only scenario showed very small residual velocities near the coastline, adding swell changed this by increasing the velocity along the coastline and turning the direction of the residual velocities north-east. This resulted in the observed offshore residual current and particle movement. Over the ebb-tidal delta, residual velocities differ more due to the differences in bathymetry. There is more bottom friction in the shallower areas, causing more diverse directions in velocity. Most of the particles in the scenario tides-only were close to the tidal inlet 20 days into the simulation, while for the tides + swell scenario particles were further offshore as a result of the offshore residual current caused by swell (see figure 4.3).

As was already briefly suggested in section 3.3, adding swell resulted in a more significant north-south movement of particles, next to the west-east movement caused by the tides. The depth-averaged velocity near the location of the incident showed the difference between the scenarios tides + swell and tides-only (see figure 4.4a). The scenario tides-only showed nearly the same velocity in either directions, but the scenario tides + swell showed the velocity was stronger in the northern direction. By only forcing swell in the simulation (without the tides), no north-south oscillations were observed anymore in the depth-averaged velocity (see figure 4.4). Instead the velocity had a constant value towards the north. This caused the stronger north direction in velocity in the scenario tides + swell and thus explains why particles moved more towards the north compared to tides-only. However, the effect of swell was stronger at the coastline, where it resulted in the offshore residual current. This was not caused by Stokes drift, as that is in the direction of wave propagation (here to the south-east). The effect of swell weakened with increasing distance from the coast (see figure 4.4b).
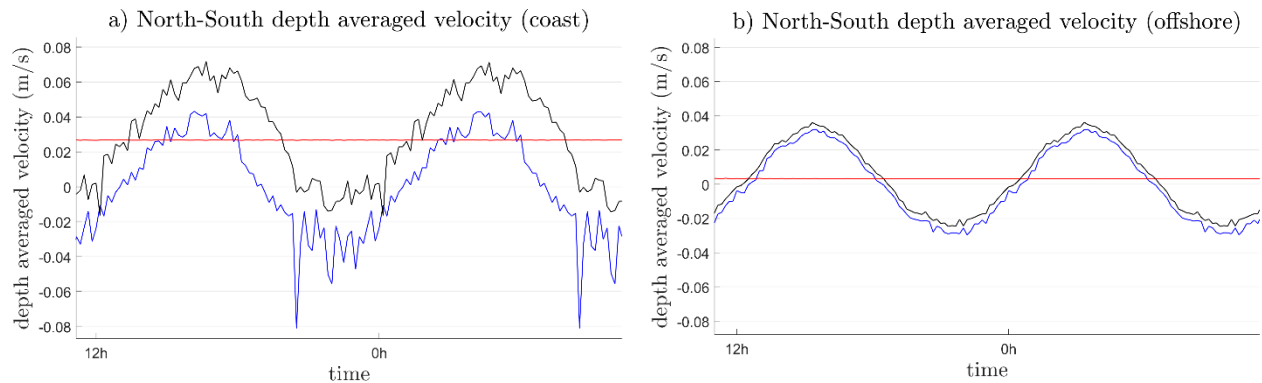

Figure 4.4: Depth-averaged velocities on the y-axis (north-south direction), 600 m from the coast (a) and offshore at the location of particle release (b). The lines represent depth averaged velocities caused by tides-only (blue), swell-only (red) and tides + swell (black).

The beaching quantity in this scenario was largest for the simulation in which particles were released during the ebb-slack phase, although the differences between the simulations were minor. Nevertheless, the larger number for ebb-slack could be explained by the time particles oscillated with the tides before reaching the inlet area. This was shortest compared to the other simulations (as explained in the previous section) so particles were transported less towards the north and therefore not in the channels as clearly as in the other simulations.

In general, however, particles in the scenario tides + swell beached significantly less compared to the scenario tides-only. As indicated earlier, this was caused by the offshore residual current as a result of adding swell. Although this research used a model in depth-averaged mode and therefore cannot separate surface residual currents from bottom residual currents, another research that analysed the vertical profile of the water column in shelf seas found that observations showed the bottom current (i.e. undertow) was the dominant component of the depth-averaged circulation, especially in shallow

waters (approximately 15m) (Lentz, et al., 2008). This is a possible explanation to why an offshore residual current was observed in the results here. However, this observed current was still in contradiction with the principle of mass conservation as it would mean more water flows away from the coast than towards the coast. It therefore requires further attention in future research.

Influence of adding wind on transport of plastics

In the previous scenarios without wind conditions, the residual velocities pointed towards the east. For the scenarios including wind from 270 degrees, 315 degrees and 0 degrees, the main direction was not different. However, for the wind directions 45 degrees and 90 degrees (westward wind) the residual velocities showed to also be westward (see figure 4.5), suggesting wind played a large role in determining the residual velocity and with that the direction of particle transport. This corresponds with similar research that found wind plays a large role in determining the speed and direction of particle transport (Neumann, Callies, & Matthies, 2014). A research on modelling the fate of marine debris along the Great Barrier Reef World Heritage Area by using a high resolution model, found that wind conditions have a large effect on the speed and direction of floating debris (Critchell, et al., 2015). This corresponds with the findings of this research as both speed and direction of particle transport changed significantly by adding wind. Critchell, et al. found that the diffusion of floating debris is larger for particles that are influenced by currents and wind, than that of currents alone, because wind and currents are generally not parallel to each other. This corresponds with the findings of this research as particle movement was much faster, providing the chance for increased diffusion.
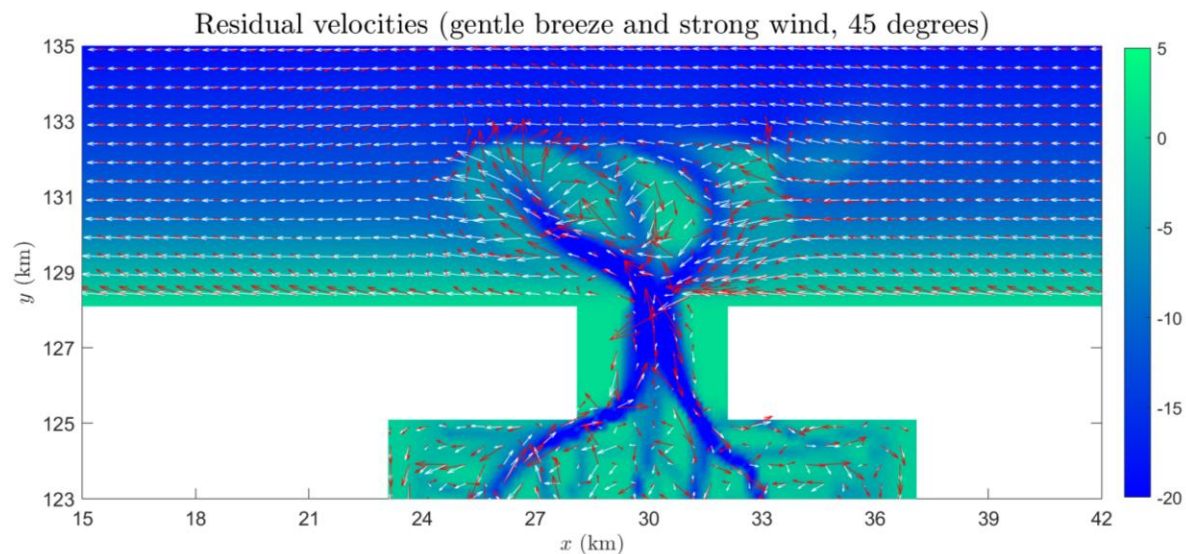

Figure 4.5: Residual velocities for the scenarios with a wind direction from 45 degrees. Gentle breeze (red) and strong wind (white). Colour bar indicates bathymetry. The residual velocity for wind from 90 degrees is given in appendix I.

For the eastward wind directions (270 degrees and 315 degrees), the residual velocities were also eastward, but to a stronger extent compared to the scenario of 'tides + swell' (see figure 4.6). Another difference with 'tides + swell' is that by adding wind, the residual offshore current seemed to be suppressed. This indicates wind influences the residual velocity, and therefore particle transport, more than swell. Other research found similar results. Although some included the effect of wind drift coefficients on the litter particles, for many the result showed wind had the largest influence on particle transport (Janssen, 2019; Gutow, et al., 2018; Critchell, et al., 2015; Neumann, Callies, & Matthies, 2014).
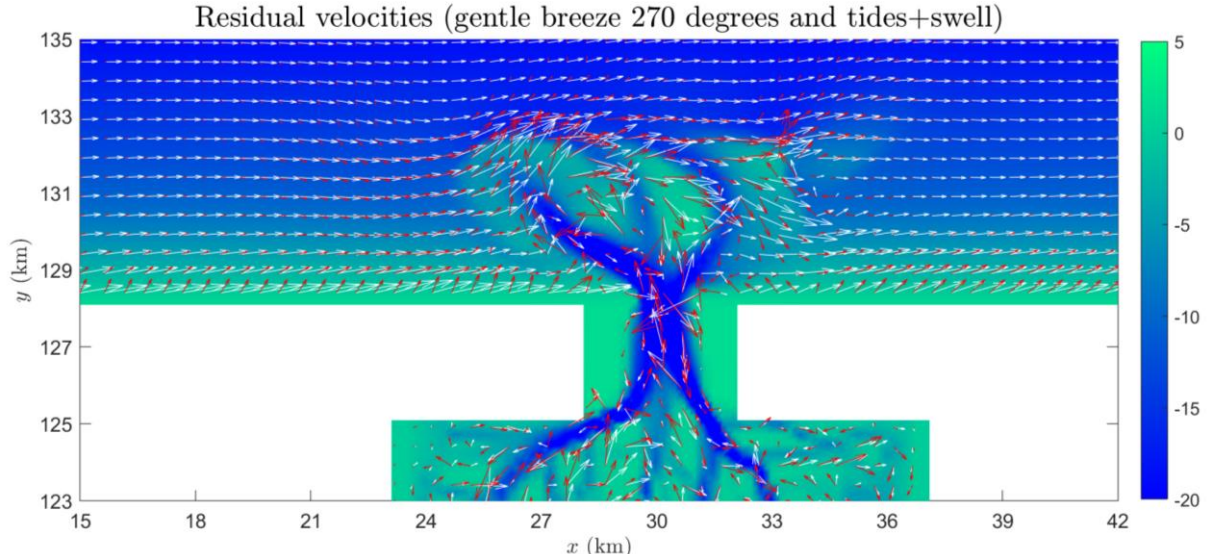
Figure 4.6: Difference in residual velocities for the scenarios gentle breeze from 270 degrees (white) and tides + swell (red). Colour bar indicates bathymetry. The scenario 315 is not plotted due to the difference with 270 not being significantly large enough. The difference between gentle breeze from 270 degrees and strong wind 270 degrees is given in appendix I.

One interesting result was that for the scenarios with wind from the north, as they were remarkably similar to the results of the tides + swell scenario. It was already briefly indicated that it seemed that wind from the north did not influence particle spreading. The residual velocity pattern supports this theory, as it was rather similar to the residual velocities of the scenario tides + swell (see figure 4.7). The most obvious difference was that the offshore residual current seen along the coastline, seemed to decrease by adding wind from the north. This was again observed in the residual velocities of a strong wind from the north, in which the offshore residual current was even smaller (given in appendix I). The reason for this is that wind adds to the residual velocity of the scenario tides + swell: the wind direction was opposite to the offshore residual current and therefore decreased its strength in the scenario that included wind. In contrast to the other scenarios with wind conditions, particle transport with wind from the north seemed to be influenced more by tides and swell.
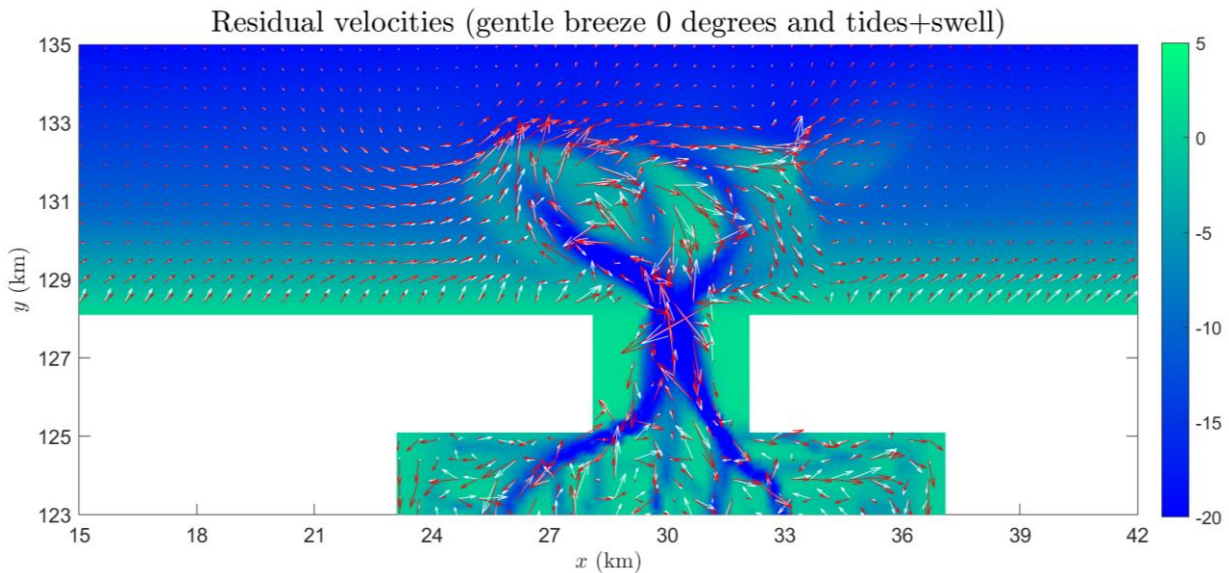

Figure 4.7: Difference in residual velocities between scenario gentle breeze 0 degrees (red) and tides + swell (white). Colour bar indicates bathymetry. The difference in residual velocities between a gentle breeze and strong wind from north is given in appendix I. Arrows were computed at each grid point for both scenarios, but red was plotted on top of white.

44

Interestingly, there was less beaching in the scenario with wind from north compared to the scenario tides + swell, thus it cannot be concluded wind from the north did not influence particle transport at all. In fact, particles influenced by wind from the north moved further towards the north compared to particles in the scenario tides + swell. Considering wind from north is perpendicular to the coast in the model used here, it indicated that beaching of particles was influenced by the orientation of the coastline to the wind direction. Similar results were found by Critchell, et al. (2015), who found that the orientation of beaches to the wind direction influenced accumulation rate.

Although the offshore residual current along the coastline was decreased by adding a northern wind, the residual velocities plotted further north in the domain, seemed to have increased. This would explain why particles were pushed towards the north. However, this movement is counterintuitive with the idea that a wind-induced current would push particles in the same direction it is going, as was seen for the simulations with other wind directions. A possible reason for this is the concept of pressure-driven currents (explained in section 2.1). The onshore wind-induced surface current leads to an offshore current in the water column below. However, considering the model used in this research is in its 2D mode, these two currents cannot be separated, therefore leaving the depth-averaged current of both, which was apparently offshore. This result was similar to the offshore residual current along the shoreline in the tides + swell scenario. Similar to the tides + swell scenario, the offshore depth-averaged current was in contradiction with the principle of mass conservation and requires further attention in future research to identify why the model would give this transport pathway.

Another interesting result was that many more particles beached under the influence of a strong wind from the west compared to other simulations with wind conditions. A huge blob of particles almost immediately was pulled into the tidal inlet and reached far into the tidal basin, whereas this pull into the tidal inlet seemed less strong for the other wind direction (north-west). This seemed to be the result of the western wind pushing particles faster towards the east. Consequently, particles entered right into the first channel simultaneously with the start of the flood current, whereas particles in the scenario with a strong wind from north-west reached the channel a few hours later (relative to the tide changing to the flood phase). This indicated the tides are important to some extent in modelling particle transport.

Influence of adding varying wind conditions (MSC Zoe based) on transport of plastics

As was already briefly indicated in section 3.5, wind direction and speed seemed to have a large influence on the spreading of particles at specific moments. Considering particles moved out of the computational domain in five days, the residual velocity was plotted here over the period January 2nd 00:00 to January 5th 00:00 (see figure 4.8).

It can immediately be seen that the residual velocities in many locations were in an eastward direction. Of the five days included in the residual velocities here, in the last two days (January 4th 00:00 to January 5th 23:59) wind came from a north-west direction and the windspeed was on average above 10 m/s. The two days before (January 2nd 00:00 to January 3rd 23:59) wind came from an almost northern direction with a wind speed of on average 7 m/s.
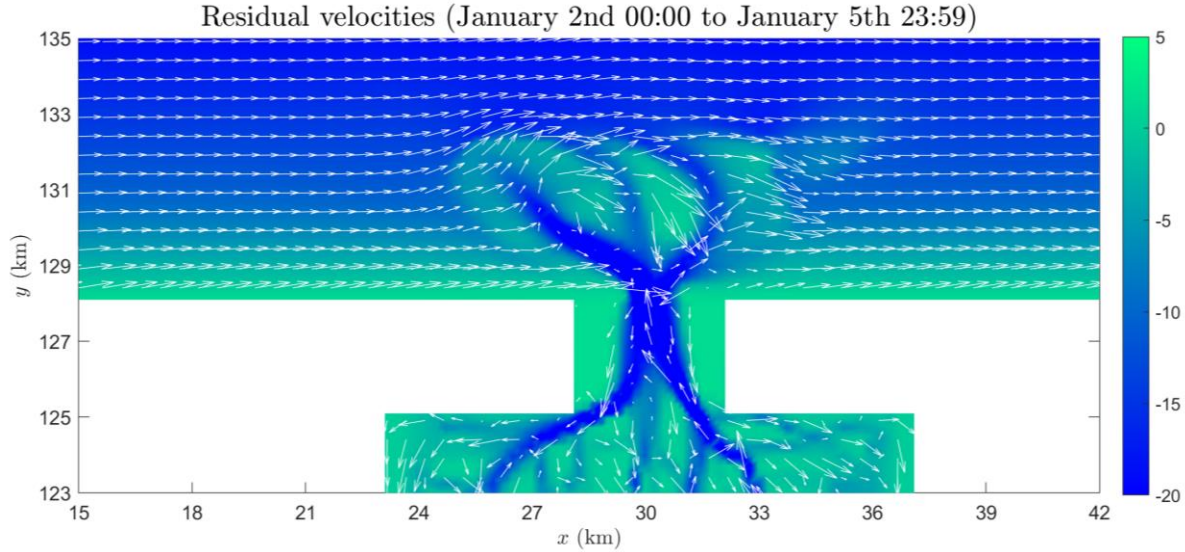
Figure 4.8: Residual velocities over a period of January 2nd 00:00 to January 5th 23:59 for the MSC Zoe scenario (varying wind conditions over time). Colour bar indicates bathymetry.

Plotting the residual velocity separately for these two periods, showed noteworthy differences (see figure 4.9). In the first period, residual velocities pointed slightly more towards the north, explaining why particles initially moved towards the north. Especially at the west side of the ebb-tidal delta, the residual current was towards the north. The middle of the ebb-tidal delta showed a residual current heading for the tidal inlet. However, by the time particles reached this area, wind direction had changed, causing the residual current to head more towards the west. This caused particles to be pushed away from the tidal inlet in a very short time, resulting in almost no particles beaching. Although wind seemed to be the main driver of particle transport in this scenario, it should be kept in mind that the bathymetry also played a role in particle transport, as was already seen for the tides-only scenario in the form of ebb- and flood-dominance. Similarly, Critchell, et al. (2015) also suggest that topography plays a strong role in determining the location of accumulation areas.
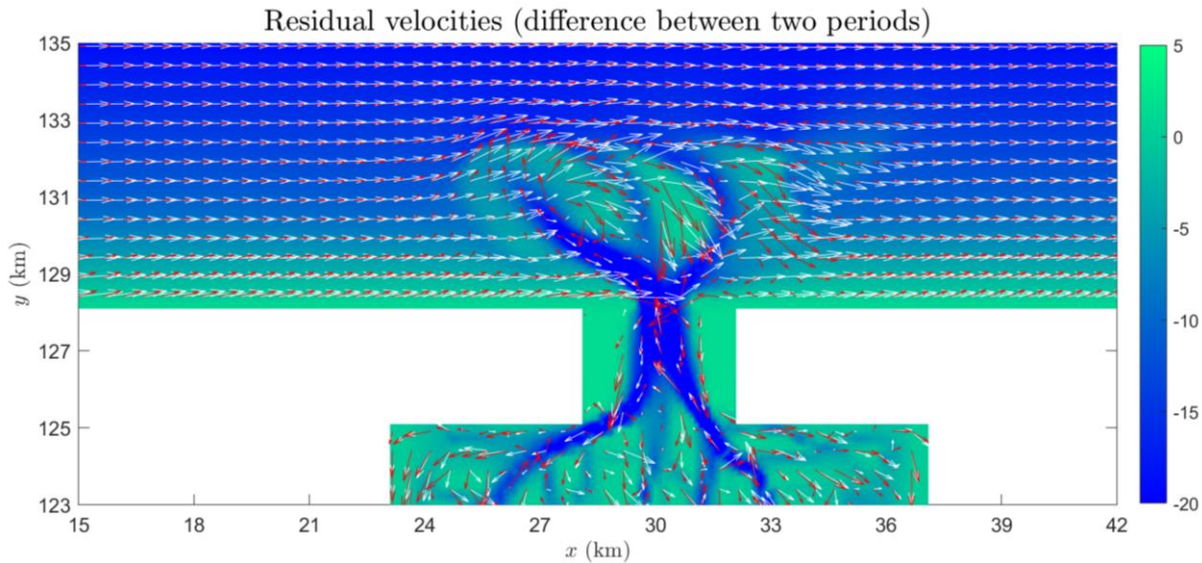

Figure 4.9: Difference in residual velocities between period 1 (January 2nd 00:00 to January 3rd 23:59) and period 2 (January 4th 00:00 to January 5th 23:59). Period 1 = red; period 2 = white. Colour bar indicates bathymetry.

Furthermore, if wind conditions had changed in a different way, particle transport would most likely also have been very different. Next to this, the reason very small differences were seen between the results of the four release times, most likely also has to do with the fact that wind conditions remained relatively the same over these four release times. Had there been a sudden change in wind direction before releasing for example particles in the last two simulations, the transport would have probably been very different.

The findings for this scenario correspond to some extent to the results of Janssen (2019). As mentioned in the first chapter, this research modelled the spreading of particles under similar conditions as during the MSC Zoe event. Janssen (2019) released particles in two lines above approximately the length of the Dutch Wadden Sea and found that particles moved towards Germany, which corresponds with the results found in this research, although here a much smaller spatial scale was analysed and particles were released closer to the coast. Next to this, Janssen (2019) found that many particles beached along the Dutch coast, with high densities on the Frisian coast and on Terschelling but no beaching on Vlieland (west of release location). Although this corresponds to some extent to field observations, the field study showed a larger beaching quantity on Schiermonnikoog and the coast of Groningen (see figure 1.4). Thus, the accuracy of the model used by Janssen can still be improved. What corresponds with the research here is that no particles moved towards the west in the MSC Zoe scenario, but different from the results found by Janssen, here almost no beaching was observed. However, as particles moved out of the computational domain within five days, it cannot be concluded that particles would not have beached further east than the computational domain (e.g. eastern part of Terschelling, Ameland, Schiermonnikoog), or whether particles would have transported into the Wadden Sea between tidal inlets further east. This theory can be supported by another similar research, also mentioned in the previous section, by Critchell, et al. (2015), who found that when floating debris was under the influence of variable wind conditions for a longer period of time (e.g. by releasing particles further offshore), a larger variety in beaching locations resulted. Although Critchell, et al. (2015), as well as Janssen (2019), analysed on a longer time scale and larger spatial scale, that start of increased spread in particle distribution was observed in the results of the short-term small-scale simulations here, before particles left the computational domain. Critchell, et al. (2015) also found that changing the start date of simulations (i.e. here release time), in scenarios with varying (normal) wind conditions, such as conditions based on the MSC Zoe event, did not influence the location of the highest debris accumulation. This corresponds with findings here, as the difference between simulations in this scenario having different release times was very small.

4.2 Limitations of modelling

This research made use of an idealized model to gain a fundamental understanding of the hydrodynamic processes at play, so the importance of these hydrodynamic processes in tidal inlet systems could be assessed. It should be considered that the model is only moderately successful because of assumptions that were made.

One such assumption is that the depth-averaged velocities were used in computing the hydrodynamics. Thus, variation of currents in the vertical plane is not accounted for. This is what might have caused the counterintuitive results for the scenario with swell and wind from the north. One would expect particles to move in an onshore direction, as is the case with the surface layer of the sea when forced by wind and waves. However, one assumption in the model resulted in an offshore residual current, which unfortunately has not been recognised so far. It would be relevant for future research to model in 3D mode, as this would provide the separation of vertical differences in currents.

Secondly, the 12-hour tidal period used in the model corresponds with the S2 wave, whereas usually the M2 wave (a period of 12 hours and 25 minutes) is more dominant. Nevertheless, this difference of 25 minutes resulted in a fault marge in the calculations of less than 10% and therefore does not significantly influence the results.

Thirdly, in the Delft-3D model, swell is generated outside the computational domain and enters at the north-oriented open boundary. In the tides-only and tides + swell scenarios, a wave grid was applied the same size as the study area but swell had a direction of 335 (north-west). As the swell entered the domain from the northern boundary, a shadow area existed in the south-west corner of the domain (see figure 4.10). In the scenarios including wind conditions, the wave grid was enlarged in length of the domain to remove the shadow area, even though it resulted in marginal differences for the depth-averaged velocity (see figure 4.11) and was therefore no major issue. A different assumption that might have influenced the results more is that no correlation between waves (i.e. swell) and wind was included in the Delft3D-WAVE module. Wind was included in the Delft3D-FLOW module and therefore only generated wind-driven currents, rather than also including wind-driven waves.
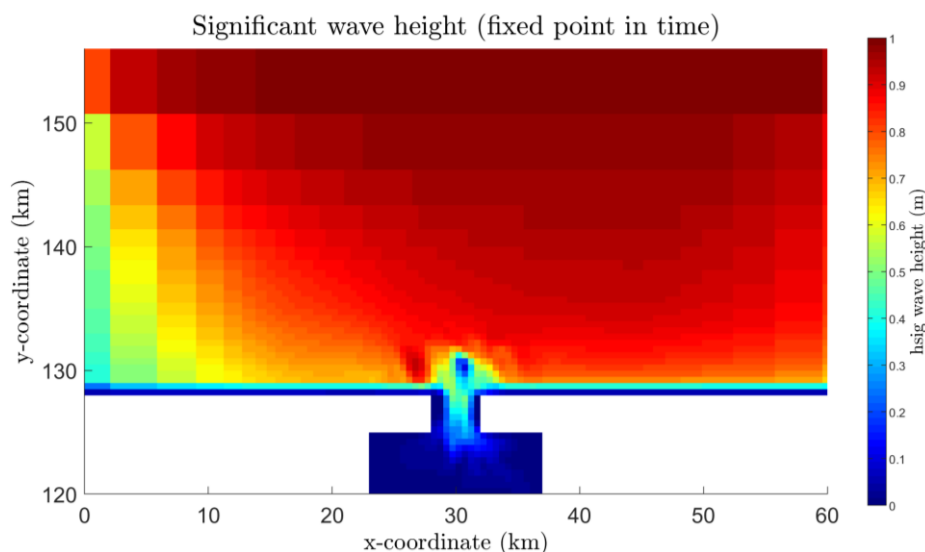

Figure 4.10: Significant wave height over the computational domain when forcing swell in a grid with the same size (not extended). The left part (blue/green/yellow) is the so-called shadow area. By extending the grid, this shadow area is located outside of the computational domain. The release location of particles is between x=10 and x=20.
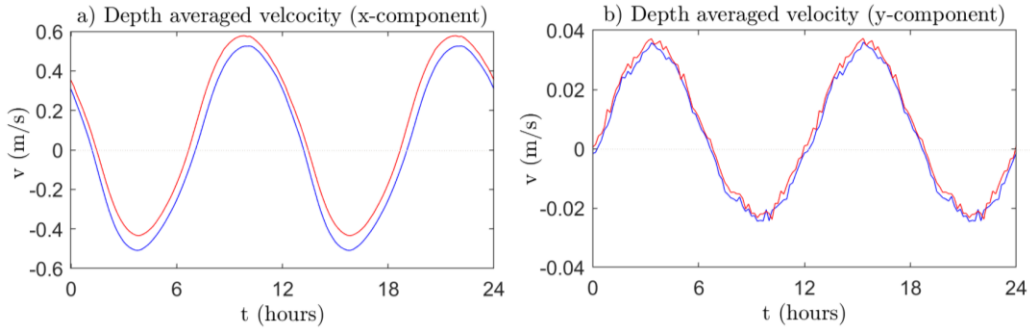
Figure 4.11: Difference in depth-averaged velocity when using two different wave-grids: short grid (blue), extended grid (red).

Fourthly, the beaching of a particle was assumed to be its final location, even though in reality some particles might be resuspended into the water column by waves or tides. Nevertheless, this research did not aim to predict actual particle locations, but to improve the understanding of buoyant particle behaviour. Other similar numerical modelling researches included the same method of simulating the process of beaching and still showed moderately successful results, even though it is a major assumption (Critchell, et al., 2015; Janssen, 2019; van Utenhove, 2019).

On the same topic, in calculating the mean of particles, beached particles were included. With that, it affected the mean pathways and residence times of the mean of particles. In case the interest lies with following the mean transport of unbeached particles, the beached particles should be excluded from this calculation.

Despite of the stated assumptions and model limitations, results did correspond in multiple ways with findings in other literature.

4.3 Relevance to practice

This research aimed "*to understand the behaviour of buoyant particles and the extent to which their transport characteristics are influenced by different hydrodynamic processes that are fundamental to tidal inlet systems, by modelling the transport of buoyant particles under specific hydrodynamic conditions*". Before presenting the conclusions, it is important to discuss the relevance of this research to practice.

There are many pathways of marine debris into the ocean and plastic is found worldwide, as well as in the deep sea. There are different fates for plastic particles in the marine environments. "*It can reside in sediment, biota, and ice, and may be trapped along the coastline or in estuaries, waterways and lakes, and can even be suspended in the atmosphere*" (Hardesty, et al., 2017). To predict the transport of plastic particles in the ocean, an improved understanding of the processes affecting particle transport is required. Understanding the transport of plastics in small coastal zones at short time scales is important to prevent further spreading of plastics over the ocean. However, efforts to monitor plastic in the marine environments is expensive, time consuming and hard to uphold (Hardesty, et al., 2017). There are many processes, physical and biotic, that interact with plastic particles and influence their fate (see figure 4.12).
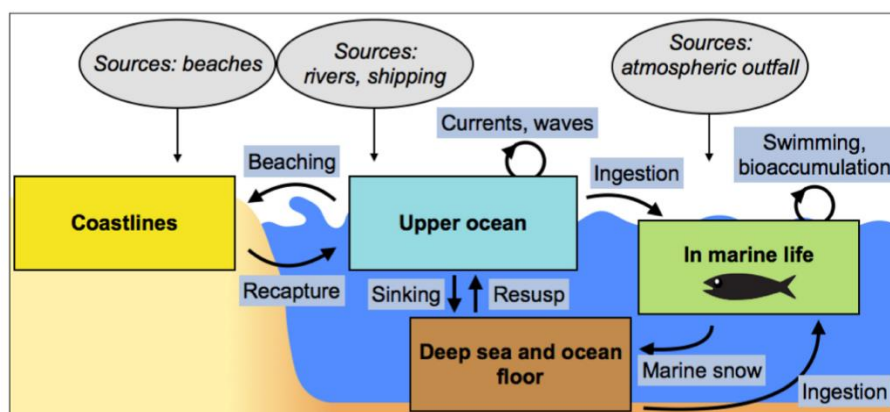

Figure 4.12: "The sources of anthropogenic debris entering the ocean (ovals), reservoirs, or oceanic compartments where debris occurs (boxes) and processes through which debris moves between compartments" (Hardesty, et al., 2017).

Numerical modelling provides a possible solution to predict particle transport in the marine environment and determine their fate. Ocean circulation models have been used to predict potential accumulation zones of marine debris, by estimating the ocean currents (Hardesty, et al., 2017). These models provide the opportunity to analyse major processes in the ocean and their contribution to particle transport. However, much research and available knowledge is focussed on larger scales, with coarse grid (i.e. lower resolution) models. In coastal zones, smaller-scale high resolution models are necessary to predict the hydrodynamics more accurately as they are more complex in shallow seas. Yet, the processes influencing particle transport on these scales are less understood (van Utenhove, 2019). By using idealized models to analyse the degree to which specific hydrodynamic processes contribute to particle transport, the accuracy of models used to predict transport pathways of plastic particles in seas can be improved. According to Dagestad & Röhrs (2019) "*The variable degree of ocean-, wind and wave forcing is highly relevant for the practical problem of predicting the drift of particles and aid search and clean-up operations*". Improving the understanding of the extent hydrodynamic processes influence transport characteristics of buoyant particles contributes to solving this 'practical problem'.

Some models are used to track back where marine debris originated, in order to raise awareness about the wide spread of plastic debris in the oceans and the adverse effects plastic pollution has on people,

planet and profit, as well as inform policy and decision makers as this information is considered critical to improve waste management strategies and with that contributing to the sustainability transition of society (Lebreton, Greer, & Borrero, 2012). Thus, understanding the dynamics in e.g. intertidal ecosystems is essential for managing purposes (Brakenhoff, Reussing, & van der Vegt, 2019).

Other models are used to predict particle transport right after a spill, such as the MSC Zoe container loss, to improve targeted clean-up and emergency response strategies. For the North Sea and Wadden Sea, for example, such emergency response strategies are coordinated and monitored by Rijkswaterstaat, as they are responsible for the management of the Dutch North Sea and Wadden Sea. After the MSC Zoe container loss, first clean-up activities were coordinated by 'Coördinatieteam Waddeneilanden' (CoWa) and 'Veiligheidsregio Fryslân' and many volunteers participated in the clean-up activities (Wijkhuijs, van Duin, Domrose, & Leentvaar, 2019). As this was a large amount of debris, volunteers had a sense of achievement afterward, which is important to maintain their interest (Critchell, et al., 2015). To make such clean-up actions as effective as possible, the location of marine debris after a spill such as the MSC Zoe is important.

The results of this research give the extent to which three critical processes (tides, swell, wind) in tidal-inlet systems influence the transport of particles, which can be used to improve the complex models that are used for accurate predictions of particle pathways and therefore aid policy decision making about emergency response strategies as well as future management. As the results reveal the contribution of the processes to particle transport, emphasis can be put on the processes that are important in tidal inlet systems in order to limit computing time in complex models and therefore speed up emergency response.

Although this research took one tidal inlet in the Wadden Sea as an example, results can be incorporated in models for similar systems over the world. Thus, this research would help short-term targeted clean-ups and emergency response strategies worldwide in case of a spill as it would provide stakeholders with the opportunity to improve their predictions on particle dispersal after a spill near tidal inlet systems.

5. Conclusions

In order to answer the research question: "*To what extent are transport characteristics of buoyant particles, released from a perturbing source outside of the tidal flat system, influenced by the hydrodynamic processes in a tidal inlet system?",* sub-questions were formed and answered below.

1. To what extent are transport characteristics of buoyant particles influenced by tides only and how do these characteristics depend on release times (tidal phases)?
The extent to which the tides influence transport of buoyant particles was seen in the particle spreading direction. With the tide falling and rising, particles also oscillate in the direction of the flood and ebb currents. The different release times influenced particle transport by affecting the spreading time (time it takes for particles to enter the tidal inlet) and beaching quantity per location.

2. To what extent are transport characteristics of buoyant particles influenced by the contribution of swell to tides and how do these characteristics depend on release times?
The extent to which swell influences the transport of particles was seen in the offshore residual current it generated, which caused particles to move further away from the coast. This offshore residual current contributed in particles entering the ebb-tidal delta further offshore, leading to particles entering the tidal inlet via the channels. This in turn influenced the beaching quantity greatly compared to the tides-only scenario. Release time determined how far offshore particles entered the tidal inlet system, yet it only caused small differences in beaching quantity.

3. To what extent are transport characteristics of buoyant particles influenced by the contribution of wind-driven currents to tides and swell?
Wind influenced particle transport more than swell or tides. Although the influence of the tides was visible when forcing a gentle breeze, a strong wind suppressed this almost completely. Relative to the tides and swell, wind most strongly determined the particle spreading time and direction, as well as the beaching quantity. The only exception was when the wind direction was perpendicular to the coast and onshore, which resulted in particle movement driven by tides and swell, although there was significantly less beaching compared to the scenarios not including wind.

4. To what extent are transport characteristics of buoyant particles influenced by realistic time-variable wind conditions (based on the MSC Zoe incident), in combination with tides and swell and how do these characteristics depend on release times?
The extent time-variable wind conditions influence particle transport was seen in particle spreading time, motion direction and beaching quantity. The sudden changes of wind conditions caused sudden changes in the transport of particles. As the wind direction turns and wind speed changes, this can significantly increase or decrease the amount of time that particles spend in the tidal inlet system and therefore increase or decrease the beaching quantity, considering the supressing effect wind has on tides. The release time seemed to be no critical parameter here, although the influence might be stronger in combination with more rapidly changing wind conditions.

Combining the answers to these sub-questions, an answer on the extent to which transport characteristics of buoyant particles were influenced by the hydrodynamic processes in a tidal inlet system was now acquired. Wind has the most significant effect on transport characteristics as it determines the general direction of particles, trumping the net transport caused by tides. However, the influence does depend on the given wind conditions. With decreasing windspeed, the effect of tides and swell become

increasingly important. The offshore transport caused by swell is then more apparent, as well as the back and forth movement by the rising and falling tide. Release time determines at what point in time and space particles enter the tidal inlet system and therefore influences the beaching quantity.

6. Recommendations

The results of this research give the extent to which three critical processes (tides, swell, wind) in tidal inlet systems influence the transport of buoyant particles. This can be used to improve the complex models, used for accurate predictions of particle pathways, and can therefore aid policy decision making about emergency response strategies as well as future management.

The focus of the processes analysed should be altered based on the aim of modelling. The influence of different tidal phases at release time is an important process in predicting particle pathways on a very short term (days), whereas wind is more important on a longer term, especially for variable wind conditions. The process of swell is more important to include when the aim is to include vertical particle transport in shallow coastal areas, as including this process in a 2D model might result in counterintuitive residual velocities. The results of the behaviour of particles in this research can be used to compare the behaviour when modelling in 3D mode.

In using complex models to predict the fate of buoyant plastics in a tidal inlet system after a spill, the focus on the processes included in the model should depend on the weather conditions at the time of the spill. In the case of fair-weather conditions (e.g. wind speed < 4 m/s), time of release is a critical parameter. Whereas in case of stronger wind conditions (>10 m/s), the tides have a less critical influence on particle spreading. Wind direction is especially critical in modelling the fate of plastics in complex models.

Future research
Firstly, some of the processes in tidal inlet systems could not be reproduced accurately in this research because the model was limited to two dimensions. This does, however, provide a representation of the model behaviour which can be used to compare with a 3D model. In future research, it would be interesting to model buoyant particle dispersal by adding more layers to the water column, creating a 3D model, as that is essential to isolate surface currents from deeper currents. This is especially relevant in shallow seas, when swell and wind are forced in an onshore direction, as it results in compensating offshore currents below the surface layer.

Secondly, considering the small spatial and time scale of the study area in this research, subtle variations caused significantly different outcomes between simulations relative to these scales. For future research, it might be interesting to analyse the sensitivity of more parameters in the model, such as variations in release location, variations in wave direction, the inclusion of wind-driven waves in a 3D model and the inclusion of spring and neap tides and storm surges. As the computational domain of this research was focussed on one tidal inlet and particles were only released west of it, there were no results on in and outflow or beaching in the inlet of particles in the scenarios with wind directions towards the west. It might be interesting to include a second release location east of the tidal inlet in future research. Furthermore, this research did not analyse different particle characteristics (e.g. size and density), but it might be interesting to include this in future research. An example is to include windage coefficients, to analyse the direct effect of wind on floating particles. In the case of 3D models, the effect of sinking can be included. Including such particle characteristics in future research provides a way to analyse the behaviour of plastic particles less similar to surface water parcels.

Lastly, to improve accuracy of complex models, for which findings in this research can be used, it is also recommended to compare results with field observations when these data are available. This way the capability of numerical models to reproduce observed particle dispersal in tidal inlet systems can be assessed more in-depth.

References

Baptist, M. J., Brasseur, S. J., Foekema, E. M., van Franeker, J. A., Kühn, S., & Leopold, M. F. (2019). *Mogelijke ecologische gevolgen containerramp MSC Zoe voor Waddenzee en Noordzee.* Den Helder: Wageningen Marine Research. doi:10.18174/473406

Brakenhoff, L., Reussing, G., & van der Vegt, M. (2019). Characteristics of saw-tooth bars on the ebb-tidal deltas of the Wadden Islands. *Ocean Dynamics, 69*, 1273-1285. doi:10.1007/s10236-019-01315-w

Buonaiuto, F. S., & Bokuniewicz, H. J. (2008). Hydrodynamic Partitioning of a Mixed Energy Tidal Inlet. *Journal of Coastal Research, 245*, 1339-1348. doi:10.2112/07-0869.1

Burchard, H., & Badewien, T. H. (2015). Thermohaline residual circulation of the Wadden Sea. *Ocean Dynamics, 65*, 1717-1730. doi:10.1007/s10236-015-0895-x

Critchell, K., Grech, A., Schlaefer, J., Andutta, F. P., Lambrechts, J., Wolanski, E., & Hamann, M. (2015). Modelling the fate of marine debris along a complex shoreline: Lessons from the Great Barrier Reef. *Estuarine, Coastal and Shelf Science, 167(B)*, 414-426. doi:10.1016/j.ecss.2015.10.018

Dagestad, K., & Röhrs, J. (2019). Prediction of ocean surface trajectories using satellite derived vs. modeled ocean currents. *Remote Sensing of Environment, 223*, 130-142. doi:10.1016/j.rse.2019.01.001

Deltares. (2019). Manuals. *Delft3D-FLOW user manual*. Retrieved February 20, 2020, from https://content.oss.deltares.nl/delft3d/manuals/Delft3D-FLOW_User_Manual.pdf

Dutch Safety Board & Bundesstelle für Seeunfalluntersuchung. (2019). *Joint Interim Investigation Report on Very serious marine casualty 3/19.* Investigation report. Retrieved May 11, 2020, from https://www.bsu-bund.de/SharedDocs/pdf/EN/Investigation_Report/2019/Interim_Investigation_Report_3_19.pdf;jsessionid=E82BCD1980EB6E06EE2DA2B1966F1A29.live21301?__blob=publicationFile&v=2

Dyke, P. P. (1980). On the Stokes' drift induced by tidal motions in a wide estuary. *Estuarine and Coastal Marine Science, 11(1)*, 17-25. doi:10.1016/S0302-3524(80)80026-0

FitzGerald, D. M., & Buynevich, I. V. (1978). Tidal inlets and deltas. In G. V. Middleton, M. J. Church, M. Coniglio, L. A. Hardie, & F. J. Longstaffe, *Encyclopedia of Sediments and Sedimentary Rocks.* Dordrecht: Springer. doi:10.1007/978-1-4020-3609-5_237

Groningen University. (2019). *First Waddenplastic.nl research outcomes*. Retrieved May 25, 2020, from rug.nl: https://www.rug.nl/news/2019/03/eerste-onderzoeksresultaat-waddenplastic.nl_-schiermonnikoog-hotspot-van-aangespoelde-plastic-ko?lang=en

Guannel, G., & Özkan-Haller, H. T. (2014). Formulation of the undertow using linear wave theory. *Physics of Fluids, 26*, 056604. doi:10.1063/1.4872160

Gutow, L., Ricker, M., Holstein, J. M., Dannheim, J., Stanev, E. V., & Wolff, J. (2018). Distribution and trajectories of floating and benthic marine macrolitter in the south-eastern North Sea. *Marine Pollution Bulletin, 131(A)*, 763-772. doi:10.1016/j.marpolbul.2018.05.003

Haigh, I. D. (2017). Tides and Water Levels. In J. Carlton, P. Jukes, & Y. S. Choo, *Encyclopedia of Maritime and Offshore Engineering.* John Wiley & Sons. doi:10.1002/9781118476406.emoe122

Hardesty, B. D., Harari, J. I., Lebreton, L., Maximenko, N., Potemra, J., van Sebille, E., . . . Wilcox, C. (2017). Using numerical model simulations to improve the understanding of micro-plastic distribution and pathways in the marine environment. *Frontiers in Marine Science, 4*, 30. doi:10.3389/fmars.2017.00030

Henry, D. (2019). Stokes drift in equatorial water waves, and wave-current interactions. *Deep Sea Research Path II: Topical Studies in Oceanography, 160*, 41-47. doi:10.1016/j.dsr2.2018.08.003

Herrling, G., & Winter, C. (2018). Tidal inlet sediment bypassing at mixed-energy barrier islands. *Coastal Engineering, 140*, 342-254. doi:10.1016/j.coastaleng.2018.08.008

Hir, P. L., Roberts, W., Cazaillet, O., Christie, M., Bassoullet, P., & Bacher, C. (2000). Characterization of intertidal flat hydrodynamics. *Continental Shelf Research, 20(12-13)*, 1433-1459. doi:10.1016/S0278-4343(00)00031-5

Howell, E. A., Bograd, S. J., Morishige, C., Seki, M. P., & Polovina, J. J. (2012). On North Pacific circulation and associaed marine debirs concentration. *Marine Pollution Bulletin, 65(1-3)*, 16-22. doi:10.1016/j.marpolbul.2011.04.034

Janssen, M. (2019). *Predicting the dispersion and beaching of floating plastics from the 2019 MSC Zoe accident in the North Sea using numerical simulations.* Utrecht: Institute for Marine and Atmospheric Research Utrecht. Retrieved February 20, 2020, from https://dspace.library.uu.nl/handle/1874/383364

Kilina, Y. (2019). *Frisian student maps plastic pollution on Schiermonnikoog [photo]*. Retrieved March 1, 2020, from northerntimes.nl: https://northerntimes.nl/frisian-student-maps-plastic-pollution-on-schiermonnikoog/

KNMI. (2020). *Uurgegevens van het weer in Nederland.* Retrieved February 20, 2020, from project.knmi.nl: https://projects.knmi.nl/klimatologie/uurgegevens/selectie.cgi

Kump, L. R., Kasting, J. F., & Crane, R. G. (2014). *The Earth System* (3rd ed.). Harlow, UK: Pearson.

Lavidas, G., & Polinder, H. (2019). North Sea Wave Database (NSWD) and the Need for Reliable Resource Data: A 38 Year Database for Metocean and Wave Energy Assessments. *Atmosphere, 10(9)*, 551. doi:10.3390/atmos10090551

Lebreton, L. C.-M., Greer, S. D., & Borrero, J. C. (2012). Numerical modelling of floating debris in the world's oceans. *Marine pollution bulletin, 64(3)*, 653-661. doi:10.1016/j.marpolbul.2011.10.027

Lentz, S. J., Fewings, M., Howd, P., Fredericks, J., & Hathaway, K. (2008). Observations and a Model of Undertow over the Inner Continental Shelf. *Journal of Physical Oceanography, 38*, 2341-2357. doi:10.1175/2008JPO3986.1

Lesser, G. R., Roelvink, J. A., van Kester, J. A., & Stelling, G. S. (2004). Development and validation of a three-dimensional morphological model. *Coastal engineering, 51(8-9)*, 883-915. doi:10.1016/j.coastaleng.2004.07.014

Mansui, J., Molcard, A., & Ourmieres, Y. (2015). Modelling the transport and accumulation of floating marine debris in the Mediterranean basin. *Marine Pollution Bulletin, 91(1)*, 249-257. doi:10.1016/j.marpolbul.2014.11.037

Murray, A. B. (2003). Contrasting the Goals, Strategies, and Predictions Associated With Simplified Numerical Models and Detailed Simulations. *Geophysical Monograph series, 135*. doi:10.1029/135GM11

Netherlands Coastguard. (2020). *Schip verliest containers*. Retrieved February 13, 2020, from kustwacht.nl: https://www.kustwacht.nl/nl/node/579

Neumann, D., Callies, U., & Matthies, M. (2014). Marine litter ensemble transport simulations in the southern North Sea. *Marine Pollution Bulletin, 86(1-2)*, 219-228. doi:10.1016/j.marpolbul.2014.07.016

Oost, A. P., de Groot, A. V., Duren, L. A., & van der Valk, L. (2014). *Preparing for climate change: a research framework on the sediment - sharing systems of the Dutch, German and Danish Wadden Sea for the development of an adaptive strategy for flood safety.* Deltaris. Retrieved February 29, 2020, from https://research.wur.nl/en/publications/preparing-for-climate-change-a-research-framework-on-the-sediment

Plastic Soup Foundation. (2019). *Extensive loss of pellets at sea remains without sanctions*. Retrieved May 25, 2020, from plasticsoupfoundation.org: https://www.plasticsoupfoundation.org/en/2019/01/extensive-loss-of-pellets-at-sea-remains-without-sanctions/#top

Ridderinkhof, W., de Swart, H. E., van der Vegt, M., & Hoekstra, P. (2014). Influence of the back-barrier basin length on the geometry of ebb-tidal deltas. *Ocean Dynamics, 64(9)*, 1333-1348. doi:10.1007/s10236-014-0744-3

Rijkswaterstaat. (2020). *Rijkswaterstaat Waterinfo*. Retrieved May 11, 2020, from waterinfo.rws.nl: https://waterinfo.rws.nl/#!/details/publiek/astronomische-getij/Wierumergronden(WIERMGDN)/Waterhoogte___20berekend___20Oppervlaktewater___20t.o.v.___20Normaal___20Amsterdams___20Peil___20in___20cm/NAP/2019-01-01T00:00:00.001Z,2019-01-02T23:59:59.999Z,E. E

Rynne, P. (2016). Observations and Modeling of Exchange and Residence Time in Tidal Inlets. *Open Access Dissertations*, Paper 1579. University of Miami. Retrieved May 15, 2020, from https://www.researchgate.net/publication/299351942_Observations_and_Modeling_of_Exchange_and_Residence_Time_in_Tidal_Inlets

Sheavly, S. B., & Register, K. M. (2007). Marine Debris & Plastics: Environmental Concerns, Sources, Impacts and Solutions. *Journal of Polymers and the Environment, 15(4)*, 301-305. doi:10.1007/s10924-007-0074-3

Stichting de Noordzee. (2020). *Het jaar van de containerramp*. Retrieved February 13, 2020, from noordzee.nl: https://www.noordzee.nl/het-jaar-van-de-containerramp/

Stommel, H. M., & Farmer, H. G. (1952). *On the nature of estuarine circulation* (Vol. 2). Woods Hole: Woods Hole Oceanographic Institution.

The Open University. (1999). *Waves, Tides and Shallow-Water Processes* (Second ed.). Oxford: Butterworth-Heinemann. doi:10.1016/B978-0-08-036372-1.X5000-4

UNESCO. (2020). *Wadden Sea*. Retrieved February 22, 2020, from whc.unesco.org: https://whc.unesco.org/en/list/1314/

Van Sebille, E., England, M. H., & Froyland, G. (2019). Origin, dynamics and evolution of ocean garbage patches from observed surface drifters. *Environmental Research Letters, 7(4)*. doi:10.1088/1748-9326/7/4/044040

van Utenhove, E. (2019). *Modelling the transport and fate of buoyant macroplastics in coastal waters.* Delft: Delft University of Technology. Retrieved February 20, 2020, from https://repository.tudelft.nl/islandora/object/uuid:be6a41d2-6071-47b9-926d-f22c23edadba?collection=education

Wang, B., Hirose, N., Moon, J.-H., & Yuan, D. (2013). Difference between the Lagrangian trajectories and Eulerian residual velocity fields in the southwestern Yellow Sea. *Ocean Dynamics, 63*, 565-576. doi:10.1007/s10236-013-0607-3

Wang, Z. B., Louters, T., & de Vriend, H. J. (1995). Morphodynamic modelling for a tidal inlet in the Wadden Sea. *Marine Geology, 126*, 289-300. doi:10.1016/0025-3227(95)00083-B

Wijkhuijs, V., van Duin, M., Domrose, J., & Leentvaar, E. (2019). Containercalamiteit in het Noorden: de aanpak en impact. *Een evaluatie ten behoeve van het ministerie van Infrastructuur en Waterstaat*. Insituut Fysieke Veiligheid. Retrieved May 27, 2020, from https://www.ifv.nl/kennisplein/Documents/20190613-IFV-Containercalamiteit-in-het-Noorden-de-aanpak-en-impact.pdf

Zandt, A. (2019). *Onderzoek: 24 miljoen plastic korrels op de Wadden*. Retrieved March 6, 2020, from natuurmonumenten.nl: https://www.natuurmonumenten.nl/natuurgebieden/nationaal-park-schiermonnikoog/nieuws/onderzoek-24-miljoen-plastic-korrels-op-de

Appendix I: Supporting and additional figures

Supporting figures are given here per case (1-4), including the figures referred to in the discussion.
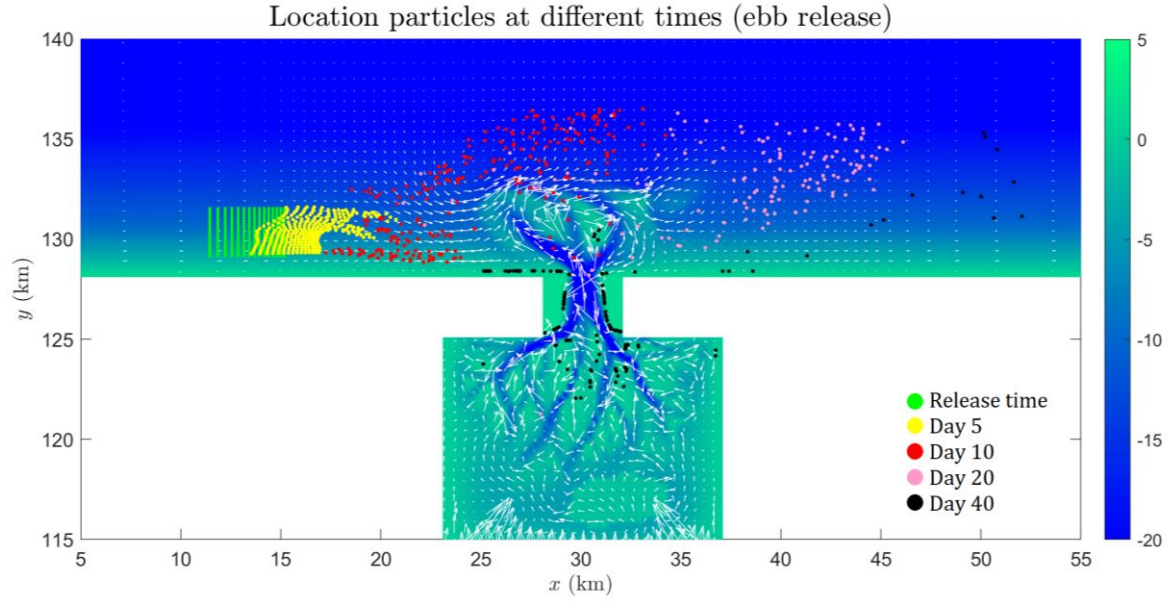
1. Scenario Tides-only

Figure I: Location of particles at different times into the simulation, particles released during ebb phase. Colours indicate bathymetry.
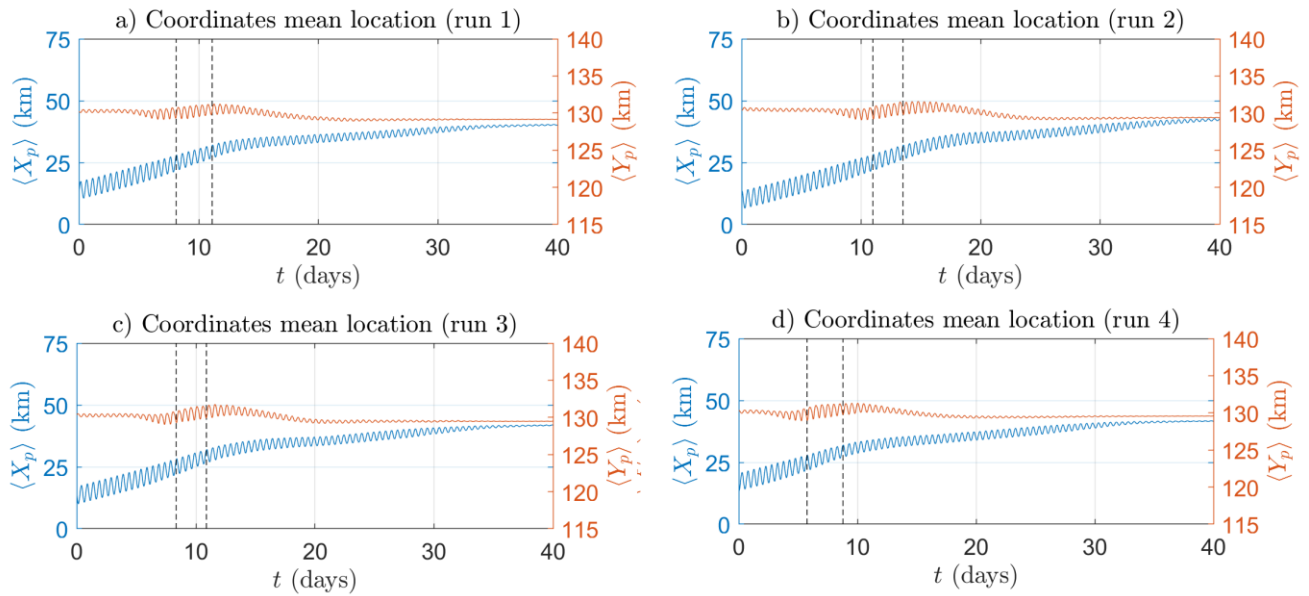

Figure II: X- and y-coordinates of the mean particle location over time. Dashed lines indicate the moment of entering and passing the tidal inlet area. Run 1 = flood release; run 2 = flood-slack release; run 3 = ebb release; run 4 = ebb-slack release.

Figure III: Mean particle pathways and final locations of run 1 (flood) and run 3 (ebb). Green dots represent release location. Colour bar indicates bathymetry.

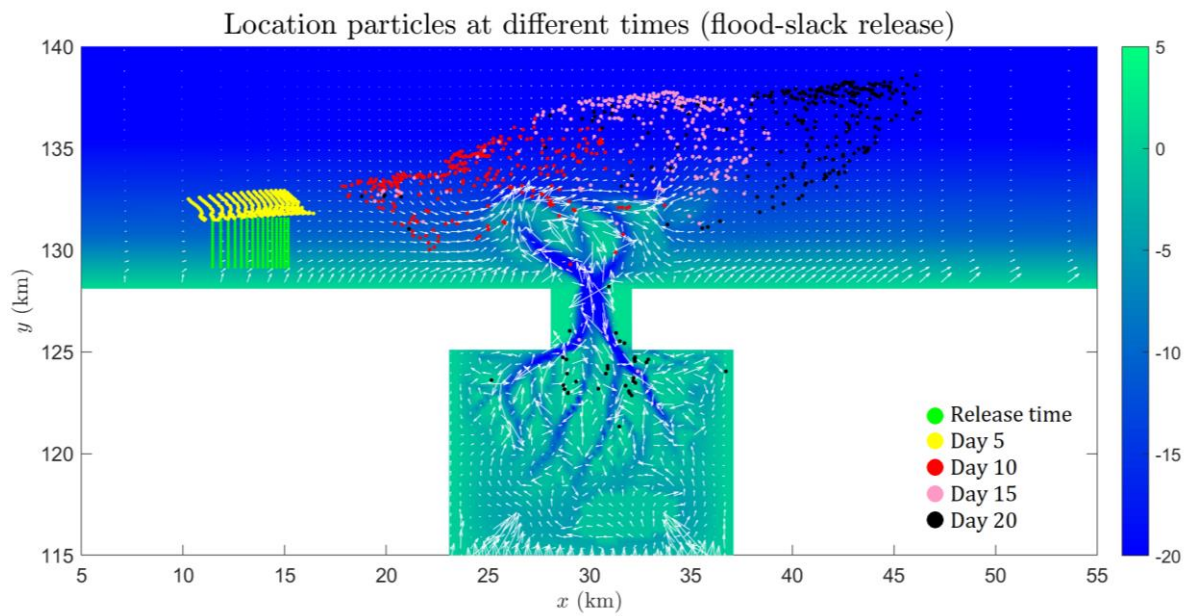## 2. Scenario Tides + Swell

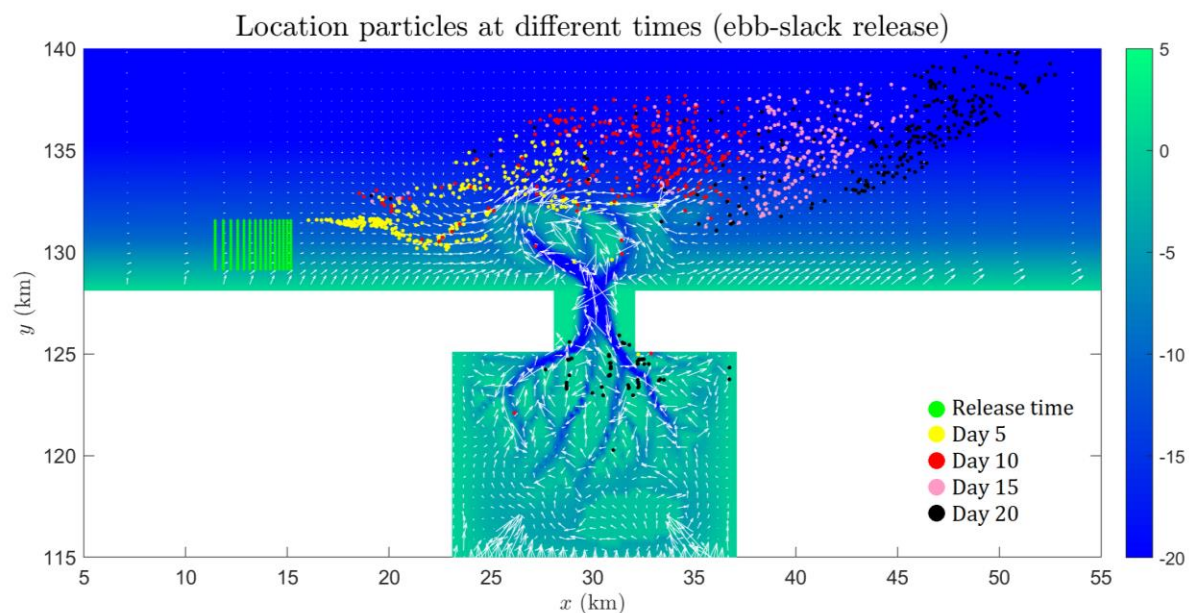*Figure IV: Location of particles at different times for run 6 (flood-slack release). Colour bar indicates bathymetry.*

Figure V: Location of particles at different times for run 7 (ebb release). Colour bar indicates bathymetry.
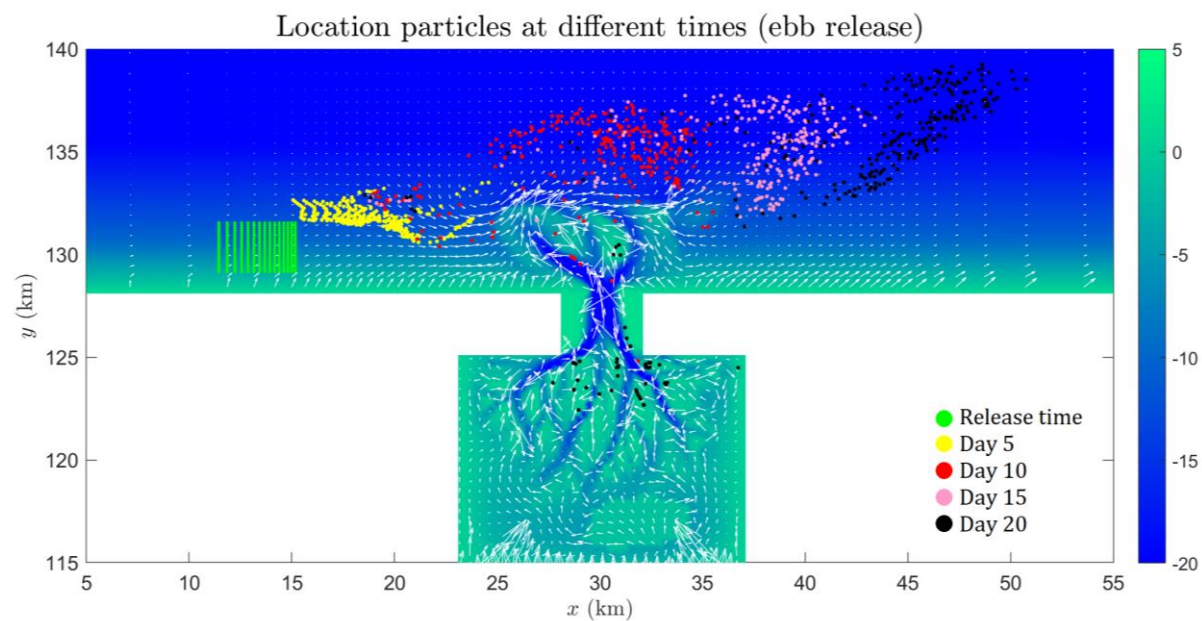

Figure VI: Location of particles at different times for run 8 (ebb-slack release). Colour bar indicates bathymetry.
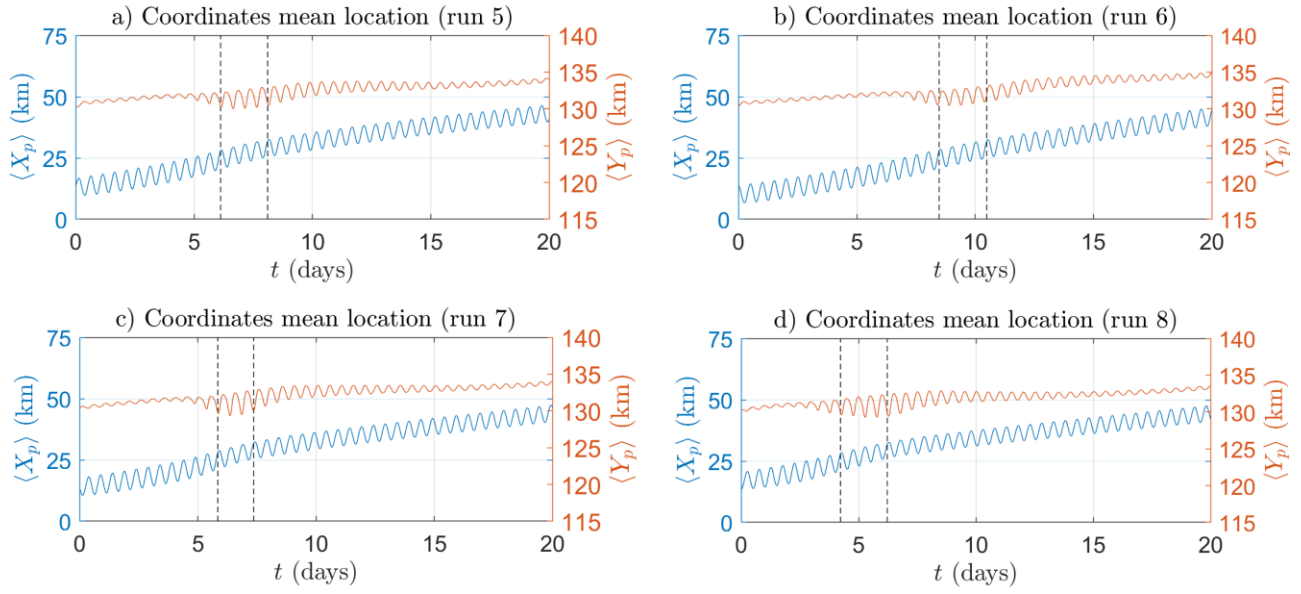
Figure VII: X- and y-coordinates of the mean particle location over time. Dashed lines indicate the moment of entering and passing the tidal inlet area. Run 5 = flood release; run 6 = flood-slack release; run 7 = ebb release; run 8 = ebb-slack release.
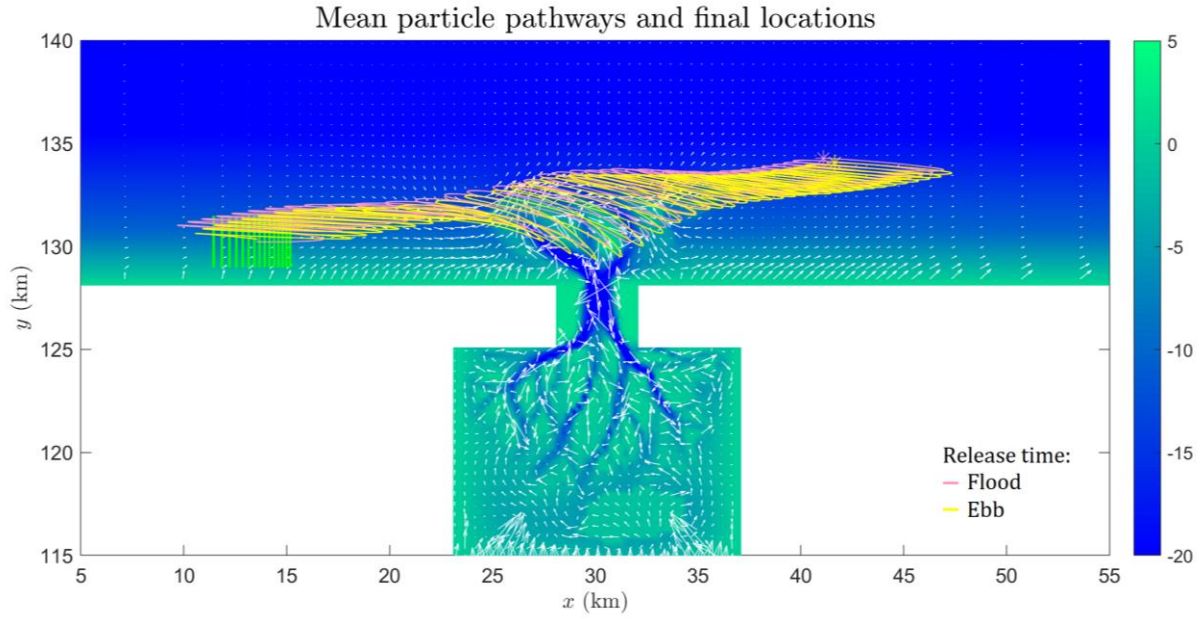

Figure VIII: Mean particle pathways and final locations of run 5 (flood) and run 7 (ebb). Green dots represent release location. Colour bar indicates bathymetry.
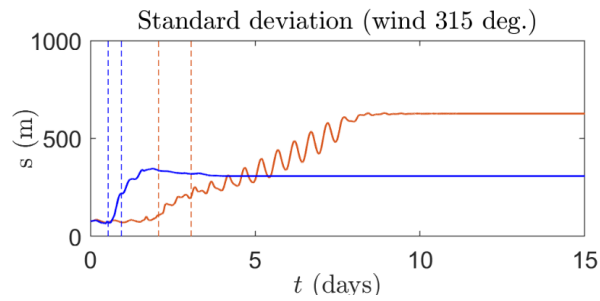
3. Scenario Tides + Swell + Wind

Figure IX: Standard deviation scenarios wind from 315. Gentle breeze (orange) and strong wind (blue).
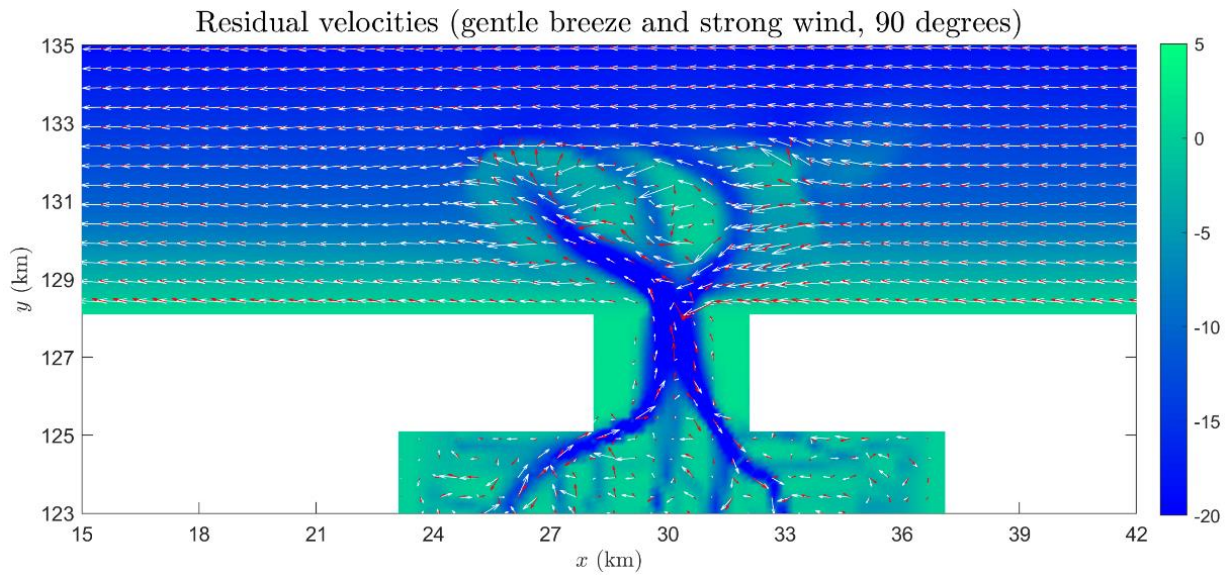

Figure X: Residual velocities for gentle breeze (red) and strong wind (white) from 90 degrees. Colour bar indicates bathymetry.

Figure XI: Difference in residual velocity between scenarios with gentle breeze (red) and strong wind (white) from 270 degrees. Colour bar indicates bathymetry.

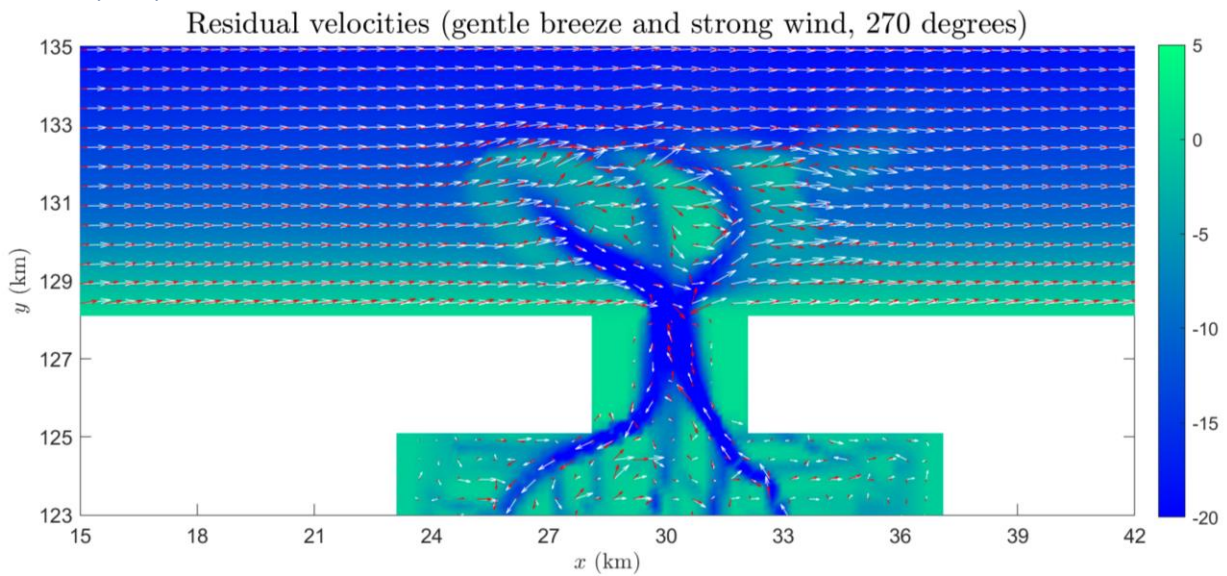*Figure XII: Difference in residual velocity between scenarios with gentle breeze (red) and strong wind (white) from 0 degrees. Colour bar indicates bathymetry.*

4. Scenario varying wind (MSC Zoe)
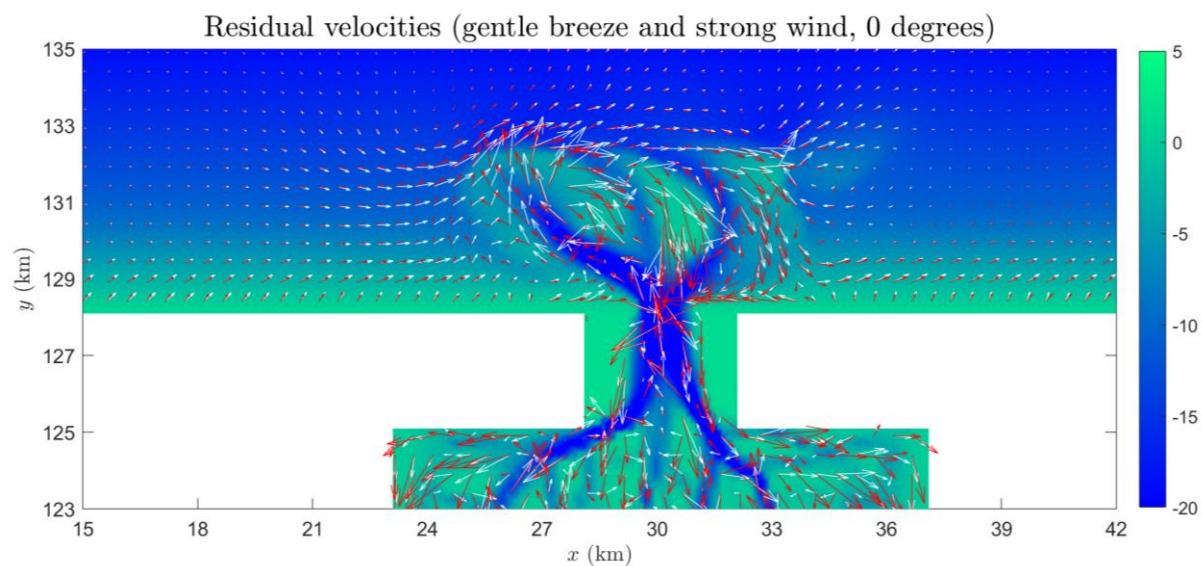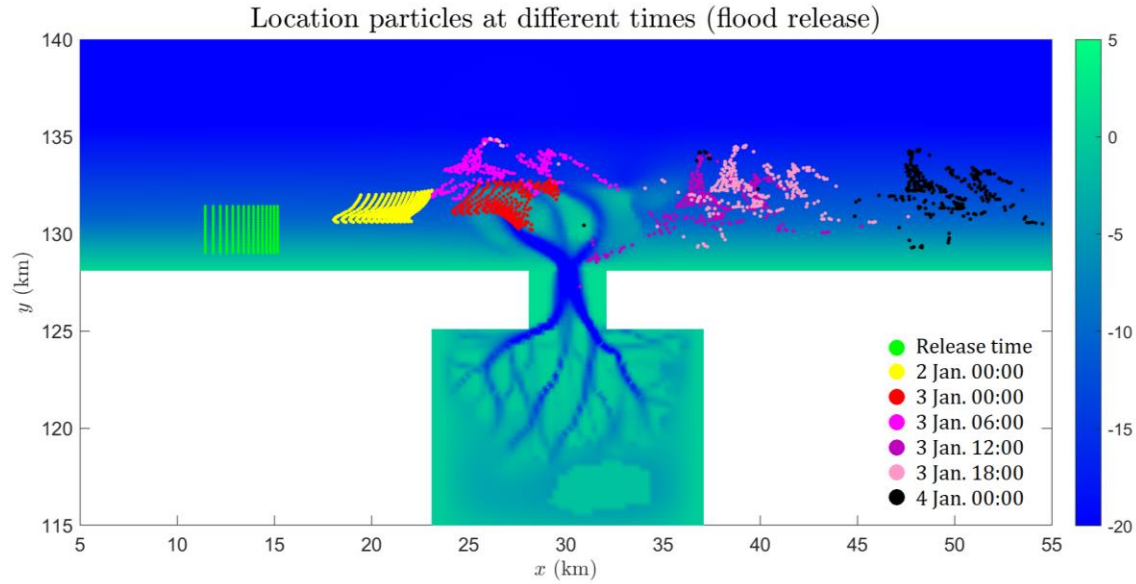

Figure XIII: Location of particles at different times for run 19 (flood release). Colour bar indicates bathymetry.
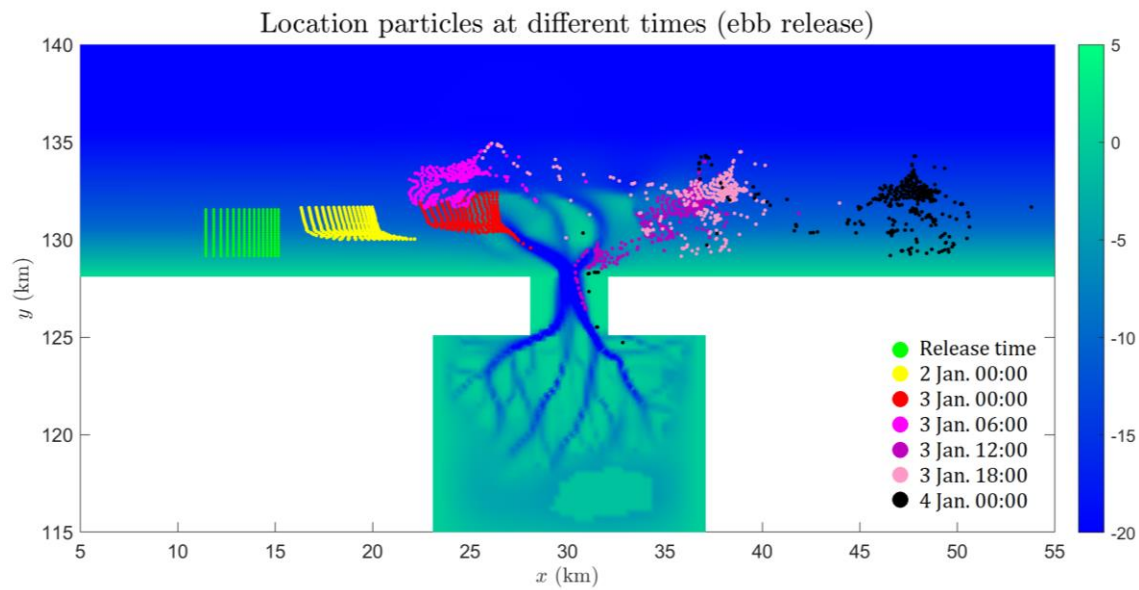

Figure XIV: Location of particles at different times for run 21 (ebb release). Colour bar indicates bathymetry.

Appendix II: Weather conditions during MSC Zoe disaster

Table A1: Weather conditions for dates December 31st, 2018 to January 20th, 2019 measured on Vlieland (KNMI, 2020). Wind conditions at time periods of 6 hours (1=00:00-06:00, 2=06:00-12:00, 3=12:00-18:00, 4=18:00-24:00). Wind direction in degrees (360=north, 180=south).

Date (YYYY-MM-DD)	Period (1-4)	Wind direction (in degrees)	Mean windspeed (in m/s)
2018-12-31	1	303	5.8
	2	283	5.2
	3	257	7.2
	4	263	10.0
2019-01-01	1	272	12.2
	2	323	11.3
	3	330	15.0
	4	342	15.7
2019-01-02	1	350	13.8
	2	3	11.8
	3	8	8.8
	4	348	7.8
2019-01-03	1	352	8.2
	2	348	7.7
	3	355	6.2
	4	340	6.7
2019-01-04	1	307	8.0
	2	313	10.3
	3	325	10.0
	4	322	10.0
2019-01-05	1	325	11.7
	2	328	12.2
	3	320	10.7
	4	323	9.7
2019-01-06	1	318	8.5
	2	313	6.7
	3	317	5.2
	4	353	4.3
2019-01-07	1	270	5.3
	2	243	7.2
	3	253	12.0
	4	280	14.5
2019-01-08	1	303	17.2
	2	322	18.5
	3	330	18.0
	4	338	15.5
2019-01-09	1	2	12.8
	2	5	11.5
	3	12	12.7
	4	22	10.7
2019-01-10	1	23	7.0

	2	325	2.7
	3	283	3.5
	4	297	6.2
2019-01-11	1	338	6.0
	2	325	9.2
	3	323	10.0
	4	317	9.3
2019-01-12	1	270	9.0
	2	270	12.0
	3	295	11.2
	4	290	10.3
2019-01-13	1	268	9.5
	2	280	13.2
	3	298	15.8
	4	317	14.8
2019-01-14	1	345	8.2
	2	333	13.0
	3	327	13.0
	4	302	8.3
2019-01-15	1	265	10.7
	2	260	11.7
	3	263	11.7
	4	250	10.3
2019-01-16	1	240	11.2
	2	227	12.8
	3	220	15.7
	4	267	11.7
2019-01-17	1	270	12.7
	2	307	12.2
	3	335	12.2
	4	357	11.2
2019-01-18	1	325	4.8
	2	297	4.8
	3	146	3.3
	4	185	5.0
2019-01-19	1	178	5.2
	2	160	6.5
	3	133	7.5
	4	135	7.5
2019-01-20	1	113	4.2
	2	113	2.7
	3	93	2.0
	4	158	1.7
2019-01-21	1	222	4.0
	2	258	3.3